Wildfire Risk Prediction: A Survey of Recent Advances Using Deep Learning Techniques

Zhengsen Xu[a], Jonathan Li[a,b], Sibo Cheng[c], Xue Rui[d], Yu Zhao[e], Hongjie He[a], Linlin Xu[b]

[a]*Department of Geography of Environmental Management, University of Waterloo, 100 University Avenue, Waterloo, N2L3G1, Ontario, Canada*
[b]*Department of Systems Design Engineering, University of Waterloo, 100 University Avenue, Waterloo, N2L3G1, Ontario, Canada*
[c]*CEREA, Ecole des Ponts and EDF R&D, Ile-de-France, France*
[d]*School of Emergency Management, Nanjing University of Information Science and Technology, 219 Ningliu Road, Nanjing, 210044, China*
[e]*Division of Geoinformatics, KTH Royal Institute of Technology, Teknikringen 10a, Stockholm 100 44, Sweden*

Abstract

Wildfires pose significant threats to ecosystems, wildlife, and human populations, leading to habitat destruction, pollutant emissions, and biodiversity loss. Accurate wildfire risk prediction is crucial for mitigating these impacts and protecting both environmental and human health. This paper presents a comprehensive review of wildfire risk prediction methodologies, particularly focusing on deep learning approaches. It begins by defining wildfire risk and summarizing the geographical distribution of relevant studies. Key predictive features, including meteorological, socio-economic, and fuel-related factors, are analyzed, with emphasis on feature collinearity evaluation and model interpretability to enhance predictive accuracy. Traditional methods such as wildfire danger rating systems and machine learning models are reviewed, followed by a categorization of deep learning models into time series prediction, image segmentation, and spatiotemporal prediction. Methods for translating model outputs into actionable probabilities are also discussed. The paper identifies the current challenges and limitations in existing models and outlines future opportunities for multimodal data integration and the development of architecturally efficient models for improved wildfire risk prediction.

Keywords: wildfire, risk prediction, remote sensing, deep learning, review

1. Introduction

Wildfires occur in diverse environments such as forests, grasslands, farmlands, and peatlands, with significant impacts on global ecosystems, wildlife, human health, air quality, and carbon balance (Moritz et al., 2014; Stojanovic et al., 2016; Bowd et al., 2021; Holder et al., 2023; Lopez et al., 2024). They not only destroy plant communities, habitats, and human settlements but also contribute to elevated emissions of greenhouse gases and toxic pollutants like carbon dioxide, nitrogen oxides, methane, ozone, particulate matter, and mercury (Hua and Shao, 2017; Yang et al., 2022a; Pelletier et al., 2023; McNorton and Di Giuseppe, 2024). For instance, during the record-breaking 2023 wildfire season, approximately 18.5 million hectares burned across Canada (Erni et al., 2024), the largest area recorded since national reporting began in 1972. This season resulted in the evacuation of 232,000 people (Byrne et al., 2024), with over 200 communities evacuated, hundreds of homes, and infrastructure destroyed (Jain et al., 2024). The carbon emissions for this season were estimated at 647 Tg C (Byrne et al., 2024), with potential long-term impacts on communities and ecosystems expected to last for years or even decades. In the coming decades, climate change is expected to shorten fire return intervals and increase the burned area in vulnerable regions (Parks and Abatzoglou, 2020; Holdrege et al., 2024).

In response to these challenges, wildfire risk prediction has attracted growing attention from governments, academia, and industry. Current prediction models consider essential components such as research scope delineation, data selection and processing, method establishment, setting prediction objectives, and evaluating model accuracy. However, a systematic review of these elements remains lacking. This paper addresses this gap by providing a comprehensive review of the data and deep learning methods used for wildfire risk assessment. In addition, the popular feature attribution techniques in deep-leaning-based wildfire risk prediction models are also reviewed. Finally, we also outline promising new deep learning methods.

First, wildfire ignition and spread result from complex interactions among various factors, including fuel conditions, climate, weather, socio-economic factors, terrain, hydrology, and historical wildfire data (Fuller, 1991). This paper details the definitions, calculations, proxies, and frequency of use of these features, alongside an overview of publicly available spatial datasets for wildfire spread prediction.

Second, A key concern in the design of prediction algorithms is evaluating feature collinearity and improving model interpretability. Including highly correlated features can degrade model performance and obscure feature importance (Li et al., 2022a), while model interpretability helps to clarify patterns of ignition and spread (Abdollahi and Pradhan, 2023). This paper introduces techniques for assessing feature collinearity and enhancing the interpretability of machine learning models.

Another critical aspect of wildfire prediction is the algorithm establishment. Methods range from wildfire danger rating systems and statistical models to traditional machine learning and deep learning approaches. While Jain et al. (2020) provides a comprehensive review of machine learning models, this paper

focuses on deep learning, which has seen rapid adoption and is becoming a crucial tool for wildfire predictions. To address the lack of systematic reviews in this area, we categorize deep learning-based models into three task types: time series prediction, image segmentation and classification, and spatiotemporal prediction. This study reviews existing deep learning models in these categories, providing a structured overview of their applications.

Finally, with the continuous advancements in deep learning techniques, the integration of multi-source geospatial data and deep learning models for wildfire risk prediction offers both significant opportunities and challenges. This paper also discusses the current limitations of existing algorithms and highlighting potential future developments in multimodal and architecturally efficient models.

2. Wildfire Risk Definition

In the majority of published wildfire risk methodology studies, the concept of wildfire risk is not clearly defined, leading to instances of confusion regarding the interchangeable use of terms such as risk, hazard, and danger. Consequently, this paper initiates by presenting a precise definition of wildfire risk. Miller and Ager (2012), based on the Society for Risk Analysis's definition of risk, proposed a comprehensive fire risk framework (Fig. 1), which divides wildfire risk into three components: likelihood, intensity, and effects. This framework emphasizes the impact of wildfires on human activities and the environment rather than solely considering the probability of occurrence. For instance, low-intensity and low-impact wildfires might not significantly affect areas of concern, meaning that a high likelihood of wildfire occurrence does not necessarily equate to high wildfire risk.

Additionally, their study distinguishes between commonly used terms in wildfire risk research, such as risk, hazard, exposure, threats, vulnerability, and fire danger. When summarizing related work, we focus only on studies concerning wildfire risk and danger, excluding those on hazard, exposure, and threats. The former primarily describes the outlook for fire occurrence over a certain period, while the latter tends to evaluate the hazard of wildfires (Fig.1). Consequently, if we consider only the likelihood of fire occurrence without considering its potential harm, the definition of wildfire risk can be simplified to the probability of a wildfire igniting or spreading at a specific location and time (Deeming, 1972). Many researchers in the past have described risk as the likelihood of wildfire occurrence, which also aligns with the wildfire framework established by the European Commission (Depicker et al., 2020).

More specifically, these studies often treat wildfire risk assessment as a conditional probability, where wildfire risk is defined as the probability of a wildfire igniting or spreading under the influence of factors such as fuel, terrain, and weather conditions. In this context, wildfire risk equates to wildfire probability (Yang et al., 2004). In addition, some definitions emphasize the role of causal agents and their frequency in influencing wildfire risk (Hardy, 2005). In this definition, the importance
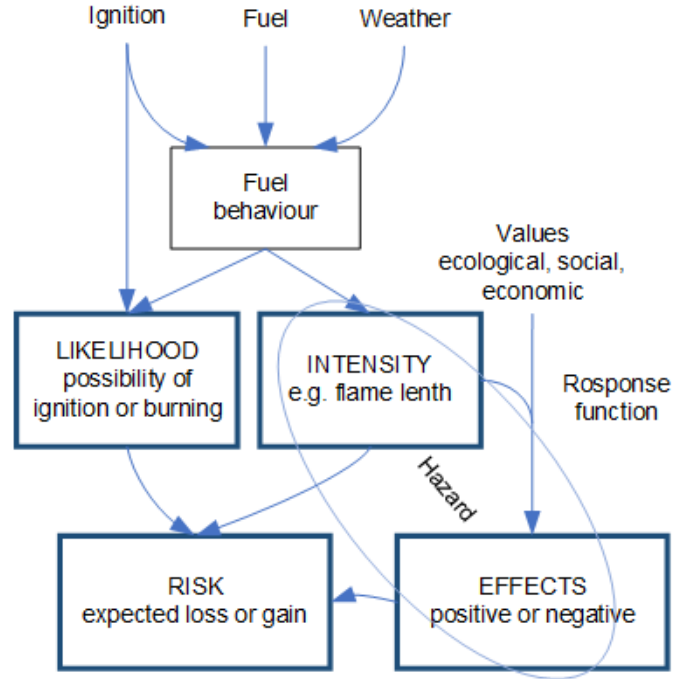

Figure 1: The generalized wildfire risk framework proposed by Miller and Ager (2012)

of "causal agents" is highlighted—without these agents, the existing hazard would have zero potential to cause harm. Causal probability refers to the conditions that trigger wildfires, such as lightning or human activities Deeming (1972).

Based on these definitions, the specific form of wildfire risk varies across studies. This paper categorizes wildfire risk definitions into four types based on the algorithms used and the research objectives: explicit definitions, implicit definitions, wildfire ignition risk, and wildfire burning risk. On one hand, definitions are categorized according to whether they explicitly represent various wildfire influencing factors and the contributions of historical wildfire records. These categories include definitions based on historical observed wildfire occurrence data, influencing factors, and simulation data, as well as data-driven machine learning implicit definitions. On the other hand, wildfire prediction research is generally divided into studies on wildfire ignition risk and wildfire burning risk. Wildfire ignition risk is typically estimated using ignition data, while wildfire burning risk refers to the risk of a fire encountering a particular place. Although this risk partly depends on ignition, it is also influenced by subsequent wildfire spread and fire suppression efforts and is generally derived from historical burn data or simulation methods (Miller and Ager, 2012).

2.1. Explicit and Implicit Definition Methods

This subsection focuses on explicit definition methods, which include directly using historical observation data to define wildfire risk, defining wildfire risk based on the weights of influencing factors, and combining these factors to simulate wildfire distribution and define risk through simulation results. It is worth noting that this subsection does not cover the details

of the simulation algorithms, but rather how to convert simulation results into wildfire risk.

Firstly, the simplest and most direct method in wildfire risk estimation is using historical fire occurrences to predict future risk. For example, Rubí and Gondim (2023) classified regions where one or more fires occurred within an hour as "high risk," while other areas were classified as "low risk." Preisler et al. (2004) selected all fire voxels within a past time (t) and spatial range and sampled a π percentage of non-fire voxels using the scheme proposed by Brillinger et al. (2003). The occurrence of fire can then be characterized using conditional probability, which can be constrained within the (0, 1) interval using a sigmoid function.

$$p(n) = \sum_{t=0}^{T} \frac{y_{t,n}}{T}, \forall n \in [N] \tag{1}$$

where $y_{t,n}$ is the wildfire occurrence at a specific time t and location (grid cell) n 0, 1; N is the duration of the wildfire season. Similarly, Umunnakwe et al. (2022) estimated the spatiotemporal ignition probability using a similar function.

$$m_{g,j} \approx \frac{n_{g,j}}{N} \tag{2}$$

where $m_{g,j}$ represents the fire ignition probability in grid cell g during period j; $n_{g,j}$ and N are the total number of wildfires and the total number of considered periods, respectively. They also introduced Monte Carlo techniques to interpolate grid cells. Lall and Mathibela (2016) assessed wildfire risk in Cape Town, South Africa, by defining daily risk ratings based on the average number of wildfires per day and their corresponding standard deviation over seven years. Specifically, fire occurrences below the average were rated as 1 or lower, those between the average and one standard deviation above were rated as 2 or moderate, those between one and two standard deviations above were rated as 3 or higher, and occurrences more than two standard deviations above the average were rated as 4 or extreme. An ANN model was then established using temperature, humidity, wind speed, and precipitation as inputs to predict wildfire risk.

The above models based on historical data do not consider the conditions for wildfire ignition or spread, thus having poor robustness and generalization ability. Moreover, due to the infrequent occurrence of wildfires over long time scales and large areas, there is a severe class imbalance between the occurrence and non-occurrence of wildfires in space and time. Therefore, the risk assessment results of these models are greatly influenced by data sampling. Consequently, some studies have begun to incorporate or solely use factors such as fuel, terrain, weather conditions, and wildfire triggers as proxies to estimate ignition risk. For example, Castro et al. (2003) used shrub moisture content, specifically live fuel moisture, as a proxy variable for wildfire risk in Spain. More complexly, Sadasivuni et al. (2013) defined wildfire risk as the interaction between human activity and fuel distribution. Specifically, they integrated population and fuel layers through additive operations as input variables for a gravity model in a spatial interaction model. The prediction results were then classified into five levels. Similarly, Gentilucci et al. (2024) categorized wildfire influencing factors and input them into a weight of evidence model, categorizing wildfire risk into low and high levels through regression of various influencing factor weights. Oliveira et al. (2021a); Bergonse et al. (2021) conducted classifications of land use, land cover, slope, elevation, and aspect. They then calculated the likelihood ratio for each category and determined fire susceptibility by summing the weight values of different categories. This process can be mathematically represented as follows:

$$\begin{cases} Lr_i = \frac{S_i/S}{N_i/N}, \\ Lr_j = \sum_{i=0}^{n} X_{ij} Lr_i \end{cases} \tag{3}$$

where Lr_i represents the likelihood ratio of the variable corresponding to category i; S_i and S represent the number of burning pixels associated with category i and the total number of burning pixels; N_i and N represent the number of pixels belonging to category i and the total number of pixels in the study area; the total likelihood ratio Lr_j of each grid cell j is obtained by summing the Lr_i values of all n variables. Similarly, South Africa's official wildfire danger rating system, the Lowveld model (Meikle and Heine, 1987; Lall and Mathibela, 2016), defines wildfire risk using the burn index (BI), wind correction factor (WCF), and rain correction factor (RCF), where BI is a function of temperature and relative humidity:

$$\begin{cases} BI = ((T - 35) - (\frac{35-T}{30})) + ((100 - RH) \times 0.37) + 30 \\ FDI = (BI + WCF) \times RCF \end{cases} \tag{4}$$

where FDI represents the fire danger index. Srivastava et al. (2014) differed from the aforementioned studies by simultaneously considering both causal and anti-causal factors, including the distribution of check dams, firelines, and fire water towers, using an expert knowledge system to quantify the likelihood of forest fires.

Simulation methods based on the above influencing factors are also commonly used in wildfire risk modeling. For instance, Ager et al. (2010) utilized the minimum travel time (MTT) fire spread algorithm, calculating the burn probability of each pixel through the burn frequency in 10,000 simulations. The simulation results defined wildfire risk as burn probability. Similarly, Salis et al. (2021) used MTT but calculated burn probability through a combination of different simulation results rather than frequency. Ujjwal et al. (2022) used the Spark model and parameters such as temperature, relative humidity, wind speed, and wind direction to model wildfire risk in Tasmania, Australia, defining risk categories as low or high based on the spread area of wildfires at different locations. Another typical example of a simulation method is the Monte Carlo algorithm. For example, Adhikari et al. (2021) defined wildfire risk through the overlap of multiple Monte Carlo algorithm predictions. Specifically, they predicted wildfire boundaries within 30 hours of ignition under various random weather and fuel moisture conditions using the Monte Carlo algorithm. The spatial overlap of all Monte Carlo predictions then generated risk levels.

On the other hand, wildfire ignition and spread are highly random and exhibit a strong nonlinear relationship with various factors (Leuenberger et al., 2018). Data-driven machine learning methods are frequently employed in wildfire risk prediction research due to their capability to effectively model nonlinear functions using large-scale datasets (Jain et al., 2020). However, these methods do not explicitly quantify the contribution of individual factors to the overall wildfire risk, compared to explici definition methods. Thus, these methods can be categorized as implicit definition methods. Further details on these methods will be provided in Section 7.

It is important to note that the wildfire risk defined by these machine learning models represents a pseudo-probability rather than a true probability density (Pelletier et al., 2023). This pseudo-probability arises from the models' limitations in explicitly defining risk. For example, in XGBoost, the predicted pseudo-probability is derived from the inverse log transformation of the sum of terminal leaf weights. In SVM, it is estimated by calculating the distance to the classification decision boundary and using these distances for probability estimation. In Random Forest, it is the average of the voting outcomes from multiple decision trees. For models such as Multilayer Perceptron (MLP), Long Short-Term Memory (LSTM), and Convolutional Neural Network (CNN), it is typically the probability estimate from the activation function of the final layer.

Apart from the impact of method selection on the prediction probability, these models also heavily depend on the construction of the label sample set. Different preprocessing techniques, such as historical resampling of wildfire data, can significantly affect the predicted probability values. Therefore, it is necessary to apply post-processing techniques, such as establishing a connection between explicit and implicit definitions, to enhance the interpretability and accuracy of the model outputs.

2.2. Wildfire Ignition and Burring Risk

Wildfire ignition refers to the first occurrence of a fire event during a wildfire. According to Badia-Perpinyà and Pallares-Barbera (2006), to combat forest fires most effectively, the importance of assessing wildfire ignition risk should be emphasized. Similarly, Catry et al. (2009) highlighted that it is not sufficient to consider only factors influencing wildfire spread and suppression difficulty, such as fuel, weather, and terrain. They cited the definitions provided by the Food and Agriculture Organization and the Glossary of Wildland Fire Terminology, which define wildfire risk as fire ignition risk, meaning "the chance of a fire starting as determined by the presence and activity of any causative agent." Furthermore, estimating wildfire ignition risk is crucial for wildfire management, as it guides decisions related to fuel treatment and the allocation of suppression resources. Generally, wildfire ignition risk can be modeled using historical ignition data (Miller and Ager, 2012) and used to generate broader or spatially continuous ignition risk maps. Therefore, the following section will focus on how various studies have identified or defined ignition points and converted these records into probability values or modeled dependent variables.

In the study of wildfire ignition risk in Central Spain, Romero-Calcerrada et al. (2008) utilized wildfire records pro-

vided by the Sección de Defensa Contra Incendios Forestales of the Madrid regional government. These records included the coordinates of ignition points, land cover of the burned area, and the time of the fire. The researchers then defined the probability of wildfire ignition during the fire season as a prior probability and calculated the posterior probability based on this prior probability. Finally, they generated predicted wildfire risk levels by comparing the ratio of prior to posterior probabilities.

In the study by Catry et al. (2009), they first cleaned and corrected a dataset of 137,204 ignition points selected from the official wildfire dataset provided by Portuguese Forest Services, ultimately retaining 127,409 fire ignition locations. To construct a balanced dataset, they randomly selected a number of non-ignition points across the country, 1.5 times the number of fire ignition locations. The ignition and non-ignition points were then encoded as binary variables, forming the final dependent variable dataset for fire ignition. The researchers used frequency analysis and the natural breaks method to convert the historical fire locations dataset into observed and expected frequencies, which were used to train a logistic regression model. In this model, the expected frequency of fire ignition was calculated proportionally to the land area of each observed frequency interval. The output of the logistic regression model was classified into six risk levels. Similarly, Ager et al. (2014b), in their study of wildfire ignition and burning risk in Sardinia, Italy, and Corsica, France, defined the dependent variable of their regression model as the frequency of wildfire ignition on a daily basis, using wildfire ignition area as a condition for burning risk. It is noteworthy that ignition points in Corsica were assumed to be the centroids of burned areas. Braun et al. (2010) used forest inventory data from Ontario's Ministry of Natural Resources to identify wildfire ignition areas and employed generalized additive models, coordinate offsets, and cubic spline interpolation to generate spatially continuous wildfire ignition probability maps, i.e., risk maps.

In the study of wildfires in Belgium, Depicker et al. (2020) defined the probability of wildfire occurrence in a given area as the average probability of ignition within a calendar year:

$$P(I|C_i) = \frac{P(I)P(C_i|I)}{P(C_i)} \quad (5)$$

where $P(C_i)$ and $P(C_i|I)$ represent the ratio of the area of ignition unit C_i to the total study area and the ratio of the number of ignitions to the total study area, respectively, while P_i denotes the ratio of the number of ignitions to the number of units over a one-year span. To mitigate the issue of class imbalance, smaller areas were merged into larger ones:

$$P_A = 1 - \prod_{i=1}^{n}(1 - P(I|C_i))^{N_i} \quad (6)$$

where n and N_i represent the number of environments within a larger area A and the number of grid cells within environment i, respectively. In the study of wildfire ignition risk in Galicia, Spain, Calviño-Cancela et al. (2017) analyzed the differences between historical ignition points obtained from the Spanish Forest Fire Statistics and an equal number of randomly selected locations, examining the relationships between wild-

fire occurrences and factors such as the wildland-urban interface (WUI), land use/land cover (LULC), and elevation. Similarly, Ying et al. (2021), in their analysis of wildfire ignition causes in Yunnan Province, China, used historical records from the Yunnan Forestry Bureau for the period 2003-2015. These records, like those in previous studies, included information on the date, location, size, and cause of each ignition. In total, 5,145 ignition events were recorded, and approximately 1.5 times as many non-ignition points were randomly selected. The relationship between wildfire risk and influencing factors was modeled based on the presence or absence of ignition, rather than frequency.

It is important to note that the studies mentioned above utilized ground-based wildfire databases rather than the more commonly used MODIS or VIIRS fire/hotspot data in wildfire risk prediction research. This may be due to the relatively low spatiotemporal resolution of these data, making it difficult to detect ignition points with very low intensity and duration. Benali et al. (2016) compared the consistency of wildfire field records in Portugal, Greece, Alaska, California, and southeastern Australia with MODIS active fire products (MCD14ML). They proposed a clustering algorithm to calculate the ignition and end dates of a wildfire in the MCD14ML product and used the Nash–Sutcliffe Model Efficiency Index to estimate the consistency between satellite-estimated fire dates and ground records. The study found that satellite data could not estimate the start and end dates of most fires smaller than 500 ha. Similarly, Coskuner (2022) compared the performance of MODIS and S-NPP VIIRS active fire or hotspot detection products, i.e., MCD14ML V6 and VNP14IMG, in detecting wildfires across five different land cover types in Turkey and compared these detections with records from Turkey's ground-based wildfire database. The authors found that both MODIS and VIIRS had very low detection capabilities for small fires (<1 ha) (<3.5%). They also cited studies by Fusco et al. (2019) and Ying et al. (2019), showing that MODIS fire products had high omission rates in the United States and China. Specifically, Fusco et al. (2019) reported detection rates for MODIS products in the United States ranging from 3.5% to 23.4%, with detection rates increasing with fire size. Similarly, Ying et al. (2019) found that in Yunnan Province, China, only 11.10% of 5,145 ground-recorded wildfire events were detected by MODIS fire products, with most omissions attributed to the small size of the fires. These analyses suggest that the commonly used MODIS and VIIRS fire and hotspot products are not suitable for estimating ignition locations and events, nor for corresponding ignition risk estimation.

In contrast to wildfire ignition risk, wildfire burning risk is more broadly defined as the risk of a fire encountering a particular location, influenced by both ignition and spread. Therefore, most studies do not distinguish between ignition and spread when defining wildfire burning risk but consider both simultaneously. In general, there are two methods for defining wildfire burning risk: using historical burn data through explicit or implicit methods, or defining it based on simulation or spread models (Finney, 1998, 2002; Scheller et al., 2007; Miller et al., 2008; Tolhurst et al., 2008; Tymstra et al., 2010; Chen et al.,

2024d). These methods have been discussed in the previous sections of this chapter, so they will not be repeated here. It is important to note that in choosing between these two methods, (Miller and Ager, 2012) suggests that for smaller fire extents (e.g., 1-10 hectares), ignition risk assessment can accurately reflect the likelihood of fire occurrence. However, for larger fire extents (e.g., 20-50 km), it is necessary to consider using burning risk to represent wildfire risk.

3. Research area distribution

This paper counts 138 recent wildfire risk prediction works in various regions around the world. Fig. 2 illustrates the geographic distribution and quantity of wildfire prediction research globally. The figure indicates that North America and Asia are the most concentrated regions for wildfire prediction studies. The United States has the highest number of studies, totaling 71, followed by China and Australia, each with 18 studies. Additionally, Canada, Iran, and India exhibit considerable research activity, with 11, 14, and 6 studies, respectively.

In Europe, the research is primarily concentrated in Western and Southern Europe. Spain, France, Greece, and Portugal have a notable number of studies, with 8, 5, 7, and 9 studies, respectively. Other countries such as Italy, Sweden, Serbia, and Turkey also have a smaller number of studies. Research on the African continent is relatively sparse, with South Africa, Algeria, Morocco, and Senegal each having one study. Similarly, South America has a limited number of studies, with Brazil and Chile each contributing one study. In Oceania, aside from Australia, no other countries have been recorded as having studies.

Furthermore, there are several studies categorized as global, totaling 18, and studies focused on the Mediterranean basin, totaling 6. These global and regional studies highlight the complexity and diversity of wildfire prediction across different climate zones and ecosystems.

Given the geographic distribution and quantity of research, future studies could focus on expanding research regions, promoting cross-regional studies, and enhancing data sharing and model validation. Specifically, although North America and Asia have concentrated research efforts, other regions such as Africa, South America, and parts of Europe have significantly fewer studies. Future research should aim to strengthen wildfire prediction studies in these underrepresented regions to address the geographic distribution gaps and emphasize the climate justice issue (Jones et al., 2024). Additionally, global and Mediterranean basin studies suggest that cross-regional research is crucial for understanding wildfire behavior under different ecosystems and climatic conditions. Enhancing international collaboration to conduct more comprehensive cross-regional studies can provide more robust prediction models and methods. Finally, many current studies rely on region-specific datasets, limiting the generalizability and applicability of the models. Future efforts should focus on promoting data sharing and openness, establishing unified data platforms, and conducting model validation across different regions to improve the reliability and applicability of prediction models.

Figure 2: The spatial distribution of included research.

4. Data

Essentially, wildfires are uncontrolled processes involving the continuous combustion of organic matter in landscapes (Duff et al., 2017). The ignition and burning processes of wildfires are influenced by factors such as fuel conditions, meteorological and climatic conditions, human interventions, topographical and hydrological characteristics, and historical wildfire occurrences (Fuller, 1991). Therefore, in this section, the data used in wildfire risk prediction are categorized into these types, and their components, definitions, and estimation or proxy methods are introduced.

4.1. Fuel Conditions

Duff et al. (2017) suggests that wildfire is a function of the characteristics of the fuel that sustains it. Compared to other factors influencing the ignition and spread of wildfires, such as meteorological conditions, climate, topography, and hydrology, fuel is relatively straightforward to control (Chuvieco et al., 2012). Some studies even posit that fuel is the only element in the landscape that can be altered to influence fire behavior (Thompson et al., 2013; Fernandes and Botelho, 2003). These studies highlight the importance of assessing fuel conditions in wildfire risk evaluations. Fuel refers to any combustible material; in the context of wildfire studies, this includes the combustible organic matter contained in both live and dead vegetation (McLauchlan et al., 2020; Leite et al., 2024). The influence of fuel conditions on wildfire potential, behavior, duration, and emissions is typically described using four variables: Fuel Moisture Content (FMC), fuel load, fuel type (fuel model), and fuel continuity. These parameters directly impact the likelihood of fire occurrence, its intensity, and its rate of spread.

4.1.1. Fuel moisture content

FMC is defined as the ratio of the weight of water (WoW) to the dry weight (DW) of the sample (Eq. 7)(Mbow et al., 2004; Chuvieco et al., 1999). FMC can be categorized into two types: Live Fuel Moisture Content (LFMC) and Dead Fuel Moisture Content (DFMC). It regulates the combustibility of the fuel (Yebra et al., 2013b) and is a significant factor influencing the spread rate of wildfires and the emissions produced during a fire (Fernandes et al., 2008; May et al., 2019).

$$FMC = \frac{WoW}{DW} \times 100\% \qquad (7)$$

In FMC, LFMC is influenced by various plant ecophysiological characteristics, adaptations, and environmental factors affecting transpiration, such as soil moisture and ambient humidity (Castro et al., 2003). In contrast, dead fuel differs from live fuel in that it cannot actively regulate its moisture content through water uptake via roots or water loss through stomatal transpiration. Instead, its moisture content is determined by fuel size, meteorological and microclimate conditions (Nolan et al., 2016), and the biochemical composition of the fuel (Viney, 1991a). These factors are generally determined through experiments or empirical data (Viney, 1991b; Ager et al., 2010). Dead fuel absorbs or loses moisture in response to environmental conditions and eventually reaches equilibrium with the surrounding atmosphere, known as Equilibrium Moisture Content (EMC). The time required to reach EMC is primarily determined by the size of the fuel (Catchpole et al., 2001). Fuel size can be classified into fine fuels, such as small twigs and leaves (1-hour fine fuels), coarser branches and small trunks (10-hour and 100-hour coarse fuels), large trunks and coarse branches (1000-hour fuels), dead grasses and forbs, as well as surface litter and fallen leaves. In some cases, soil is also considered a

type of dead fuel, and its moisture content is measured (Rother-mel et al., 1986). The moisture content of dead fuel, which is more influenced by environmental and weather factors, plays a decisive role in fire ignition and rapid spread at the beginning of the fire season, whereas the moisture content of live fuel has a greater impact on the persistence and extent of fire spread.

a) Dead Fuel Moisture Content

DFMC is a crucial input in nearly all wildfire risk assessment models (Matthews, 2013). For example, estimates of DFMC are integral to current operational fire prediction systems, including the Fire Weather Index (FWI) and the National Fire Danger Rating System (NFDRS) in the United States (Vitolo et al., 2020). Estimating DFMC involves calculating EMC based on factors like temperature, relative humidity, and fuel response time, combined with precipitation data and drying algorithms (Nieto et al., 2010). DFMC estimation methods can generally be divided into four categories: measurements at meteorological stations, field sampling, estimates based on meteorological data, and indirect retrieval using multi-source remote sensing data.

DFMC can be measured using standard wooden dowels installed 10-12 inches above the ground at meteorological stations (Rakhmatulina et al., 2021). However, due to the sparse network of DFMC measurement stations and the limited accuracy, it is challenging to cover large areas even with interpolation of atmospheric parameters. Similarly, field sampling of DFMC is highly accurate and provides data and theoretical support for physical process models and empirical modeling. However, field measurements of fuel properties like DFMC require consideration of terrain, vegetation type, ecosystem structure, climate type, and soil type, making it time-consuming, costly, and limited in scope (Duff et al., 2017). Therefore, studies combining field measurement data with station or numerical weather prediction and meteorological reanalysis data to develop empirical and mechanistic models for estimating FMC are more common (Matthews, 2013). Physical process models primarily consider energy and water balance equations, with the Nelson Dead Fuel Moisture Model, proposed by Nelson Jr (2000), being the most widely used for DFMC estimation. This model predicts DFMC by calculating heat conduction and moisture transfer between a wooden cylinder, the surrounding atmosphere, and external conditions, using hourly input data on temperature, humidity, radiation, and precipitation.

Additionally, McNorton and Di Giuseppe (2024) designed a new method for estimating DFMC by grouping fuels and simplifying the Nelson model. Other models used for DFMC estimation include bulk litter layer models, Byram's diffusion equation-based models, and complete process-based models (Matthews, 2013). Empirical methods for estimating DFMC rely on observed relationships between measured DFMC and factors such as air temperature, relative humidity, wind speed, soil moisture content, and vapor pressure deficit. These data-driven methods include statistical techniques (Ferguson et al., 2002; Ray et al., 2010; Cawson et al., 2020; Rakhmatulina et al., 2021), but their primary limitation is that they are entirely data-driven, making it difficult to explain the relationship between driving factors like temperature, heat and water vapor fluxes,

radiation, and precipitation, and DFMC. Consequently, some studies have started to combine data-driven approaches with physical process models (Fan and He, 2021; Fan et al., 2024).

Apart from the meteorological data-based FMC estimation methods mentioned above, indices such as the Cellulose Absorption Index (CAI), the Lignocellulose Absorption Index (LCAI), the Normalized Difference Tillage Index (NDTI), the Normalized Difference Vegetation Index (NDVI), and the Shortwave Infrared Normalized Difference Residue Index (SINDRI) have been shown to correlate with DFMC (ZORM-PAS et al., 2017; Zacharakis and Tsihrintzis, 2023b). This forms the theoretical basis for DFMC estimation using remote sensing. However, research on DFMC estimation using multi-source remote sensing data is still limited (McCandless et al., 2020).

b) Live Fuel Moisture Content

In early research, LFMC was measured analogously to DFMC through field sampling and weighing, with broader area estimates obtained via interpolation or inversion techniques (Bianchi and Defossé, 2015). While locally precise, this method is neither scalable nor efficient for landscape or global applications due to its time-consuming and labor-intensive nature (Yebra et al., 2013a). Additionally, meteorological parameter-based LFMC estimation benefits from near real-time predictions but faces challenges due to the active regulation of water content by plants and their phenological differences (Pellizzaro et al., 2007; Ruffault et al., 2018).

As such, many studies favor multi-source geospatial data for large-scale and near real-time LFMC estimation, utilizing the growing capabilities of Earth observation technologies for high-resolution data (Rao et al., 2020a; Capps et al., 2021). These contemporary approaches utilize environmental variables such as precipitation and soil moisture, along with spectral, thermal infrared, and microwave data, often in combination with machine learning algorithms, to enhance prediction accuracy (Bowyer and Danson, 2004; Yebra et al., 2013a; ?).

LFMC inversion methods based on multispectral reflectance data exploit water absorption bands in the near-infrared and shortwave infrared spectral regions. Drought stress leads to changes in chlorophyll concentration and leaf structure, enabling LFMC estimation through spectral reflectance relationships (Knipling, 1970; Yebra et al., 2013a). Physical models simulate these relationships, but they are complex; empirical methods using spectral indices like NDVI, EVI, and NDWI provide simpler alternatives and perform well at local scales (Hunt Jr et al., 1987; Fensholt and Sandholt, 2003). Studies have demonstrated the effectiveness of shortwave infrared bands and vegetation indices for LFMC estimation, though improvements through integrating meteorological data have also been suggested (Chuvieco et al., 2002; Myoung et al., 2018).

Thermal infrared bands, such as land surface temperature (LST), are also incorporated to enhance LFMC estimation since canopy temperature correlates with plant water stress (Chuvieco et al., 2004). Machine learning methods have further combined spectral and thermal data to model LFMC, revealing varying importance levels among predictors (McCandless et al., 2020).

Remote sensing methods often face limitations in lighting conditions and cloud coverage, prompting the use of microwave sensors for LFMC estimation due to their ability to penetrate clouds and sensitivity to water content (Rao et al., 2020b). Both active and passive microwave sensors have been employed, with studies showing promising results for vegetation monitoring and LFMC estimation (Dorigo et al., 2017; Lu and Wei, 2021). For example, integrating SAR and multispectral data with vegetation indices improves LFMC predictions, as shown in studies using Sentinel-1 and Landsat-8 data (Jia et al., 2019; Rao et al., 2020b).

Overall, advancements in combining multi-source data and modeling techniques present significant opportunities for accurate LFMC estimation. However, it is important to note that due to the complexity of real-world scenarios, LFMC estimation still faces significant challenges. These challenges include separating the effects of vegetation dry matter, soil moisture, and atmospheric and canopy structure interference on backscatter and optical reflectance and emissivity. Moreover, LFMC ground truth data remain scarce and sparsely distributed, hindering the development of data-driven algorithms.

4.1.2. Fuel load

Another crucial variable in fuel conditions is fuel load, which refers to the total biomass per unit area and provides a baseline for the available biomass in wildfires (McNorton and Di Giuseppe, 2024). Fuel load influences the severity and spread of fires (García-Llamas et al., 2019; Alonso-Rego et al., 2020; McNorton and Di Giuseppe, 2024). It can be categorized into live fuel load and dead fuel load, or further divided by size into fine fuel load—such as grass, small shrubs, twigs, and leaves—and coarse fuel load, including trunks and logs (Gould et al., 2011). Moreover, the definition of fuel load varies slightly across different studies. For instance, Lee et al. (2022) defines fuel load as the amount of fuel in the upper parts of trees, specifically canopy fuel load, while McNorton and Di Giuseppe (2024) defines the above-ground component of fuel load as above-ground biomass. Notably, there is an emphasis on dead fine fuel because it is the primary carrier of fire ignition and spread (Cruz et al., 2003; Elia et al., 2020; D'Este et al., 2021), while canopy fuel load is highlighted because crown fires typically consume fine fuel, resulting in more intense and faster-spreading fires (Arellano-Pérez et al., 2018; Walker et al., 2020; de Groot et al., 2022).

The methods for estimating fuel load are similar to those for estimating FMC, including direct sampling and the use of physical models or multispectral and microwave remote sensing data. Direct measurement involves collecting field samples, weighing, drying them, and then estimating biomass in the area, which is considered the most accurate assessment method and can provide a data foundation for physical or empirical model evaluations. First, fuel load estimation methods based on ground-measured data combined with vegetation or forest growth models can predict or estimate fuel load by forecasting future vegetation growth, forest structure, and more. For example, Lee et al. (2022) used a Weibull function and mortality model based on forest inventory data to predict the fuel load

of Korean red pine (Pinus densiflora) for the next 20 years in Korea. Meanwhile, Nolan et al. (2022) modeled above-ground biomass in the shrub layer of eucalyptus forests in southeastern Australia using allometric equations, considering it as fuel load.

While ground sampling offers high accuracy, it is inefficient and costly. In contrast, remote sensing technology provides an efficient and comprehensive method for assessing fuel load. For example, Saatchi et al. (2007) used airborne SAR data and a semi-empirical algorithm to estimate the distribution of forest biomass and canopy fuel load in Yellowstone National Park. Additionally, Duff et al. (2012) developed a biophysical model to explore the feasibility of using satellite-based NDVI to estimate forest fuel load in southeastern Australia. Li et al. (2020) estimated changes in live fuel load in shrubs and grasslands in the Owyhee Basin, southern Idaho, using MODIS NPP products combined with the Biome-BGC model, and calculated changes in dead fuel load based on the estimates. The study found that even with the same productivity, the fuel load of shrubs was higher than that of grasslands.

In addition to fuel load estimation using physical or semi-empirical models based on remote sensing data, empirical model-based methods are simpler and more commonly used. For instance, Arellano-Pérez et al. (2018) used the random forest method and Sentinel-2 multispectral and vegetation index data to estimate the canopy fuel load of Pinus radiata and Pinus pinaster stands in northwestern Spain. However, due to the low penetration capability of optical sensors, the accuracy of canopy fuel load estimation in this study was limited. Furthermore, Li et al. (2021a) compared the effectiveness of L-band SAR (ALOS-PALSAR) and Landsat 7 ETM+ in estimating fuel load in coniferous mixed forests and found that L-band SAR outperformed optical data in all three fuel load types, with estimation accuracy further improved when both were integrated. Li et al. (2022b) used a data-driven random forest model to correlate long-term spatiotemporal characteristics derived from Landsat 8 OLI and Sentinel-1 data with field-measured fuel load, estimating the fine fuel load (FFL) of pine forests in some areas of Sichuan Province, China. The study found that combining SAR and multispectral data improved FFL estimation accuracy, and temporal features were more important than spatial features.

The comparison between optical and SAR sensor-based fuel load estimation accuracy highlights the importance of canopy structure information in remote sensing-based fuel load estimation. Compared to the fuel load assessment methods based on optical or SAR imagery mentioned earlier, airborne LiDAR provides more detailed information about vegetation's three-dimensional structure (Aragoneses et al., 2024). Therefore, airborne and satellite-based LiDAR sensors can more directly and accurately estimate fuel load at different scales. For instance, Skowronski et al. (2011) used a LiDAR system to estimate canopy fuel load in pine-dominated forests in New Jersey, USA, predicting crown bulk density and canopy fuel weight. Chen et al. (2017) effectively estimated ground fuel load in Western Australia's Jarrah forests by combining LiDAR data with previous year fire data, canopy density, elevation, and fuel types. Bright et al. (2017) compared the performance of airborne LiDAR and Landsat time-series data in estimating forest

canopy and surface fuel load in a study area in Grand County, Colorado, USA, finding that Landsat provided limited improvement in fuel load estimation. Labenski et al. (2023) further combined Sentinel-2 multispectral data with airborne LiDAR data to extract forest structure and composition information for two forest areas in southwestern Germany, using a random forest model to predict and map surface fuel load. In another study, D'Este et al. (2021) incorporated Sentinel-1 SAR data into a fuel load estimation model based on Sentinel-2 multispectral data and airborne LiDAR data for southeastern Italy, estimating dead fine fuel load. The study found that compared to NDVI and C-band SAR data, LiDAR variables had a stronger capacity to estimate dead fine fuel load. The study also found that woody vegetation contributed more to fuel load, consistent with the findings of Li et al. (2020).

In addition, the more recent NASA Global Ecosystem Dynamics Investigation (GEDI) full-waveform LiDAR sensor has been widely used for large-scale above-ground biomass estimation and vegetation canopy structure analysis (Myroniuk et al., 2023; Liang et al., 2023; Aragoneses et al., 2024; Guerra-Hernández et al., 2024), aiding wildfire simulation, assessment of wildfire impacts on vegetation, and understanding wildfire severity. However, only a few studies have directly used GEDI LiDAR data to estimate fuel load. For example, Leite et al. (2022) used unmanned aerial vehicle (UAV) simulations and GEDI data to study the ability to stratify fuel load in grasslands, savannas, and forests within tropical savannas in Brazil. The study found that GEDI performed poorly in estimating fuel load for ground and low-lying vegetation, and was significantly affected by terrain.

Finally, it is worth noting that due to the similarity in definitions, particularly the emphasis on crown fires, some studies have used above-ground biomass as a proxy for fuel load (Eames et al., 2021; Vega et al., 2022). Additionally, other studies have used different proxies for fuel load. For instance, Su et al. (2021) used fractional vegetation cover (FVC) as a proxy for fuel load in a study on wildfire drivers in tropical rainforests in southern China. FVC represents the percentage of an area covered by green vegetation within a statistical region. In practical applications, the MODIS NDVI product is commonly used as a proxy for FVC. Helman et al. (2015) analyzed time-series NDVI data from MODIS to distinguish between woody and herbaceous vegetation in Mediterranean forest regions, using long-term mean woody NDVI and its trends as a proxy for fire fuel. In actual wildfire risk prediction, using proxies instead of directly estimating fuel load is more common because it is simpler and avoids cumulative errors.

4.1.3. Fuel types

Another method to describe fuel properties, aside from fuel moisture code and fuel load, is by categorizing fuels into homogeneous groups that exhibit similar characteristics under specified burning conditions. These groups are defined as "fuel types" or "fuel models" (Arroyo et al., 2008). The description of fuel types is generally complex, taking into account various fuel characteristics such as vegetation type, canopy height, canopy base height, canopy bulk density, vegetation cover ratio,

horizontal and vertical continuity, fuel load, fuel moisture, and biomass (Chuvieco et al., 2003; Pettinari and Chuvieco, 2020; Aragoneses and Chuvieco, 2021). In recent years, various standardized fuel classification systems have been proposed in different regions (Table 1), including the NFDRS (Cohen, 1985), Northern Forest Fire Laboratory (NFFL) (Albini, 1976; Burgan, 1984), Fuel Characteristics Classification System (FCCS) (Sandberg et al., 2001; Ottmar et al., 2007), McArthur fuel types (McArthur, 1966, 1967), Canadian Fire Behaviour Prediction (FBP) (Group et al., 1992), and Prometheus (Riaño et al., 2002).

Table 1: Comparison of Fuel Classification Systems (Arroyo et al., 2008)

Fuel classification system	Number of fuel types	Country of application
NFDRS fuel types	20	USA
NFFL fuel types	13[a]	USA
FCCS	216[b]	USA
McArthur fuel types	3	Australia
FBP fuel types	16	Canada
Prometheus fuel types	7	Europe[c]

[a] Option of developing custom fuel types.
[b] New fuelbeds added periodically.
[c] Mediterranean countries.

Similar to the assessment methods for fuel load and fuel moisture, fuel type mapping can also be conducted through field sampling and remote sensing techniques, including the use of optical, microwave, and LiDAR sensors (García et al., 2012; Pettinari and Chuvieco, 2020; Aragoneses and Chuvieco, 2021). This generally involves the classification of vegetation types and the retrieval of vegetation structure and biochemical parameters such as canopy, followed by the classification of fuel types using expert knowledge or experimental data (Chuvieco et al., 2020). At large scales, such as global or continental levels, fuel type maps are usually created by combining satellite imagery with land use types and the aforementioned fuel classification systems (Pettinari et al., 2013; Pettinari and Chuvieco, 2016; Aragoneses and Chuvieco, 2021).

In addition to detailed classification of fuel types, many wildfire risk assessment studies based on multi-source remote sensing data employ simpler, but coarser, land use type maps as proxies for fuel types to analyze the impact of different land cover types or human activities on wildfire risk. For instance, Jaafari et al. (2019) used logistic regression to analyze the impact of various explanatory variables, including topography, elevation, TWI, meteorological factors, and land use, on wildfire risk in the Zagros ecoregion of western Iran. They found that the most important variable was land use type, with dry farmland and forests being the most susceptible to wildfires. Additionally, the type and continuity of vegetation determined the likelihood of large fires. Similarly, Ager et al. (2014b) analyzed wildfire occurrence and size on the islands of Sardinia, Italy, and Corsica, France, finding that early in the fire season, the probability of large fires was ten times higher in agricultural lands in southern Sardinia compared to forest and shrubland land use types near roads. However, by the end of the fire season, the latter land use types exhibited a higher probability of fires. Conversely, Calviño-Cancela et al. (2016) an-

alyzed the wildfire risk in the wildland-urban interface (WUI) and LULC in northern Spain, finding that primary forests and agricultural areas had the lowest fire risk. Similarly, Donovan et al. (2020) assessed wildfire risk in the Great Plains ecoregion of the United States, considering five land use types: grasslands, woody vegetation, croplands, pastures and hayfields, and developed areas. Their study found that woody vegetation and grasslands were most prone to wildfires and large fires, while other land use types had lower risks. Among them, croplands had the lowest probability of large fires, and as the percentage of crop cover increased, the likelihood of large fires decreased.

4.1.4. Fuel continuity

Since fire lines spread both horizontally and vertically, fuel continuity is generally considered in terms of both vertical and horizontal directions. Vertical canopy continuity primarily refers to the vertical structure of fuels, also known as ladder fuels. These are composed of low-lying shrubs, seedlings, upper canopy trees, and intermediate understory vegetation. In areas where vertical fuels are present, this structure can cause low-intensity surface fires to escalate into severe crown fires (Agee and Skinner, 2005; Menning and Stephens, 2007). There has been significant research on ladder fuels, including methods for precise field measurements of fuel structure (Kilgore and Sando, 1975; Pye et al., 2003) and approaches combining field measurements with expert knowledge (Menning and Stephens, 2007). However, due to the complexity of field measurement, the more common proxy for vertical fuel continuity is the estimation of canopy base height (CBH) (Scott, 2001).

CBH is defined as the height above which there is sufficient canopy fuel per unit volume to support vertical fire spread into the canopy (Scott, 2001). It has widespread application in various wildfire behavior models (Hall and Burke, 2006). CBH can be estimated using allometric equations based on species, diameter at breast height (DBH), and tree height, or it can be retrieved from remote sensing data. However, due to the limitations of passive optical remote sensing signals and synthetic aperture radar (SAR) in penetrating the canopy, studies using multi-angle observations or bidirectional reflectance distribution function (BRDF) retrievals to obtain three-dimensional vegetation structure information are rare in wildfire prediction (Pisek et al., 2015; Canisius and Chen, 2007). More commonly, LiDAR is used to estimate CBH at the individual tree or local scale (Andersen et al., 2005; Luo et al., 2018; Wang et al., 2022a). Some studies suggest that while the definition of CBH is clear, its practical application is complicated by the lack of a clear fuel threshold per unit volume and the potential neglect of fine fuels, which can lead to errors in modeling canopy fire risk (Cruz et al., 2004; Kramer et al., 2014). As a result, a quick and simple method to estimate ladder fuels is by estimating the coverage area or coverage rate of low-lying fuels as a representation of ladder fuel (Clark et al., 2009; Wing et al., 2012).

In addition to vertical continuity, horizontal fuel continuity is also crucial. However, there are various definitions of horizontal continuity. For example, Frandsen et al. (1979) defines horizontal continuity as the degree of variation in the physical characteristics of fuels within a given area, with an emphasis on the

impact of fuel type. Conversely, a more commonly used definition in describing horizontal continuity focuses on the spacing between fuels (Ritter et al., 2023). Tree spacing significantly affects the intensity and scale of wildfires (Kim et al., 2016). For instance, Qadir et al. (2021) showed in a study on wildfire risk prediction in Nepal that areas with high forest cover density have a higher risk of fires. In contrast, when there is canopy discontinuity, fire spread may slow down or even be extinguished (Taneja et al., 2021). For example, Kim et al. (2016) used the Fire Dynamics Simulator (WFDS) to model fire behavior in Korean pine (Pinus densiflora) and found that when the spacing between trees is 6 meters or more, most crown fires stop spreading within 100 meters. Therefore, fuel management techniques that fragment fuels can be used to suppress wildfires (Srivastava et al., 2014; Harrison et al., 2021). Based on our review, research on horizontal fuel continuity is less prevalent compared to vertical continuity, likely because many studies use proxies rather than directly assessing horizontal continuity. For instance, many crown fire spread models use canopy bulk density to describe horizontal fuel continuity (Wagner, 1993; Cruz et al., 2005). Additionally, proxies such as fraction vegetation cover, canopy cover, vegetation cover density, and various vegetation indices are also commonly used.

In summary of fuel conditions, it is noteworthy that various fuel state description parameters are generally used in studies evaluating their effectiveness in wildfire risk modeling but are rarely directly utilized in wildfire risk assessment models. Commonly used wildfire risk assessment models often directly employ raw multispectral or microwave data or indices derived from these data. This could be due to several reasons:

Firstly, evaluating fuel state is complex, often requiring multiple sensors, and the models built for this purpose tend to have poor generalization ability, making them suitable only for specific regions. Additionally, the availability of sensors is a limiting factor for the application of certain fuel state description parameters. For example, estimating vertical canopy structure typically requires LiDAR data. However, satellite-based LiDAR canopy structure is limited by spatiotemporal resolution, and airborne LiDAR has limited coverage and high costs.

Moreover, most wildfire risk assessment studies require long time series data, which, due to cost constraints, are often based on low-cost and readily available data such as multispectral or microwave satellite data. These data, due to limitations in spatiotemporal resolution and canopy penetration, often struggle to accurately retrieve various descriptive parameters. The descriptive parameters obtained from inaccurate data inversions may lead to error accumulation, which can further impact prediction accuracy.

Lastly, data-driven wildfire risk prediction algorithms are becoming increasingly popular, and these algorithms can either rely on or bypass manual feature engineering, allowing them to directly learn the necessary abstractions from features or raw data.

4.2. Weather and climate conditions

Weather and climate factors are major drivers of wildfire activity, influencing the occurrence, burned area, and fire behav-

ior (Swetnam and Betancourt, 1990; Bessie and Johnson, 1995; Abatzoglou and Kolden, 2013). Weather conditions are central to almost all global fire danger risk systems. High temperatures, low relative humidity, insufficient precipitation, and strong winds have been proven to be key factors in the ignition of fires in the short term (Keane et al., 2001; Zacharakis and Tsihrintzis, 2023b), and they also affect fire size and spread (Abatzoglou and Kolden, 2011). On the other hand, climate conditions generally refer to the long-term weather conditions of a region and their variations. Some studies specifically define these as the collective atmospheric conditions months or even years before the start of the fire season, emphasizing the use of prior climate conditions to convert fuel conditions into wildfire potential (Abatzoglou and Kolden, 2013). This approach enables predictions of large-scale fire risks over seasonal, annual, or even multi-decadal time scales.

4.2.1. Weather conditions

Short-term weather conditions focus primarily on predicting the impact of weather conditions over quarters, months, weeks, or days on fire risk. These include short-term temperature, wind, relative humidity, soil moisture, precipitation, and lightning, as well as corresponding indices like the Palmer Drought Severity Index (PDSI) and the FWI. Temperature and various humidity conditions affect fuel conditions, such as evapotranspiration and moisture content, which in turn influence the wildfire risk. Wind direction, wind speed, and other related metrics like Mean Wind Power Density (MWPD) and Mean Wind Speed (MWS) affect fire spread and intensity, making them commonly used parameters in wildfire prediction. Unlike other parameters, lightning can act as an ignition factor for wildfires.

Short-term weather parameters are widely used in wildfire risk prediction. For example, Tavakkoli Piralilou et al. (2022) used temperature, precipitation, MWPD, and MWS as parameters in their wildfire prediction model for the forested areas of Gilan Province, Iran. In another study conducted in Pakistan, Kanwal et al. (2023) utilized 16 meteorological parameters, including monthly average precipitation, evapotranspiration, wind speed, soil temperature, humidity, heat flux, albedo, average land surface temperature, soil moisture, actual evapotranspiration, moisture deficit, downward surface shortwave radiation, precipitation accumulation, minimum/maximum temperature, and vapor pressure. An assessment of their importance indicated that heat flux, evapotranspiration, and vapor pressure were relatively more important compared to other meteorological parameters, although the differences in importance were not significant. Bergado et al. (2021) used seven meteorological factors in their wildfire prediction study for Victoria, Australia: daily maximum temperature, daily minimum relative humidity, daily total solar radiation, daily total precipitation, daily average wind speed, daily average wind direction, and lightning frequency. The lightning data was derived from an annual lightning climatology dataset that provided estimates of lightning density for each day of the year. Their study found that total precipitation, lightning density, and surface temperature consistently held high weight in all models. In contrast, Quan et al. (2023) used various meteorological variables from the ERA5 dataset, including precipitation, relative humidity, temperature, wind speed, and the Keetch-Byram Drought Index, to predict wildfire risk in parts of the western Tibetan Plateau in China. The study revealed that relative humidity was the most critical factor in the occurrence of forest and grassland fires in the region. Higher relative humidity leads to higher DFMC, thereby reducing the likelihood of ignition.

4.2.2. Climate conditions

Climate conditions primarily refer to annual or multi-year meteorological parameters such as temperature, humidity, precipitation, and evaporation. Unlike short-term meteorological conditions that affect fuel status temporarily, climate conditions play a crucial role in determining fuel types, distribution, life cycles, and other factors that influence fuel characteristics, such as fuel load and continuity (Aldersley et al., 2011; Jaafari et al., 2017; Tavakkoli Piralilou et al., 2022). These fuel characteristics respond to climatic patterns accumulated before the start of the fire season (Chen et al., 2016). Consequently, climate variables are often the primary drivers of long-term wildfire activity (Pollina et al., 2013; Jain et al., 2020). Furthermore, climate conditions also explain strong seasonal variations in wildfire risk in certain regions (Martell et al., 1989), particularly in the context of intensified climate change in recent years, which has raised concerns about its long-term impact on the occurrence of large-scale wildfires (Prior and Eriksen, 2013; Jolly et al., 2015; Jain et al., 2024).

Climate conditions are widely used in wildfire risk prediction. Specifically, Chen et al. (2016) used large-scale sea surface temperature anomalies to predict the severity of the fire season in South America on a seasonal time scale. Their study found that using a single ocean climate index could predict about 48% of the burned area globally for up to three months or longer before the peak burning month. In a study by Jaafari et al. (2019) in the Zagros ecoregion of western Iran, they used three climate conditions: annual temperature, rainfall, and wind effects. However, the results showed that only the annual temperature parameter was relatively important. Similarly, Naderpour et al. (2020) studied the northern beaches of New South Wales, Australia, using three climate factors: annual rainfall, annual humidity, and annual wind speed. Holdrege et al. (2024) studied the Great Basin sagebrush regions across 13 western U.S. states and used three climate factors: annual mean temperature, annual precipitation, and the proportion of summer (June to August) precipitation to total annual precipitation. The study found that areas with low summer precipitation proportion, medium to high annual precipitation, and high temperatures had the highest wildfire probability. Similarly, Aldersley et al. (2011) used annual cumulative precipitation, annual lightning frequency, monthly precipitation frequency, monthly average temperature, and climate data from the British Atmospheric Data Centre (BADC) to study the drivers of monthly fire area on a global and regional scale. They found that climate factors such as high temperatures, moderate precipitation, and drought were the most important drivers globally. Mansuy et al. (2019) conducted a study across the U.S. and Canada and found that climate variables were the primary control factors

for the burned area in most ecoregions, both inside and outside protected areas, surpassing landscape and anthropogenic factors. The climate data used in their study included annual average precipitation, annual average relative humidity, the Hargreaves climate moisture deficit (an annual measure of energy and moisture), and degree days below 18°C. Abdollahi and Pradhan (2023) conducted a wildfire prediction study in the Gippsland region of Victoria, Australia, and found that humidity, wind speed, and rainfall were the most influential factors in wildfire prediction. Zhao and Liu (2021) used data from over 600 meteorological stations in forest, grassland, and shrubland areas to calculate two drought indices, the Keetch-Byram Drought Index and the Standardized Precipitation Index. They then used global-scale PDSI data to mask these indices and assess long-term wildfire risk in China. The results showed that drought indices had a stronger correlation with seasonal and annual fire occurrences compared to climate indicators such as temperature and precipitation.

From the analysis above, it is evident that various forms of temperature, wind, humidity, and evaporation data are commonly used as meteorological or climate variables in wildfire prediction models. A few studies have combined both meteorological and climate factors to analyze their roles in the occurrence, spread, and scale of wildfires. For example, Abatzoglou and Kolden (2011) found in their study on the influence of weather and climate factors on the occurrence and scale of individual wildfires in Alaska that prior climate conditions had no significant effect on the final fire size, whereas post-ignition weather conditions, such as precipitation, had a greater impact over days to weeks. Thus, the authors suggest using short-term weather factors in wildfire risk assessment models and spread models. From another perspective, weather variables are more important than climate variables for small-scale and short-term wildfire risk and spread assessments.

4.3. Socio-economic factors

In the early stages of wildfire risk assessment, considerable attention was given to factors influencing wildfire spread and suppression difficulty (McArthur, 1958, 1966; Hollis et al., 2024). However, numerous studies have shown that the proportion of fires caused directly or indirectly by human activities surpasses those triggered by natural factors, such as lightning (FAO, 2006). Indirect human activities typically refer to the impact of human actions on climate change, which in turn influences wildfire risk. This effect can be modeled by analyzing the influence of climate on wildfire risk. Furthermore, the impact of indirect human activities on wildfire risk also includes changes in vegetation types, land use patterns, and landscape fragmentation, as well as alterations in fuel load and fuel continuity due to activities like grazing, planting, and harvesting (Harris et al., 2023). These changes can significantly affect local wildfire risk. Direct human activities, on the other hand, primarily involve ignition and suppression. The risk of wildfires caused by direct human ignition is particularly significant. For instance, from 1992 to 2012, 84% of wildfires in the United States were human-induced (Balch et al., 2017). Similarly, Vilar et al. (2016) found that 95% of wildfires in Mediterranean

Europe between the 1980s and 2010s were caused by human activities. Notably, human factors not only increase the frequency of fires but also extend the fire season and lead to more random distributions of fire locations (Balch et al., 2017). This randomness introduces greater uncertainty into wildfire risk prediction, as wildfires may occur in areas with infrequent lightning or where lightning does not coincide with high temperatures, dryness, and strong winds (Abatzoglou et al., 2016).

Since Chuvieco and Congalton (1989) first introduced human activity variables into wildfire risk research by considering the proximity of road networks and areas with high human activity, such as recreational zones, an increasing number of studies have incorporated human activity variables into wildfire risk prediction models. These variables include the distance of various locations from nearby roads, power lines, villages, and cities, as well as road density, population density, and land use. The assumption underlying the inclusion of these variables is that wildfire frequency is negatively correlated with distance from human infrastructure and positively correlated with road density and population size (Gilreath, 2006; Martínez et al., 2009). In addition to these easily describable features, there are more complex factors influencing wildfire risk, such as the potential for urban development to increase fuel loads in rural areas, or the possibility that controlled burns for agricultural purposes in remote areas may increase the likelihood of uncontrolled wildfires (Martínez et al., 2009). Several studies have confirmed these assumptions. For example, Jaafari et al. (2019) found a strong correlation between high wildfire probability and road network density in the Zagros ecoregion of western Iran. Ghorbanzadeh et al. (2019), in their study of the forest areas in Amol County, Mazandaran Province, northern Iran, similarly found that human activities near major roads significantly influenced wildfire risk. The interaction between human settlements and vulnerable infrastructure in areas with high or moderate forest fire susceptibility leads to the emergence of high-risk zones on wildfire risk maps.

Therefore, most wildfire risk prediction studies consider the socio-economic factors mentioned above. For instance, Sadasivuni et al. (2013) generated a population interaction map based on forest resources and human settlement patterns and studied wildfire risk in Mississippi, southeastern United States. They found that areas with dense fuel and sparse populations were most likely to experience wildfires. Malik et al. (2021) mapped wildfire risk in a densely vegetated area of approximately 63 km^2 between Monticello and Winters, California, using the location of power lines as a proxy for socio-economic factors, given that power lines can serve as ignition sources during high wind events. Nami et al. (2018) considered land use/land cover (LULC) and proximity to roads and settlements when mapping wildfire risk in the Hyrcanian ecoregion of northern Iran. They found that the probability of fire occurrence was highly dependent on human infrastructure and related activities. Additionally, the study revealed a positive correlation between fire occurrence and landscapes within 4,000 meters of human settlements, and a negative correlation for areas beyond 4 kilometers. Rubí and Gondim (2023) conducted a study in Brazil's Federal District, dividing the region into zones based

on the coverage of different weather stations and calculating the distance from each zone's center to the nearest road and building as proxies for socio-economic factors. Bergado et al. (2021) carried out a wildfire prediction study in Victoria, Australia, and found that land cover categories (such as farmland, forests, mines, and quarries) and distance from power lines were relatively low in importance. In their wildfire risk assessment in Guangdong Province, China, Jiang et al. considered socio-economic factors such as gross domestic product (GDP), distance from roads, and population density. The results showed that, aside from meteorological factors, GDP was the most significant factor in wildfire risk. Similarly, Jiang et al. (2024b) in their wildfire risk assessment in Guangdong Province, China, also utilized GDP, distance to highways, and population density as socio-economic factors. However, their results indicated that the contribution of socio-economic factors to wildfire risk was not significant. Furthermore, in a study conducted in the western part of the Tibetan Plateau in China, Quan et al. (2023) found that although government reports indicated that the majority (about 95%) of wildfires in the region were caused by human activities, the importance of distance from roads and residential areas was relatively low compared to meteorological factors.

It is noteworthy that current research on the impact of human activities on wildfire risk primarily focuses on using the distribution density of population, roads, and other infrastructure, as well as the straight-line distance of different locations within the study area from infrastructure, as input features for models. However, the consideration of these distances is typically limited to simple linear measurements, without accounting for human accessibility. This limitation may reduce model performance in regions with rugged terrain. Additionally, current research on human factors mainly focuses on human-induced wildfires, with little consideration given to the mitigating effects of firefighting facilities, such as fire stations, firebreaks, and lookout towers.

4.4. Terrain and hydrological features

Terrain factors used in wildfire prediction studies include elevation, slope, aspect, hill shade, and planar curvature. Terrain indirectly determines mesoscale and microscale climate and airflow (Coen et al., 2013), thereby impacting fuel conditions and wildfire propagation. For example, to some extent, an increase in slope leads to faster fire spread (Ghorbanzadeh and Blaschke, 2018). Steeper slopes result in faster fuel preheating and ignition rates, and compared to flat terrain, the rate of fire spread on a 20° slope increases by about four times (Lecina-Diaz et al., 2014). The slope aspect influences prevailing winds, humidity, solar radiation, and plant species distribution. In many regions of the Northern Hemisphere, north-facing slopes are typically cooler and more moist than south-facing slopes, making south-facing slopes at higher risk of forest fires (Sayad et al., 2019). Curvature and valley depth are geomorphic indicators of soil moisture and vegetation distribution (Kalantar et al., 2020). In larger valleys, downslope-driven cold air pooling has a significant impact on vegetation density and composition (Kiefer and

Zhong, 2015). Additionally, elevation can also influence human activities, as lower elevations tend to have higher human population density and are more prone to wildfires compared to higher elevation areas (Guo et al., 2016). In addition, the main hydrological feature is the distance between fuel and water bodies, soil moisture, and the topographic wetness index (TWI). TWI represents soil saturation and surface runoff rates. Land with higher TWI is more saturated, and high moisture content can prevent fire ignition (Achu et al., 2021).

For example, Ghorbanzadeh et al. (2019) studied the forestry area of Amol County in the Mazandaran province of northern Iran and used slope, slope aspect, and altitude as terrain factors. They found that steep areas were generally more prone to forest fires. Nami et al. (2018) considered terrain factors such as slope, slope aspect, altitude, planar curvature, TWI, and topographic roughness index (TRI) when mapping wildfire risk in the Hyrcanian ecological region in northern Iran. Their further collinearity analysis revealed significant collinearity between TWI and slope with other parameters, leading to their exclusion from subsequent modeling tasks. A study conducted by Tran et al. (2023) on the island of Oahu in the Hawaiian Islands also utilized terrain and hydrological features such as elevation, slope, aspect, plan curvature, profile curvature, valley depth, TWI, and proximity to rivers. The assessment of their significance indicates that slope, elevation, and TWI are of secondary importance compared to proximity to roads and temperature in relation to fire risk. Gentilucci et al. (2024) also used TWI in a study in the Marche region of central Italy. Their research shows that areas of the terrain with less accumulation of moisture are most susceptible to fires.

Soil moisture information can serve as a complement or substitute for drought indices and is commonly used in wildfire risk prediction models. It can be utilized in modeling fuel moisture and other related factors (Krueger et al., 2022). For example, Bakke et al. (2023) conducted a study in Fennoscandia, Finland, to explore the primary hydro-meteorological factors influencing wildfire occurrence. They found that shallow soil moisture anomalies were the main influencing factor. Similarly, in the study by Vissio et al. (2023) on the prediction of summer burning area in Italy, the ERA5 soil moisture reanalysis data product was used. The research found that using only a single variable, namely surface soil moisture, for predicting wildfire burn area yielded good results. This is because surface soil moisture can serve as a proxy for the combined effects of temperature and precipitation. In the study by Nur et al. (2023) focusing on Sydney, Australia, the MODIS Terra Climate dataset was used, which provided drought indices and soil moisture data. However, due to the low resolution of the dataset (4 km), the importance of soil moisture as a factor was not fully reflected. In research conducted by Yahia et al. (2023), to improve the resolution of soil moisture, temperature vegetation dryness index (TVDI), perpendicular drought index (PDI), optical trapezoid model (OPTRM), and modified normalized difference water index (MNDWI) were used as proxies for soil moisture. These variables, along with a Gaussian Naive Bayes (GNB) classifier, were employed to generate wildfire risk maps. Beyond, the NDVI can be used to estimate soil moisture anoma-

lies (Tucker, 1979; Liu et al., 2010). However, when modeling moisture anomalies using NDVI, it can only directly detect surface soil moisture, and a physical or empirical relationship must be employed to further obtain deep soil moisture. In addition, it is worth noting that the estimation of soil moisture based on optical or SAR remote sensing imagery still faces significant challenges. This is due to the influence of factors such as tree canopy obstruction, absorption, reflection, and scattering, which result in a mixed signal received by the sensor containing information on both soil and fuel moisture (Pelletier et al., 2023).

4.5. Wildfire historical records

Wildfire historical records are indispensable in all studies and form the data foundation for wildfire risk prediction models. The sources and scales of wildfire historical records vary widely. For example, in Canada, many provinces, cities, or forestry management agencies maintain their own wildfire historical records. Additionally, the Canadian Natural Resources Department maintains its wildfire information data system, such as the Canadian Wildfire Information System. Specifically, commonly used public global or regional scale wildfire historical records include the National Burned Area Composite dataset (NBAC), the Canadian National Fire Database (CNFDB), the National Institute for Space Research database (INPE), the Fire Planning and Analysis Fire Occurrence Database (FPA-FOD), the Global Fire Emissions Database (GFED), and FireCII. In regions without systematic wildfire records, most studies use satellite-derived thermal anomalies or wildfire products from MODIS, Suomi-National Polar-orbiting Partnership (S-NPP), National Oceanic and Atmospheric Administration (NOAA) VIIRS, GOES, AVHRR, Sentinel, Landsat, Himawari, FY-4, among others.

Specifically, Pelletier et al. (2023) used the NBAC dataset from the Canadian Forest Service for their study on the northern Canadian forest peatlands. Liang et al. (2019) utilized the CNFDB dataset for wildfire research in Alberta, Canada, which includes fire location (latitude and longitude points), ignition date, extinguishment date, burned area, and cause of fire provided by provincial, regional, and the Canadian Parks Service firefighting agencies. Rubí and Gondim (2023) employed the INPE database for their study in the Federal District of Brazil. The INPE fire database is primarily based on thermal anomaly data collected from satellites such as AQUA, TERRA, NOAAs-15, 16, 17, 18, and 19, METEOSAT-02, and GOES-12. It covers the geographic location and timing of fires (latitude, longitude, and date/time) since the year 2000. Wang et al. (2021) used the FPA-FOD dataset to assess the drivers of wildfires in the continental United States, which includes discovery date, burned area, and geographical location (longitude and latitude) of wildfires from 1992 to 2020. The dataset intentionally excludes prescribed fires that escaped and required suppression response. Despite the possibility of missing data on smaller fires, the omission is tolerable for analytical purposes since the largest 5% of all fires account for the majority of the burned area. Song and Wang (2020) utilized the Global Fire Emissions Database version 4.1 (GFEDv4) for predicting global monthly wildfire risks throughout the year. This dataset covers monthly wildfire areas globally from 1997 to 2016, with a spatial resolution of 0.25° x 0.25°. It also includes daily burned area data globally from August 2000 to 2015. Bakke et al. (2023) employed the FireCCI dataset in their study in Fenno-Scandinavia, Finland, which provides global-scale pixel products at spatial resolutions of 250m or 300m, or gridded products at a resolution of 0.25 x 0.25 degrees, with a temporal resolution equal to or less than one month.

Satellite thermal anomaly products are commonly used in wildfire risk prediction studies, such as the MODIS MCD14 and MCD64A1 products (Giglio et al., 2003, 2016). The MCD14 series dataset has a spatial and temporal resolution of 1km and one day, respectively, offering a long time series (from 2006 to present) and providing near-real-time wildfire hotspot maps. The MCD64A1 dataset has a higher spatial resolution of 500m, although it does not offer near-real-time products. In specific studies, Abdollahi and Pradhan (2023) used MODIS fire and thermal anomaly data in their wildfire prediction research in the Gippsland region of Victoria, Australia, along with the NPWS Fire History - Wildfire and Prescribed Burning dataset provided by the New South Wales Department of Climate Change, Energy, the Environment, and Water. Ghorbanzadeh et al. (2019) acquired polygon data for 34 wildfire areas through field surveys and assessed data for the forested regions of Amol County, Mazandaran Province, northern Iran using MODIS data. Jaafari et al. (2019) and Nami et al. (2018) also employed historical data, field surveys, and validated using MODIS hotspot products in their studies in the western Zagros ecoregion and the northern Hyrcanian ecoregion of Iran, respectively, to enhance the reliability of historical data. Kanwal et al. (2023) in their study in Pakistan used MODIS data from the Fire Information for Resource Management System (FIRMS) as wildfire historical data, setting a 60% confidence threshold to reduce false alarm errors.

Additionally, some studies argue that MODIS products may overlook fires that are smaller in scale or shorter in duration (Hantson et al., 2013; Benali et al., 2016; Fusco et al., 2019; Ying et al., 2019). Therefore, other satellite data are also used in conjunction with MODIS data or independently for fire hotspot detection or burned area mapping, and for generating historical datasets. For instance, the study by Zhang et al. (2021) used the GFED dataset, which utilizes the MODIS MCD64A1 dataset and VNPIMG14ML dataset (Schroeder et al., 2014; Hall et al., 2024), to mitigate errors of commission and omission in agricultural fire detection in the MODIS dataset. Moreover, some studies have begun to explore using other high temporal resolution data to build global or regional wildfire detection datasets, such as the Sea and Land Surface Temperature Radiometer (SLSTR) sensor on Sentinel-3A/B (Xu and Wooster, 2023).

4.6. Frequency of different data utilization

In the "Fuel Conditions" category, the NDVI is the most frequently utilized variable, with a frequency of 27, underscoring NDVI's critical role in assessing vegetation health and fuel availability. Other significant variables include Tree Species, which appears 8 times, and LAI and Vegetation Type, each

Climate and meteorological conditions

Temperature, Wind, Precipitation, Humidity, Moisture, Evapotranspiration, Fuel moisture code, Radiation, Drought, Vapor pressure, Pressure, Aridity, Lighting, Heat flux, Albedo, Water deficit, Summer duration, Frost daily frequency, Number of dry-storm days, Soil water retention

Fuel conditions

NDVI, Tree species, LAI, Vegetation type, Fractional vegetation cover, Canopy cover, Forest land density, NDII, GNDVI, Brightness, Greenness, Wetness, Fuel type, Fuel load, Vegetation cover density, FWI, Forest age, Hereafter annual biomass, Hereafter perennial biomass, Canopy height, Build-up index, Gross stem volume, EVI, NDVIW, NDVIT, SAVI, Shrub biomass load, Quadratic mean diameter, Stand dominant height, Stand basal area, Stand structure, Fuel model

Terrain & hydrological attributes

Slope, Aspect, Elevation, Plan curvature, TWI, Latitude, Landform, Longitude, Illumination, Hill shadow, Soil bulk density, Soil taxonomy, Soil texture, Topographic position index, Valley depth, Stream power index, Soil type, Surface roughness

Socio-economic variables

LULC, Road proximity, Settlement proximity, River proximity, Population density, Road density, Railway proximity, Recreation area distribution, GDP, Distance to cropland, Distance to anthropogenic features, Non-forested area distance, Powerline, Agriculture area, Village density, Road distribution, Railway distribution, Settlement distribution, Nightlight intensity, Travel speed, WUI, Road carrying capacity, Availability of wildfire suppression resource
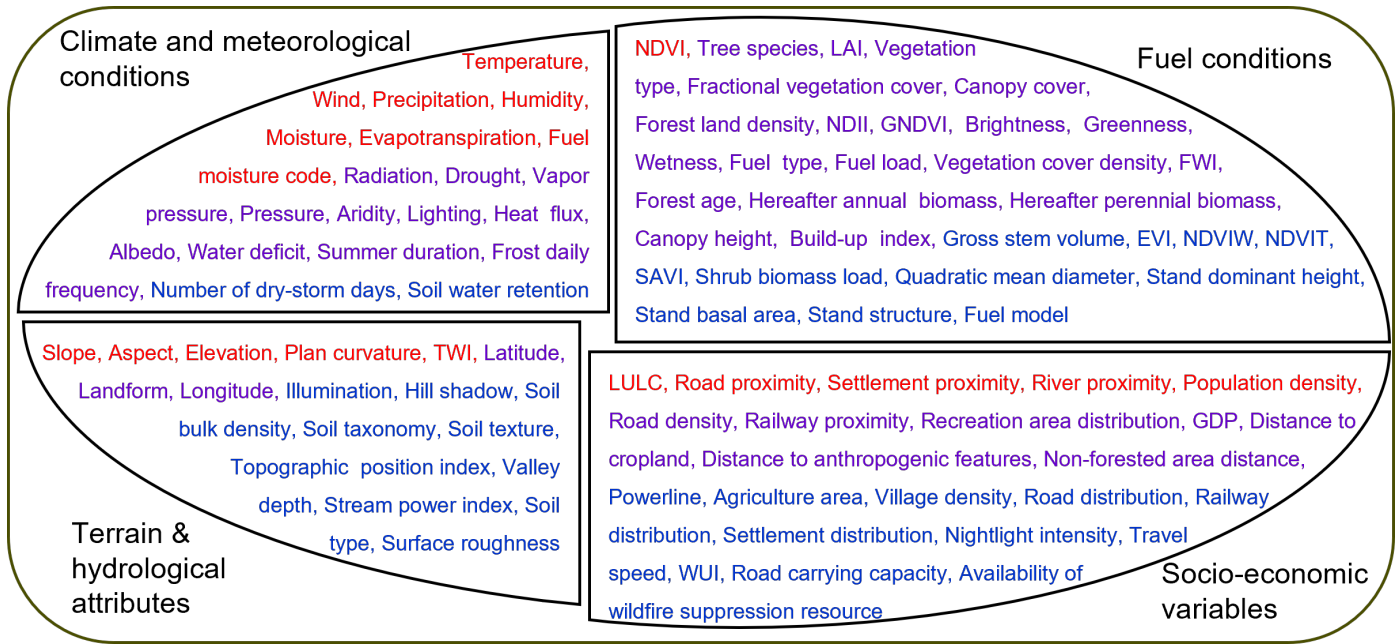
Figure 3: Feature utilization frequencies is classified into four categories: fuel conditions, weather and climate conditions, socio-economic variables, and terrain and hydrological attributes. The color scheme in this visual representation signifies the prevalence of these features, with red, green, and blue denoting utilization frequencies exceeding 20, 10, and 0 occurrences, respectively.

with a frequency of 6. These variables are essential for understanding the characteristics of biomass that contribute to wildfire risk. The presence of numerous variables with lower frequencies, such as Enhanced Vegetation Index (EVI) and NDWI, each used only once, highlights the complexity of this category. This diversity of variables reflects the multifaceted nature of fuel dynamics, requiring a broad range of factors to be considered in fire risk modeling, as depicted in Fig. 3(a).

In the "Climate and Weather Conditions" category, Temperature emerges as the dominant variable, with a frequency of 65. Precipitation follows closely with 53 occurrences, and Wind is also significantly utilized, with a frequency of 42. These variables are fundamental in understanding fire behavior, particularly in their influence on fire ignition, spread, and intensity. Humidity, used 27 times, and Moisture, used 16 times, further contribute to this category, reflecting the central role of atmospheric conditions in fire risk assessments. Other variables, such as Fuel Moisture Code, utilized 11 times, and Vapor Pressure, with 9 occurrences, are less frequently employed but remain crucial in specific contexts. The data presented in Fig. 3(b) emphasizes that climate variables, particularly Temperature and Precipitation, are among the most critical factors in fire dynamics, with a wide array of related variables also contributing to detailed climatic modeling.

Land Use and Land Cover (LULC) stands out as the most frequently utilized socio-economic variable, appearing 32 times, underscoring its importance in assessing how human activities and changes in land use influence fire risk. Road Proximity, with 23 occurrences, and Settlement Proximity, with 18, follow, indicating the significance of infrastructure and human settlement patterns in fire studies. Population Density, appearing 16 times, and Road Density, with a frequency of 4, also play

roles, although to a lesser extent. The data in Fig. 3(c) suggest that while variables like Gross Domestic Product (GDP), used 5 times, and Distance to Cropland, also used 5 times, are relevant, they are more context-specific. This analysis indicates that socio-economic factors are essential for understanding the human impact on fire dynamics, particularly in areas where land use and human infrastructure intersect with natural landscapes.

In the "Terrain and Hydrological Features" category, Slope is the most frequently used variable, appearing 46 times. This reflects the critical role of slope in influencing fire spread and intensity. Aspect, with a frequency of 34, and Elevation, with 32, are also key factors in understanding how topography affects fire behavior. These variables are particularly important in regions with complex terrain, where physical landscape features significantly impact fire dynamics. Plan Curvature, used 11 times, and TWI, used 10 times, are less frequently applied but remain relevant in specific contexts, often related to hydrological modeling. Other variables like Latitude, used 5 times, and Landform, with 3 occurrences, indicate their more specialized application. The analysis of these features highlights that while terrain and hydrological factors are crucial for understanding the physical environment's impact on fires, certain variables like Slope, Aspect, and Elevation consistently prove to be more influential.

Overall, when comparing the categories, climate and weather conditions emerge as the most frequently utilized, with Temperature and Precipitation leading the way. Fuel conditions follow closely, with NDVI being the most prominent indicator of vegetation health and fuel availability. Socio-economic factors, while important, are used more selectively, with LULC, Road Proximity, and Settlement Proximity being the primary variables. Finally, terrain and hydrological features, particularly

Slope, Aspect, and Elevation, are critical for understanding how the physical landscape influences fire behavior. However, it is worth noting that the frequency of use of the aforementioned features is not solely dependent on their importance but also on their ease of availability. For example, in the "Fuel Conditions" category, NDVI is more readily accessible compared to other features; similarly, variables like Temperature, LULC, Slope, Aspect, and Elevation are also more easily obtained.

4.7. Open-source wildfire spread prediction datasets

With the growing reliance on machine learning methods for wildfire risk prediction, the need for standardized datasets to establish, evaluate, and compare models has become evident. To address this, several open-source wildfire spread datasets have been released, providing varying spatial, temporal, and thematic coverage for research. These datasets support the development of machine learning-based wildfire risk prediction models and offer standardized benchmarks for evaluating model generalization.

The datasets presented in Table.2, including FireCube (Prapas et al., 2022; Kondylatos et al., 2023), Next Day Wildfire Spread (Huot et al., 2022), WildfireDB (Singla et al., 2020), WildfireSpreadTS (Gerard et al., 2023), CFSDS (Barber et al., 2024), and SeasFire Cube (Alonso et al., 2023), encompass various factors critical to wildfire spread prediction. These factors include spatial-temporal coverage of fuel conditions, climate and weather conditions, socio-economic factors, terrain, and historical records. Each dataset differs in the spatial-temporal coverage, and resolution of these factors, providing diverse perspectives and data for wildfire modeling.

First, the datasets vary significantly in their spatial and temporal resolutions. For instance, FireCube and Next Day Wildfire Spread focus on coarse-resolution data with a spatial coverage of 1 km for daily observations. WildfireDB offers more localized coverage at 375 m but over a broader temporal range (2012-2018). The CFSDS dataset provides highly detailed data at 180m resolution, though its temporal span is longer (2002-2021). SeasFire Cube offers the broadest coverage globally, albeit at a coarser resolution of 0.25 degrees and 8-day intervals.

Regarding fuel conditions, the datasets primarily utilize vegetation indices such as MODIS EVI and NDVI. FireCube combines MODIS EVI, LAI, and NDVI to provide a detailed view of vegetation. Similarly, Next Day Wildfire Spread and WildfireSpreadTS rely on VIIRS NDVI, offering 8-day data at 500m resolution. WildfireDB stands out by incorporating LANDS-FIRE data, which includes specific details like canopy base density and height, providing a more comprehensive fuel description, although at a lower temporal resolution. CFSDS uses specialized Canadian forest inventory data, adding complexity by considering forest composition and peatland presence.

For climate and weather conditions, most datasets rely on re-analysis products. FireCube integrates ERA5-Land data, covering a broad range of climatic variables, including temperature, precipitation, and soil moisture. Next Day Wildfire Spread and WildfireSpreadTS use GRIDMET data for similar parameters, with WildfireSpreadTS further incorporating Global Forecast System data for temperature and wind predictions. WildfireDB

uses NOAA Ground Station data, focusing on ground-based observations, which may offer more accuracy but less spatial coverage.

The inclusion of socio-economic factors varies widely among the datasets. FireCube incorporates multiple socio-economic variables, including LULC, population distribution, and proximity to roads and waterways, offering a comprehensive view of human impact on wildfire spread. Next Day Wildfire Spread and SeasFire Cube focus solely on population density, while WildfireSpreadTS considers only LULC. WildfireDB does not include socio-economic factors, limiting its ability to account for human influences on wildfire ignition.

Terrain and hydrological features are primarily derived from DEM products, providing data on elevation, slope, and aspect. FireCube uses the EU-DEM, while Next Day Wildfire Spread and WildfireSpreadTS rely on SRTM products. CFSDS employs ASTER data for terrain variables, while WildfireDB and SeasFire Cube use various unspecified sources for elevation data. Despite different products, all datasets achieve similar resolutions of around 30m.

Historical wildfire records are crucial for validating wildfire spread and risk prediction models. FireCube incorporates both MODIS and EFFIS records, offering detailed fire occurrence accounts. Next Day Wildfire Spread relies on the MOD14A1 product, while WildfireDB and WildfireSpreadTS use VIIRS data at 375m resolution. SeasFire Cube integrates multiple sources, including FireCCI, GWIS, and MODIS, to provide a comprehensive historical dataset, though at a coarser resolution.

It is important to note that we only consider time series wildfire observation datasets stored in a spatially explicit format and encompassing multiple wildfire impact factors. Datasets that do not have a clearly defined spatial distribution (Sayad et al., 2019), datasets containing only historical wildfire extent (Short, 2014; Andela et al., 2019; Artés et al., 2019; Lizundia-Loiola et al., 2020; Hargrove et al., 2022; Gincheva et al., 2024), fire detection datasets (Chino et al., 2015; Toulouse et al., 2017; Shamsoshoara et al., 2020; Mou et al., 2020; El-Madafri et al., 2023), and simulation datasets (Wang et al., 2024), are not included.

It is worth noting that, as shown in Table.2, the number of available open-source wildfire spread datasets is limited, with most coverage concentrated in the United States and Mediterranean, while other regions, such as the wildfire-prone Canada and Australia, are underrepresented. Additionally, some studies using these datasets have overly simplistic considerations of fuel conditions, such as relying solely on vegetation indices as proxies. This approach fails to accurately and comprehensively describe the state of fuel load, moisture content, and continuity. Similarly, using MODIS or VIIRS to record historical burned areas lacks precision, potentially overlooking small fire spots, offering low spatial and temporal resolution, and being prone to false alarms (Zubkova et al., 2024). Furthermore, there is a lack of quantitative evaluation of how the accuracy of different products impacts the accuracy of wildfire spread predictions.

Table 2: Open-access Wildfire Spread Prediction Datasets

Dataset	Spatial-temporal Coverage and Resolution	Fuel Conditions	Climate and Weather Conditions	Socio-economic Factors	Terrain and Hydrological Features	Historical Records
FireCube	Greece and Eastern Mediterranean (1 km), 2009-2021 (Daily)	MODIS: EVI (MOD13A2, 16d, 1 km), LAI (MOD12A2H, 500 m, 8d), NDVI (16d, 1 km)	ERA5-Land: Avg, max, min of dew point temperature, relative humidity, surface pressure, air temperature, total precipitation, U and V wind components (1d, 9 km); MODIS: Total evapotranspiration (MOD16A2, 8d, 500 m), day and night LST (MOD11A1, 1d, 1 km), FPAR (8d, 500 m); Europe-EDO: Soil moisture index anomaly, Soil moisture (10d, 5 km)	Corine Land Cover: LULC (2006, 2012, 2018); WorldPop: Population density (2009-2021), distance from roads, distance from waterways	EU-DEM: Elevation, aspect, roughness, slope (2016, 30m)	EFFIS & MODIS: Ignition points, burn area, daily fire count
Next Day Wildfire Spread	USA (1 km), 2012-2020 (Daily)	VIIRS: NDVI (VNP13A1) (8d, 500 m)	GRIDMET: Wind direction and speed, minimum and maximum temperatures, humidity, precipitation (1d, 4 km), drought index, energy release component (ERC) (5d, 4 km)	GPWv4: Population density (1 km)	SRTM: Elevation (30 m)	MODIS: MOD14A1 V6 (1d, 1 km)
WildfireDB	California, USA (375 m), 2012-2018 (Daily)	LANDFIRE: Canopy base density, base height, cover, canopy height, and existing vegetation cover, height, and type (2012, 2014, 2016, 30 m)	NOAA Ground Station Data: Temperature (avg, min, max), total precipitation, atmospheric pressure, and wind speed (1d, 5787 stations)		Elevation and slope (2016, 30 m)	VIIRS: Active Fire (1d, 375 m)
WildfireSpreadTS	USA, 2018-2021 (Daily)	VIIRS: EVI (VNP13A1) and NDVI (8d, 500 m)	GRIDMET: Surface temperature (min, max), total precipitation, wind speed and direction, specific humidity, Palmer Drought Severity Index (PDSI) (1d, 4.6 km); Global Forecast System: Temperature and wind (avg, direction, speed) (1d, 27.83 km)	MODIS: Land Cover Type Yearly Global product (MCD12Q1, 1y, 500 m)	SRTM: Elevation, slope, and aspect (2013, 30m)	VIIRS: Active Fire (1d, 375 m)
CFSDS	Canada (180m), 2002-2021 (Daily)	SCNFI: Percentage deciduous component, percentage coniferous component, biomass in tonnes/ha, and crown closure percentage (30m); Peatland presence and class (250m); ERA5-Land: FFMC, DMC, DC, ISI, BUI (1d, 0.1deg)	ERA5-Land: The maximum daily temperature, 24 hr precipitation, noon wind speed, noon relative humidity, and 24hr maximum vapour pressure deficit (1d, 0.1deg)	CanVec Transport Features: Road density, distance to road	ASTER: elevation, slope, aspect, and TWI; National Ecological Framework for Canada: Ecozones	National Burned Area Composite; VIIRS: VNP14IMGT (375m); MODIS: MCD14ML (1km)
SeasFire Cube	Global (0.25deg), 2001-2021 (8d)	MODIS: NDVI (MCD15A2, 8d, 500m), LAI (MOD13C1, 16d, 5600m)	ERA5: Mean sea level pressure, total precipitation, relative humidity, vapor pressure deficit, sea surface temperature, skin temperature, wind speed, 2m temperature (mean, min, max), surface net solar radiation, surface net solar radation, surface solar radation downward, volumetric soil water (level1-4), land-sea mask (0.25deg); Copernicus CEMS: Drought code (max, avg), fire weather index (max, avg) (1d, 0.25deg); CAMS: Carbon dioxide emmision from wildfire, fire radative power (1d, 0.1deg); MODIS: LST (MOD11C1, 1d, 0.05deg); NOAA climate indices	GPWv4: Population density (1km); ESA CCI: LULC (7d, 300m/1km); Biomes		FireCCI: Burned areas (area, mask, fraction) (250m/300m); GFED: Burned areas (area, mask) (1month, 0.25deg); GWIS: Burned areas (area, mask)

5. Features Collinearity and Attribution

The relationships between wildfires and driving environmental factors have always been a focal point in wildfire prediction research. Considering the interplay between wildfire occurrences and factors such as fuel conditions, climate, meteorological variables, topographical features, and human activities is crucial. However, including highly collinear independent variables in a model may impair its performance (Chen et al., 2019). Moreover, when two or more independent variables are significantly correlated, they provide redundant information in regression analysis, complicating the interpretation of each variable's individual impact on the dependent variable. Therefore, it is essential to examine the collinearity and contributions of different features to provide predictive insights for wildfire management.

5.1. Assessment of Feature Collinearity

Common metrics for assessing data collinearity in wildfire risk prediction include the Variance Inflation Factor (VIF) and tolerance (Hair Jr et al., 1986; Liao and Valliant, 2012a). VIF quantifies how much the variance of a regression coefficient is inflated due to collinearity, while tolerance represents the proportion of variance in a predictor that is not explained by other predictors in the model. The formulas are as follows:

$$\begin{cases} \text{VIF} = \frac{1}{\text{Tolerance}} \\ \text{Tolerance} = 1 - R^2 \end{cases} \tag{8}$$

where R^2 is the coefficient of determination when the predictor is regressed against all other predictors. A high VIF value (typically above 10) or a low tolerance value (below 0.1) indicates significant collinearity, suggesting that one predictor is largely explained by others.

For example, Nami et al. (2018) conducted a collinearity analysis using VIF and tolerance in their study on wildfire risk mapping in the northern Hyrcanian ecoregion of Iran. They found significant collinearity between the TWI and slope with other parameters, leading to their exclusion from subsequent modeling efforts.

Similarly, Jaafari et al. (2019) assessed the collinearity of various predictors using VIF and tolerance in their study in the western Zagros ecoregion of Iran. They discovered that the VIF values for TWI and slope were below 5, and tolerance values were above 0.2, indicating insignificant collinearity with other predictors (Liao and Valliant, 2012b). Hong et al. (2019), in their modeling of wildfire susceptibility in Huichang County, China, used VIF and tolerance to assess the collinearity of multiple predictors and found no significant collinearity between slope and other features.

In another study, Li et al. (2022a) examined the drivers of forest fires in Yunnan Province, China, and found that six meteorological factors (daily average atmospheric pressure, daily minimum atmospheric pressure, daily average temperature, daily minimum temperature, daily average surface temperature, and daily minimum surface temperature) had VIF values exceeding 10 and tolerance values below 0.1, indicating significant correlations. The study also used the Pearson correlation algorithm to analyze the correlations of the remaining variables, finding a correlation coefficient of 0.77 between surface temperature and air temperature.

Similarly, in their wildfire prediction model for Maui Island in Hawaii, Rezaie et al. (2023) analyzed the correlation and collinearity among independent variables (altitude, slope, aspect, valley depth, TWI, slope length, plan curvature, distance from rivers, distance from roads, NDVI, average monthly rainfall, average annual wind speed, and average annual temperature) using Pearson correlation coefficients, VIF, and tolerance. They found the strongest correlations between average annual temperature and altitude, and the most significant collinearity between average annual temperature and distance from roads. However, the collinearity and correlations among all variables were not statistically significant.

In summary, different studies have shown varying levels of collinearity between features, indicating that no consistent conclusion can be drawn regarding the relationships between specific features across different wildfire risk prediction models.

5.2. Feature attribution

In wildfire risk prediction algorithms, explicit methods can predict wildfire risk by defining the contributions of different features to the ignition and spread of wildfires. However, these methods often have poor fitting capabilities and struggle to handle the nonlinearity and randomness characteristic of wildfire risk prediction tasks. On the other hand, machine learning models, such as deep learning and ensemble learning models, can extract patterns from highly complex datasets and demonstrate superior predictive performance. However, their decision-making processes are opaque, earning them the label of "black box models."

In wildfire risk prediction, this lack of transparency undermines the credibility of the predictions and makes it difficult for researchers and fire management agencies to understand the factors inducing wildfire ignition and spread. This, in turn, hinders the understanding of wildfire mechanisms and the prevention and management of wildfires. The interpretation of the decision-making process in machine learning models is generally referred to as explainable AI (XAI). In this paper, we define XAI as the attribution of causal responsibility or feature attribution (Josephson and Josephson, 1996), as XAI in wildfire risk prediction algorithms mainly focuses on explaining the influence of different wildfire risk factors on model predictions. Currently, common XAI methods in wildfire risk prediction include Permutation Feature Importance (PFI), Explainable Feature Engineering (Ali et al., 2023), and SHapley Additive exPlanations (SHAP).

Firstly, PFI quantitatively analyzes feature importance by randomly permuting each feature and evaluating the change in model performance. For example, Rubí and Gondim (2023) used PFI to assess the contributions of meteorological, fuel, terrain, and socioeconomic factors in models such as ANN, SVM, NB, KNN, LR, LogLR, and AdaBoost in their study in the

Federal District of Brazil. They found that analyzing individual variables might lead to contradictory results. For instance, NDVI was more important for models like AdaBoost and ANN, whereas its influence was relatively low or nonexistent in other models such as LR and SVM. This finding highlights the necessity of considering multiple variables in predictive modeling and the varying importance of different models. Additionally, Shadrin et al. (2024a) evaluated the impact of specific feature values on the final test results by setting them to zero during model testing. Similarly, Chen et al. (2024b) calculated the importance of each feature by measuring the variation in prediction error when feature values were perturbed.

Secondly, Explainable Feature Engineering (Ali et al., 2023) methods have also been applied to wildfire risk prediction. For example, Rezaie et al. (2023) used the Information Gain Ratio (IGR) to select the optimal subset of variables in their wildfire prediction model for Maui, Hawaii. They found that the distance to roads had the highest IGR value of 0.903, indicating its significant impact on mapping fire-prone areas. The next important variables were annual average temperature (0.724), elevation (0.715), and slope (0.665). Similarly, Zhang et al. (2019) used IGR to evaluate the importance of different factors in assessing forest fire risk in Yunnan Province, China. They found that temperature and wind speed contributed the most to the risk, while the importance of distance to roads and rivers was the lowest. In another example, Hong et al. (2019) modeled the spatial distribution of wildfire susceptibility in Huichang County, China, using the Analytic Hierarchy Process to assign weights to a logistic regression model and found that elevation was the most influential indicator of fire occurrence, followed by land use, NDVI, and distance to human settlements.

Finally, SHAP analysis (Shapley, 1953), which is based on game theory, is more commonly used, especially for explaining complex models, because it considers both feature importance and feature interactions while offering higher computational efficiency. SHAP explains the impact of each feature on model predictions by assigning SHAP values to them. Common SHAP methods include Kernel SHAP, Deep SHAP, and Tree SHAP (Lundberg and Lee, 2017). For instance, to address the challenge of explaining deep learning models, Abdollahi and Pradhan (2023) introduced SHAP to study the contribution of different features to the model. The authors found that relatively high NDVI, temperature, and elevation, as well as relatively low NDMI and precipitation, increased wildfire risk, while relatively high humidity reduced this risk. They also identified elevation, NDMI, and precipitation as the three most critical factors influencing wildfire occurrence.

Similarly, Wang et al. (2021) used SHAP to evaluate the drivers of large-scale wildfires in the contiguous United States and found that coordinate variables (including longitude and latitude) and local meteorological variables (such as ERC, RH, temperature, and VPD) were important predictors of burned area across the domain. This is because coordinate variables carry crucial geographic information that broadly reflects climate, land use, human activity, and other key geographic factors, helping to distinguish temporal characteristics of different fire regimes and thus aiding in predicting burned areas. Using

SHAP's local interpretability, they also explained the driving factors of large burned areas in different regions and months within the contiguous United States. For example, ERC was identified as the most important indicator of large burned areas in the western US.

Iban and Aksu (2024) conducted a local SHAP importance analysis in the İzmir region of Turkey and found that wind speed, LULC, slope, temperature, and NDVI were the five most important influencing factors. Wind speeds above 3.5 m/s, forests in LULC, slopes greater than 8 degrees, annual average temperatures above 14 degrees, and NDVI values below 0.2 all promoted wildfires, while higher NDVI reduced the likelihood of wildfire occurrence. In the wildfire risk assessment for Hawai'i Island, Tran et al. (2024) considered 14 factors, including meteorological, topographic, anthropogenic, and vegetation-related variables: elevation, slope, aspect, plan curvature, profile curvature, TWI, valley depth, annual average wind speed, NDVI, annual average precipitation, annual average temperature, distance to roads, distance to rivers, and land use. SHAP analysis revealed that the distance from a road, annual temperature, and elevation were the most influential factors, with wildfire risk increasing as distance from roads decreased and temperature increased. Additionally, low- to mid-elevation areas were generally associated with a higher likelihood of fire occurrence due to their relatively high temperatures and accessibility.

Kondylatos et al. (2022) conducted a SHAP analysis for the Eastern Mediterranean region and found that soil moisture index, humidity indicators, temperature variables, NDVI, and wind speed were the most important factors influencing wildfire risk. Notably, the study found that the relationship between NDVI and fire risk was U-shaped, meaning that both very low and very high NDVI levels were associated with lower wildfire risk.

Currently, explainability analysis in wildfire prediction faces several challenges, such as insufficient exploration of alternative explainability methods, dependency on models and explanation techniques, unclear attribution analysis, and the uncertainty of the explanations provided.

Firstly, techniques like activation maximization analysis (Erhan et al., 2009), Partial Dependence Plot (Greenwell et al., 2017), Integrated Gradients, and other additive feature attribution methods beyond SHAP—such as Local Interpretable Model-agnostic Explanations (LIME), DeepLIFT, and Layer-Wise Relevance Propagation—have not been adequately explored in the context of wildfire risk prediction. The limited application of these XAI methods leaves gaps in our understanding of how different approaches might enhance model transparency in this domain.

Secondly, many studies select the best-performing model through comparative experiments and then conduct explainability analysis based on that model. The explanations provided by these methods often estimate how a specific ML model derives predictions from input data (Good and Hardin, 2012). However, treating these analyses as direct insights into real-world phenomena can lead to misleading or erroneous conclusions, particularly if the model's learned decision rules do not align with

the actual underlying data relationships (Jiang et al., 2024a). For instance, using a single explainability method to interpret different ML models, or using different explainability methods to interpret the same ML model, might result in varying or even contradictory observations. Therefore, any inferences drawn from these post-hoc explanations should be approached with caution (Ploton et al., 2020).

Furthermore, wildfire prediction studies often employ multiple input variables and model the relationships between these variables and wildfire risk. While such models may perform well, they do not necessarily explain whether causal relationships exist between independent and dependent variables, as the modeled relationships often result from correlations among various features (Rogger et al., 2017; Molnar et al., 2020). An example of this is multicollinearity among features, which is very common in Earth sciences due to the highly complex interactions and interdependencies between geological, meteorological, ecological, and additional factors in the Earth system (Jiang et al., 2024a). For instance, features commonly used in wildfire risk prediction, such as NDVI, soil moisture, precipitation, temperature, and evapotranspiration, often exhibit complex interrelationships. A crucial condition for ML models to produce valid causal effect estimates is that their input variables must be independent of unobserved confounders. Therefore, in most cases, ML should not be considered a definitive source of causal knowledge (Jiang et al., 2024a). This highlights the need for further research into the application of causal ML (Tesch et al., 2023) in wildfire risk prediction.

Lastly, while explainability analysis enhances model transparency, these explanations are still subject to uncertainty, unreliability, and low robustness due to the influence of model selection, choice of explainability method, and the correlations within input data (Jiang et al., 2024a). Thus, it is important to explore how insights from related fields can be applied to quantitatively assess the validity of explainability analysis results in wildfire risk assessment models (Bommer et al., 2024).

6. Fire danger rating systems

Wildfire hazards are characterized by strong nonlinearity and randomness, making it challenging to calculate wildfire risk using simple statistical models. At the same time, developing accurate physical models to precisely estimate the relationship between wildfire risk and factors such as fuel, weather, terrain, and human activities is also difficult. Consequently, adaptive and scientifically grounded wildfire rating systems have been proposed and have remained a critical component of global fire management for over a century (Hardy and Hardy, 2007). These systems have evolved from early dryness indices into complex models that predict spatial and temporal variations in wildfire ignition probability, spread rate, and heat release/fire intensity by characterizing the interactions among fuel, weather, and terrain. This evolution has provided crucial decision support for wildfire management at local, regional, national, and sometimes even international scales (Jolly et al., 2024). According to Zacharakis and Tsihrintzis (2023a), com-

monly used wildfire danger rating models today include systems developed in Canada, the United States, and Australia.
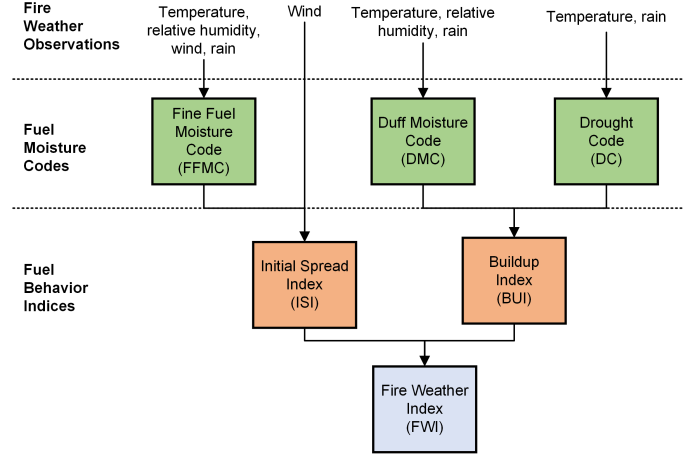

Figure 4: Illustration of FWI system.

For example, Canada developed a meteorology-based fire danger rating method in 1968, known as the Canadian Forest Fire Danger Rating System (CFFDRS). This system comprises four main subsystems: the FWI, Fire Behavior Prediction (FBP), Fire Occurrence Prediction (FOP), and Auxiliary Fuel Moisture (AFM) (Van Wagner et al., 1974; Stocks et al., 1989b; Lawson and Armitage, 2008). Among these, the FWI system is the most widely used (Fig. 4). The FWI system, based on the theory of time lag and equilibrium moisture content, calculates changes in fuel moisture codes (i.e., Fine Fuel Moisture Code (FFMC), Duff Moisture Code (DMC), and Drought Code (DC)) and fire behavior indices (i.e., Initial Spread Index (ISI) and Buildup Index (BI)) according to weather conditions. These indices are then used to classify potential wildfire danger levels in forests based on the moisture content of fuels at different locations or sizes (Stocks et al., 1989a).

Furthermore, the FWI system has been proven applicable in other countries or regions (Alexander, 1989; Fogarty et al., 1998; López et al., 2002; Taylor and Alexander, 2006; Dimitrakopoulos et al., 2011; Giannakopoulos et al., 2012). For instance, (Viegas et al., 1999) demonstrated that the FWI system is suitable for Europe, and it has been widely adopted by European countries as the optimal method for assessing wildfire danger (San-Miguel-Ayanz et al., 2018). Some countries have also developed their wildfire rating systems based on the FWI system. For example, South Africa developed the Lowveld Fire Danger Index (LFDI) based on the FWI, as shown in Eq. (4). Research has proven that this index is also applicable to the Mediterranean region of Greece (Cavalcante et al., 2021). New Zealand's wildfire rating system incorporates the Rate of Spread (ROS) and Head Fire Intensity (HFI) into the FWI system (Gregor and David, 2017). Similarly, Groot et al. (2007) developed an early wildfire risk warning system for Indonesia and Malaysia based on the FWI and FBP subsystems of the CFFDRS. This system includes a smoke potential indicator

based on the DC, an ignition potential indicator based on the FFMC, and a difficulty of control indicator for grassland fires based on the ISI of the FWI System. The ISI-based indicator was developed using the grass fuel model of the FBP System, along with a standard grass fuel load and curing level estimated from previous Indonesian studies.

In comparison, the United States National Fire Danger Rating System (USNFDRS) (Deeming, 1972) evaluates fire risk by considering not only meteorological factors, but also various terrain types, fuel types, and fuel models. By inputting meteorological data, fuel moisture, and terrain into the model, four output components are obtained: the Spread Component (SC), Energy Release Component (ERC), Burning Index, and Ignition Component (IC). The first three indices, based on combustion physics, correspond to fire behavior characteristics, while the IC provides an estimate of fire danger levels (Zacharakis and Tsihrintzis, 2023a). The system was revised in 1978 and 1988 to address issues such as poor response to prolonged droughts and the inability to capture real-time fuel dynamics (Deeming et al., 1977) and inadequate performance in moist environments (Burgan, 1988). Recently, Jolly et al. (2024) updated the US-NFDRS introduced in 1988 by emphasizing the provision of more detailed, fuel-type-dependent combustion condition assessments, proposing a new fuel moisture model, and simplifying the fuel model.

Figure 5: Illustration of AFDRS system (Hollis et al., 2024).

In Australia, widely used fire danger rating systems include the early McArthur's Forest Fire Danger Model (McArthur, 1966, 1967, 1973; Noble et al., 1980) and the Australia Fire Danger Rating System (AFDRS) introduced in 2022. The first system derived fire danger ratings based on predicted wildfire spread rates and the difficulty of suppressing fires burning in grasslands (McArthur, 1960) and dry sclerophyll forests (McArthur, 1958). This index, originally designed for eastern Australia in the 1950s and 1960s, underwent several revisions,

culminating in the final Mark 5 version. Depending on vegetation type, it is divided into the Forest Fire Danger Index (FFDI) and the Grassland Fire Danger Index (GFDI) (Zacharakis and Tsihrintzis, 2023a). However, Hollis et al. (2024) pointed out that McArthur's Forest Fire Danger Model could not utilize contemporary knowledge of fire behavior, such as new wildfire spread models (Cheney et al., 2012; Cruz et al., 2013; Anderson et al., 2015) and fire-atmosphere coupling (Mills and McCaw, 2010), and that its application has extended beyond its original design (Fogarty et al., 2010). Additionally, this system, with its low spatial resolution, cannot provide specific location-based wildfire risk recommendations. Finally, FFDI and GFDI cannot describe wildfire risks for vegetation types like shrublands (Anderson et al., 2015) and Spinifex (Burrows et al., 2018). Therefore, scientists and representatives from fire and land management agencies across all Australian jurisdictions collaborated to develop the new AFDRS. This system includes six factors: weather, fuel, fire behavior, ignition likelihood, suppression capability, and fire impact. It is designed for consistent and standardized use across Australia's states and territories, eliminating the need for ad hoc local adjustments. The main components of this system are shown in Fig. (5), which determines fire danger by establishing a forward spread rate model (Cruz et al., 2015) and incorporating hourly forecast weather data on a 1.5 km grid across Australia, as well as fuel type and fuel state, to calculate forward spread rates, fireline intensity, and other relevant information.

7. Deep Learning Methods for Wildfire Risk Prediction

Currently, methods for wildfire risk prediction include fire rating systems, statistical models, traditional machine learning, and deep learning approaches. Fire rating systems, extensively applied in regions like Canada, the USA, and Australia, combine empirical and mathematical modeling based on fluid dynamics, combustion, energy transfer, and factors like fuel, weather, and terrain conditions (Rezaie et al., 2023; Mell et al., 2007). These models are interpretable and generalizable, especially when training data is limited. However, their reliance on assumptions regarding soil moisture, fuel load, landscape structure, and other factors can reduce prediction accuracy (Bar Massada et al., 2011).

For more specific analyses, statistical models use regression to establish relationships between wildfire risks and influencing factors such as fuel conditions, meteorology, and terrain. While simple and interpretable, they have limited capacity for handling the nonlinearity and randomness typical in wildfire prediction tasks (Li et al., 2022a). Traditional machine learning methods (e.g., Random Forests, SVM, ensemble models, and Bayesian methods) improve upon statistical models by using data-driven techniques and manual feature engineering to identify patterns in historical fire data. These methods operate non-parametrically and are better suited for non-linearities (Oliveira et al., 2021b), yet they present challenges in variable interpretation compared to statistical approaches. Over the past decade, the focus in wildfire modeling has shifted from statistical algorithms to machine learning (Jain et al., 2020; Oliveira

et al., 2021b). Decision tree methods, such as Random Forests (RF), are particularly popular due to their accuracy and interpretability, as highlighted in studies like Malik et al. (2021). Nevertheless, some researchers argue that no single model is universally superior, suggesting a need for model combinations to enhance accuracy (Jaafari et al., 2019; Razavi Termeh et al., 2018).

Traditional machine learning methods often use shallow architectures that fail to exploit spatial patterns effectively, limiting feature extraction and classification accuracy (Zhang et al., 2018). In contrast, deep learning models, despite their higher data requirements, can automatically extract complex features through hierarchical structures, reducing the need for manual feature engineering and enhancing generalizability. Their larger parameter capacity also allows them to manage large datasets and minimize overfitting risks. Although deep learning has become increasingly popular for wildfire risk prediction, reviews such as Jain et al. (2020) and Zacharakis and Tsihrintzis (2023b) have only partially covered models like Recurrent Neural Networks (RNNs) and CNNs without a comprehensive systematization.

This section reviews the latest advancements in deep learning-based wildfire risk prediction models, which are typically framed as segmentation or classification tasks. These models use historical wildfire data and influencing factors as inputs, with future wildfire occurrences or risk levels as ground truth. Models are categorized into time series prediction, image semantic segmentation and classification, and spatio-temporal prediction. Time series models (RNN, LSTM, Gated recurrent unit (GRU), Transformers) predict wildfire risks using 1D feature vectors, while semantic segmentation and classification models (CNNs, Transformers) employ 2D feature maps to produce 2D risk predictions. Spatio-temporal models integrate these approaches using 2D time series data.

Deep learning models for spatio-temporal prediction often combine CNNs, Transformers, GCNs, and graph neural networks (GNNs) with RNNs, LSTMs, or GRUs, enhancing resolution with higher-resolution data over extended sequences. Despite advances in GPU technology supporting larger data scales, these models still struggle with efficiency and large spatiotemporal scales compared to newer models like Mamba (Gu and Dao, 2024). Additionally, many models use multi-branch networks that rely solely on images or nodes, missing the benefits of multimodal approaches like incorporating textual information.

While previous reviews (e.g., Jain et al. (2020); Zacharakis and Tsihrintzis (2023b)) have examined machine learning in wildfire science, they often omit post-processing techniques essential for converting model outputs into actionable risk information. Directly using these outputs can be misleading due to class imbalances and variability between models. This section also introduces methods for classifying and calibrating deep learning wildfire risk predictions to address these challenges.

7.1. Wildfire risk rating and probability calibration

Although Jain et al. (2020); Zacharakis and Tsihrintzis (2023b) systematically reviewed the application of various ma-

chine learning methods in wildfire risk research, they did not provide a description of the post-processing techniques required to convert the predictions of machine learning models into actual wildfire risk. Directly using the output of these models as the probability of wildfire risk may lack theoretical foundation and stability. This is because wildfire historical data sets typically suffer from severe class imbalance, where the spatial and temporal scope of fire occurrences is considerably smaller compared to non-fire events. To expedite model convergence, many machine learning datasets are often constructed with a balanced class ratio, typically 1:1, 1:1.5, or 1:2 (Huot et al., 2021; Kondylatos et al., 2022) between fire and non-fire instances. This may lead to an overestimation of false positives during model evaluation (Bakke et al., 2023). However, actual wildfire risk probabilities are usually much lower. For example, in wildfire risk assessments for the Mediterranean region and the United States, Ager et al. (2014a) and Preisler et al. (2004) used probabilities in the thousandths range, respectively.

Using the probability output of machine learning models as wildfire risk could be misleading to non-experts. Therefore, many studies convert continuous wildfire risk probabilities into risk levels to support wildfire management, such as conveying public warnings and guiding fire suppression measures. Among the methods for risk level classification, the Jenks natural breaks classification (Jenks and Caspall, 1971) is most commonly used. For instance, Xie et al. (2022) trained an ensemble machine learning model using binary wildfire ignition records and then classified the predicted probabilities into five groups using the Jenks method. Similarly, Iban and Sekertekin (2022) and Moayedi and Khasmakhi (2023) also classified the hazard maps generated by machine learning models into five categories using the Jenks method. Along the same lines, Chen et al. (2024c) used the Jenks method to divide the estimated potential rate of spread and fire radiative power into five levels for wildfire risk assessment.

Other methods have also been employed for risk level classification. For example, Liang et al. (2019) used the Kennard-Stone method combined with standardized duration and fire size to categorize the wildfire risk predicted by an RNN into five levels. Jalilian and Jouibary (2023) applied natural discontinuity classification methods to group the probabilities predicted by machine learning models into three classes. Bjånes et al. (2021) and Chicas et al. (2022) divided the wildfire ignition probability maps produced by the models into five levels using an equal-interval method, with intervals of 0.2. Similarly, Trucchia et al. (2022) manually defined five risk levels.

Furthermore, some methods aim to recalibrate probability outputs to obtain actual wildfire risk probabilities. For instance, Pelletier et al. (2023) constructed a semi-balanced dataset for model training, in which the numbers of burned and never-burned sites were 3,268 and 60,146, respectively. They then used the method proposed by Elkan (2001) (Eq. (9)) to convert the wildfire probabilities predicted by a time series XGBoost model into actual probability values:

$$p' = \frac{BR2 \times (p - p \times BR1)}{BR1 - p \times BR1 + p \times BR2 - BR1 \times BR2} \quad (9)$$

where p' represents the revised probability for a prediction, $BR1$ stands for the base rate of the predicted probability estimates (the average of predicted probabilities for that class), and $BR2$ denotes the base rate of the actual probability estimates derived from the target population. Here, the target population refers to the average probability of fires across all observations within the training dataset, including the unburned observations that were not utilized in model training. Similarly, Phelps and Woolford (2021) used the function proposed by Dal Pozzolo et al. (2015) to correct the neural network's probability output:

$$p_k = \frac{\pi \gamma_k}{\pi \gamma_k - \gamma_k + 1} \tag{10}$$

where p_k and γ_k represent the wildfire probabilities modeled from the original and sampled distributions, respectively, and π denotes the proportion of non-fire observations sampled.

7.2. Time Series Prediction

7.2.1. Recurrent Neural Networks

As discussed in previous sections, the occurrence and spread of wildfires are influenced by various factors, including meteorological conditions, fuel status, and historical wildfire data. These factors exhibit cumulative effects. Therefore, utilizing time series data enables models to capture the gradual changes in influencing factors, thus facilitating the prediction of future wildfire risks. The most classical methods in time series prediction tasks are RNNs, which include RNN, LSTM, and GRU.

RNN is a basic neural network structure with recurrent connections, designed to process sequential data. As shown in Fig. 6, it integrates input from the current time step with output from the previous time step to model and predict sequence data. A simple RNN structure consists of an input layer, hidden layer, and output layer. Input data are time series data, i.e., feature vectors with dimensions $f \times d$. The hidden layer includes several hidden units, where each hidden unit outputs $\mathbf{h}_{t-m}$, the 'memory' at any intermediate time $t - m(m < n)$, as a weighted sum of its previous 'memory' and current time step's input features:

$$\begin{cases} \mathbf{h}_{t-m} = \sigma_h(\mathbf{W}_{IN}\mathbf{x}_{t-m} + \mathbf{W}_{HH}\mathbf{h}_{t-(m+1)} + \mathbf{b}_h) \\ \mathbf{y}_{t-m} = \sigma_o(\mathbf{W}_{HO}\mathbf{h}_{t-m} + \mathbf{b}_o) \end{cases} \tag{11}$$

where $\mathbf{W}_{IN}$ and $\mathbf{W}_{HH}$ represent weight matrices for processing input to the hidden layer and from hidden layer to hidden layer, respectively; $\mathbf{x}_{t-m}$ and $\mathbf{h}_{t-(m+1)}$ represent the input feature vector at time $t - m$ and 'memory' from the previous time step, respectively; $\mathbf{b}_h$ and $\mathbf{b}_o$ represent bias vectors for the hidden units and output layer, respectively. Ultimately, the output $\mathbf{y}_t$ at time $(t - m(m < n))$ is a weighted sum of all hidden units. By iteratively repeating the above process, each timestep of the entire time series data $(t - n, t - (n - 1), ..., t - 1)$ is predicted. Finally, a loss function (Eq. 12) estimates the discrepancy between the prediction and labels, and model weight parameters are iteratively updated through backpropagation.

$$\iota(\mathbf{y}, \mathbf{GT}) = \sum_{t-n}^{t-1} \iota_t((\mathbf{y}_t, \mathbf{GT}_t) \tag{12}$$

where $\mathbf{GT}_t$ represents the label value at time t.
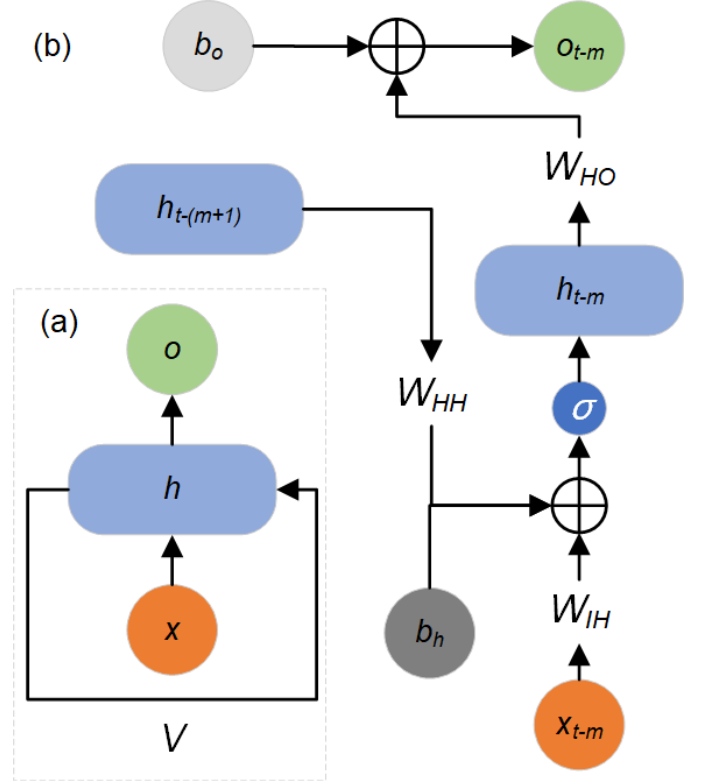

Figure 6: The architecture of RNN where (a) and (b) represent the overall architecture and detailed hiddenlayer calculation.

Classic RNN networks and their variants have been employed in wildfire risk prediction. For instance, Cheng and Wang (2008) designed a spatiotemporal Elman RNN-based prediction framework integrating historical wildfire and weather data to predict the annual average burned area in Canadian forests. Experiments demonstrated a prediction error of less than 0.5ha on areas of 500ha, validating the feasibility of using RNN for fire prediction. Similarly, a comparative study of ten artificial neural networks (ANNs) based on meteorological data for predicting wildfire incidence in Australia found that Elman RNN exhibited the best performance, with average accuracy, sensitivity, and specificity exceeding 93% (Dutta et al., 2013). Furthermore, a network composed of a dynamic autoencoder and RNN was used to predict the next month's burned area in five U.S. regions, where the dynamic autoencoder was employed to transform multidimensional time series data into RNN input features, and dual decoders were used for predicting fire spot likelihood over different time spans, i.e., one week and one month. Comparative experiments showed that their method was slightly superior to comparative methods, generative network, and GRU (Chavalithumrong et al., 2021).

While Jain et al. (2020) and others have highlighted the limited use of classical RNNs, our findings are consistent with these observations. The underutilization of RNNs may be attributed to their difficulties in handling long sequence data, where they are prone to gradient vanishing or exploding, making it challenging to capture long-term dependencies (Hochreiter, 1997; Gers et al., 2000). To address these issues, LSTM
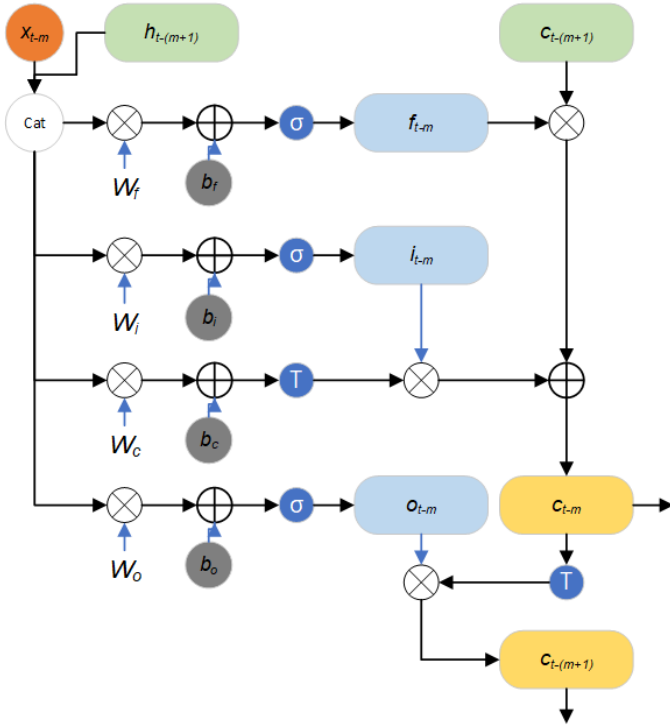
Figure 7: Schematic diagram of the LSTM architecture illustrating the flow of data through input, forget, and output gates.

networks were developed. As illustrated in Fig. 7, LSTMs incorporate three gating units: input gate, forget gate, and output gate, which control the flow and retention of information. These gates have trainable weights and decide whether to pass, forget, or output information based on the current input and the output from the previous time steps. This gating mechanism effectively resolves the issues of vanishing and exploding gradients, thereby enabling better handling of long sequences and capturing of long-term dependencies. Consequently, LSTMs are more prevalently applied in wildfire risk prediction than classical RNNs. The specific configuration of an LSTM cell is depicted in Fig. 7b and Eq.13 (Monner and Reggia, 2012; Liang et al., 2019).

- For the forget gate (f_t), the output from the hidden layer of the previous timestep $h_{t-(m+1)}$ is concatenated with the input features at the current timestep x_{t-m}, then multiplied by the forget gate weight matrix W_f and added to the forget gate bias b_f. This sum is then passed through a sigmoid activation function σ, resulting in the output of the forget gate.

- The input gate has two branches. The first branch (i_t) is similar to the forget gate, involving concatenation followed by multiplication with the input gate weight matrix W_i and addition of the bias b_i. The second branch uses a weight matrix W_c that represents candidate cell states to multiply with the concatenated result, added to the bias b_c, and activated using the hyperbolic tangent function tanh.

The outputs of these two branches are multiplied together and added to the product of the forget gate output and the output of the input gate from the previous timestep ($c_{t-(m+1)}$) to produce the output for the current timestep (c_{t-m}).

- Similarly, the output gate includes two branches. The first branch multiplies the concatenated input by the output gate weight matrix W_o, adds the bias b_o, and activates it. For the second branch, the output of the input gate at the current timestep (c_t) is activated using tanh. The final output of the hidden layer at the current timestep is obtained by multiplying the results of these two branches.

$$f_{t-m} = \sigma \left(W_f \cdot [h_{t-(m+1)}, x_{t-m}] + b_f \right) \tag{13}$$

$$i_{t-m} = \sigma \left(W_i \cdot [h_{t-(m+1)}, x_{t-m}] + b_i \right) \tag{14}$$

$$c_{t-m} = f_t \odot c_{t-1} + i_t \odot \tanh \left(W_c \cdot [h_{t-1}, x_t] + b_c \right) \tag{15}$$

$$o_{t-m} = \sigma \left(W_o \cdot [h_{t-(m+1)}, x_{t-m}] + b_o \right) \tag{16}$$

$$h_{t-m} = o_{t-m} \odot \tanh(c_{t-m}) \tag{17}$$

Studies utilizing LSTM for wildfire risk prediction often model various risk factors, including weather and climate conditions, fuel conditions, and socio-economic factors. For instance, Liang et al. (2019) found that LSTM outperformed RNN and Back Propagation Neural Network (BPNN) in predicting the class of wildfires in Alberta, Canada, based on meteorological conditions, achieving an overall accuracy of 90.9%. Similar findings were reported by Natekar et al. (2021), who assessed the wildfire risk in Indian forests using meteorological parameters and LSTM methods. The accuracy and RMSE were 94.77% and 37.5%, respectively, surpassing other benchmark methods like CNN and SVM. Additionally, Kondylatos et al. (2022) compared RF, XGBoost, and deep learning methods (LSTM and ConvLSTM) and found that deep learning significantly outperformed traditional machine learning methods in predicting next day wildfires in the Mediterranean using ERA5-Land meteorological data, MODIS NDVI, and diurnal LST data along with soil moisture, terrain data, land cover types, and distances from infrastructure. Li et al. (2023b) further integrated attention mechanisms and deep learning interpretability into an LSTM network, using monthly-scale climate, socio-economic, fuel variables, and oceanic indices to predict short-term (1–4 months) and long-term (5–8 months) wildfire burning areas in tropical regions. Experimental results demonstrated that the enhanced LSTM model outperformed traditional machine learning methods and the baseline LSTM model. Furthermore, Cheng et al. (2022, 2024) have combined LSTM with reduced order modeling techniques to improve the prediction accuracy for both regional and global scale wildfire systems. Additionally, interpretability analysis revealed that precipitation and vapor pressure deficit were critical driving factors, while oceanic indices provided more significant contributions to long-term wildfire burning area predictions.

Moreover, some studies use only historical wildfire occurrence data combined with LSTM to predict future regional

wildfire risks. For example, Kadir et al. (2023) used historical MODIS wildfire data combined with LSTM to predict the spatiotemporal distribution of wildfires in Indonesia for the following year, with a success rate exceeding 90% and an error rate of only 6.94%. Notably, to reduce the amount of data, this study grouped several days' worth of data into single days for training and testing. Furthermore, Hu et al. (2023) combined LSTM with autoencoders, using historical wildfire data from 1992-2018 to predict the level of wildfire occurrence in high-risk areas such as California. The autoencoder was employed to generalize wildfire events from the overall dataset, enhancing the accuracy of anomaly event predictions through reconstruction errors.

Similar to the LSTM, the GRU addresses the challenges of gradient vanishing and explosion inherent in traditional RNNs and involving the gate mechanisms. GRU reduces the number of gating units found in LSTM, containing only a reset gate and an update gate, as shown in Eq.18, which simplifies the model architecture and enhances computational efficiency (Chung et al., 2014). The structure of the GRU model is depicted in Fig. 8. Despite its simpler configuration, GRU retains the capability to model long-term dependencies with performance comparable to that of LSTM (Jin et al., 2020a).

$$r_t = \sigma(W_r[h_{t-1}, x_t] + b_r) \tag{18}$$

$$z_t = \sigma(W_z[h_{t-1}, x_t] + b_z) \tag{19}$$

$$\tilde{h}_t = \tanh(W_h[r_t h_{t-1}, x_t] + b_h) \tag{20}$$

$$h_t = (1 - z_t)h_{t-1} + z_t\tilde{h}_t \tag{21}$$

Studies such as Dzulhijjah et al. (2023) have compared the performance of LSTM, BiLSTM, CNN-LSTM, Stacked-LSTM, and GRU in predicting wildfire risk in the Indonesian region of Kalimantan, finding that GRU slightly outperforms the other models, though the advantage is not significant. In contrast, Gopu et al. (2023) observed better results with LSTM in a comparative study of wildfire prediction in the Montesinho Natural Park, Portugal. Additionally, Chavalithumrong et al. (2021) found that models integrating a dynamic autoencoder with RNN outperformed standard GRU models, suggesting that enhanced RNN architectures can offer superior performance.

7.2.2. Transformers for Wildfire Risk Prediction

Transformers utilize multi-head self-attention mechanisms to calculate attention scores, enabling them to capture dependencies at any position within the sequence (Vaswani et al., 2017). The attention mechanism is defined as:

$$\text{Attention}(Q, K, V) = \text{softmax}\left(\frac{QK^T}{\sqrt{d_k}}\right)V \tag{22}$$

where d_k represents the dimensionality of the key. The architecture of a Transformer, as illustrated in Fig. 9, comprises encoders, decoders, positional encoding, and multiple attention mechanisms.
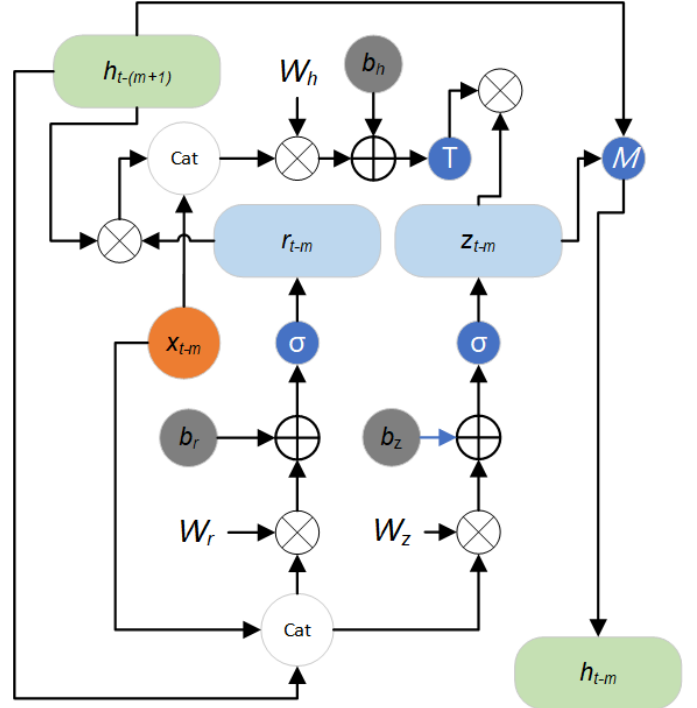

Figure 8: Schematic representation of the GRU architecture highlighting its reset and update gates.

Transformers operate on sequences transformed into tokens, which are then embedded with positional encoding to maintain the sequence order absent in traditional RNNs. The sequence of embedded tokens is processed by the encoder, which transforms it into a context vector using layers of multi-head self-attention and feed-forward networks. The decoder similarly processes the context vector to predict the output sequence. The ability of Transformers to process sequence data without relying on sequential processing allows for parallel computation during training, significantly speeding up the learning process compared to RNNs (Vaswani et al., 2017). This makes them particularly effective for long-sequence predictions or complex scenarios requiring modelling of long-range dependencies (Zerveas et al., 2021; Prapas et al., 2023).

Transformers have been adapted for several predictive tasks in wildfire risk prediction. For example, Miao et al. (2023) developed a Transformer model with a window-based attention mechanism to predict forest fire risks in Chongli District, Beijing, China, using time-series data of meteorological, topographical, vegetation, and anthropogenic factors. The window mechanism confines attention to a fixed-size window centered on each element, reducing computational complexity and memory usage. Similarly, Cao et al. (2024) employed a Transformer to predict next-day wildfire risks in Quanzhou County, Guangxi Province, China, based on three days of meteorological, topographical, and human activity data. The model's performance, analyzed using IGR, outperformed LSTM, RNN, and SVM in terms of generalization, noise resistance, and overfitting mitigation.

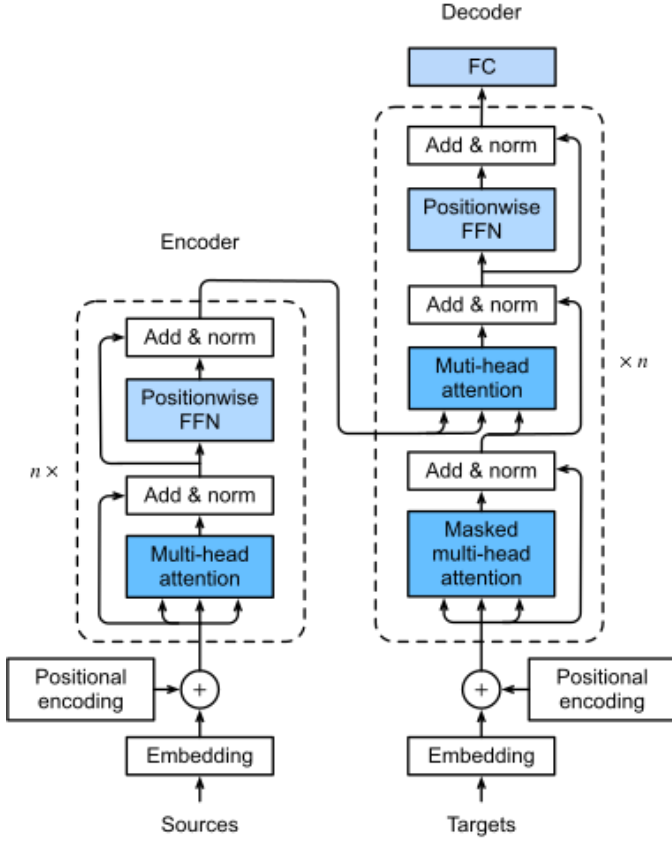From the analysis above, it is evident that both RNNs and

Figure 9: Schematic diagram of the Transformer architecture, highlighting its main components.

GRUs are less frequently used in wildfire risk prediction, which includes forecasting occurrences, susceptibility, and spread. In contrast, LSTM networks have a relatively higher usage rate. RNNs, compared to LSTMs, are particularly challenged by issues such as vanishing and exploding gradients and exhibit weaker capabilities in modeling long-distance dependencies. Furthermore, although some studies argue that GRUs perform comparably to LSTMs (Viswanathan et al., 2019; Gao et al., 2020; Liu et al., 2021a; Gao et al., 2021; Zarzycki and Ławryńczuk, 2022), the simplified structure of GRUs may result in inferior performance when processing highly complex sequences or capturing intricate relationships (Cahuantzi et al., 2023), especially in wildfire risk prediction tasks that do not require high real-time processing capabilities or are intended for edge computing devices. Recently, however, with the advent of Transformers, these models are gaining popularity in wildfire risk prediction due to their complex architecture, larger parameter capacity, and the advantages of parallel computation.

7.3. Image Semantic Segmentation and Classification Methods

Although RNNs and Transformers excel at capturing temporal dependencies for sequence-to-sequence learning tasks, these methods primarily classify individual pixels' temporal sequence data. However, wildfire occurrences are not only influenced by local conditions but also by neighboring areas (e.g.,

wind propagation). When RNNs use 1D data inputs, the spatial structure of the image is often lost (Hu et al., 2020). Consequently, several studies have explored the use of image semantic segmentation and classification methods, such as CNNs, GNNs, and Transformers, to predict wildfire risk at time t using the influencing factors (e.g., fuel, weather) from time $t' < t$. These methods rely on 2D image inputs, which explicitly model the spatial dependencies of input features, while also implicitly modeling the influence of current driving factors on future wildfire risk by having different input features and predicted time steps. In wildfire risk prediction, CNNs are commonly used, with GNNs and Transformers increasingly adopted in recent studies.

7.3.1. Convolutional Neural Networks

CNNs are foundational network structures in deep learning, designed to extract local spatial features through convolution operations, making them well-suited for capturing the spatial information necessary for wildfire risk prediction, as shown in Fig.10. For example, Zhang et al. (2019) employed a modified AlexNet (Krizhevsky et al., 2012) using annual fire point maps and springtime mean influencing factors for Yunnan Province, China, to classify image patches as wildfire-prone areas. The model outputs a probability map of wildfire risk through softmax mapping in the final CNN layer. When comparing the CNN model's performance with RF, SVM, MLP, and kernel logistic regression models, the authors found that CNN achieved the highest overall accuracy. They also analyzed the contributions of various wildfire drivers using the information gain ratio, identifying temperature, wind speed, surface roughness, precipitation, and elevation as the most influential factors.

Building upon this, the authors extended the modified AlexNet to generate a global quarterly wildfire susceptibility map (Zhang et al., 2021). They compared its performance with MLP-2D, CNN-1D, and MLP-1D models, finding that CNN-2D and MLP-1D models outperformed CNN-1D and MLP-2D. Additionally, they applied an improved permutation importance (PI) method and partial dependence plots (PDP) to investigate the interpretability of the CNN-2D model. The PI analysis highlighted that maximum monthly temperature, soil temperature, NDVI, and soil moisture were significant factors affecting the model. Furthermore, PDP analysis revealed a negative relationship between cumulative precipitation and wildfire prob-
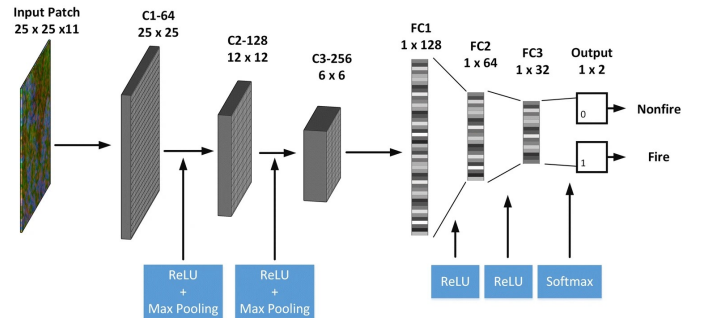

Figure 10: The architecture of CNN classification network where the center pixel is classified using surrounding information (Zhang et al., 2019).

ability, while maximum monthly temperature and soil temperature positively influenced wildfire occurrence.

Moreover, using a similar CNN approach, they predicted the spatiotemporal variation of wildfire risk under different climate scenarios, discovering that global warming would lead to an increase in burned areas and a northward shift of wildfire-prone regions (Zhang et al., 2024). In another study, Kanwal et al. (2023) explored CNN-1D and CNN-2D classification models along with other machine learning algorithms for evaluating seasonal wildfire risks in Pakistan, finding that CNN-2D outperformed CNN-1D and other machine learning algorithms.

In addition, some studies have employed deeper or structurally optimized CNN networks. For instance, Oak et al. (2024) utilized VGG16 with ReLU, BatchNorm, Dropout, and a sigmoid layer to predict wildfire susceptibility in Quebec, Canada. Comparative experiments demonstrated that this model outperformed other architectures like Xception, VGG16, ResNet50, and Inception V3. Similarly, Nur et al. (2022) applied a meta-heuristic optimization algorithm to fine-tune the hyperparameters of a CNN model for wildfire susceptibility mapping in the Plumas National Forest, USA. Their IGR analysis revealed that land use, drought index, and maximum temperature had the greatest impact on wildfire susceptibility, and the model's performance improved significantly after optimization. Likewise, (You et al., 2023) used particle swarm optimization to refine the structure and parameters of a CNN classification model for assessing annual forest fire risk across China, showing that this approach outperformed both standard CNN and traditional machine learning methods. Using SHAP for interpretability analysis, they identified NDVI, land cover, and temperature as the most significant factors.

Additionally, Eddin et al. (2023) introduced location information to the CNN by adding a separate convolution branch to differentiate between dynamic variables (those changing over time) and static variables (those that remain constant over the study period). To address the causal effects of static variables on dynamic ones, they incorporated a LOAN layer to adjust the activation maps in the dynamic branch based on static features. They also used sinusoidal encoding of Julian days to provide the model with explicit time information. Their experiments on the FireCube dataset, which covers parts of the Mediterranean (Prapas et al., 2022; Kondylatos et al., 2023), demonstrated that the proposed model's predictions of $t + 1$ wildfire spread outperformed baseline models, including LSTM, ConvLSTM, RF, and XGBoost. In a similar vein, Dong et al. (2024) proposed an architecture that models dynamic and static variables separately in the encoding phase, improving the accuracy in predicting fire radiative power.

Beyond classification-based methods, some studies have implemented end-to-end models for higher-resolution predictions. For example, Hodges and Lattimer (2019) proposed a deep convolutional inverse graphic network comprising convolution and deconvolution layers to simulate wildfire spread over homogeneous and heterogeneous landscapes for 6-hour and 24-hour intervals, demonstrating the high efficiency of CNNs in wildfire spread prediction. Similarly, Santopaolo et al. (2021) used an end-to-end CNN image segmentation model to predict wildfire risk in Sicily, Italy, and California, USA, based on driving factors from 8 days prior.

Furthermore, (Allaire et al., 2021) developed a hybrid architecture combining convolutional and fully connected layers to emulate the output of a numerical fire spread simulator based on the Rothermel model of fire propagation. Similarly, Bergado et al. (2021) designed an AllConvNet, a fully convolutional network, to predict wildfire burn probability for the next 7 days in Victoria, Australia. This model achieved higher prediction accuracy compared to logistic regression, SegNet, and MLP models. Feature extraction and normalization of logistic regression coefficients revealed that total rainfall, lightning density, and surface temperature were among the most influential variables.

Additionally, Li et al. (2023c) introduced spatial and channel attention mechanisms to enhance an end-to-end CNN model's focus on critical features while suppressing irrelevant ones for predicting the next moment's wildfire spread. This model also incorporated the burning map from the previous time step, outperforming other CNN models and ConvLSTM. Similarly, Shadrin et al. (2024b) used the MA-Net segmentation model, which includes position attention and multi-scale attention blocks, to predict wildfire extent for the next 1-5 days. Unlike previous studies, they included short-term weather forecasts along with various wildfire drivers. Experimental results showed that their model accurately predicted wildfire spread within 3 days, with the wind components, land cover, NDVI, EVI, and LAI being the most influential factors.

Lastly, Marjani et al. (2024a) combined CNN with atrous spatial pyramid pooling to model wildfires at different scales and shapes, adopting an end-to-end approach for next-day wildfire spread prediction. They used linear regression and Grad-CAM heatmap correlations to demonstrate how different dilation rates help extract both large-scale and small-scale wildfires. Similarly, Jiang et al. (2023) employed a three-branch network to process static DEM and fuel data, dynamic wind speed, temperature, humidity data, and the previous time step's wildfire status. Their experiments showed that this model's inference efficiency significantly surpassed that of cellular automata and Farsite models, accurately predicting burned areas in real wildfire scenarios.

7.3.2. Other Methods

In addition to CNNs, other image segmentation methods, such as GNNs and Transformers, have also been applied to wildfire risk prediction. GNNs, compared to CNNs, are better suited for handling non-Euclidean structured data (Asif et al., 2021), while Transformers' multi-head self-attention mechanisms are more effective in modeling long-range semantic dependencies within images (Vaswani et al., 2017). For example, Jiang et al. (2022) proposed using an irregular graph network to simulate wildfire spread in variable-scale landscapes, addressing the issue of fixed-grid data being unable to adaptively differentiate landscape heterogeneity. The model adjusts graph node density based on terrain complexity to achieve uniformity in nodes and edges at varying scales. Comparative experiments with cellular automata and FARSITE demonstrated that the proposed model exhibits competitive accuracy and efficiency.
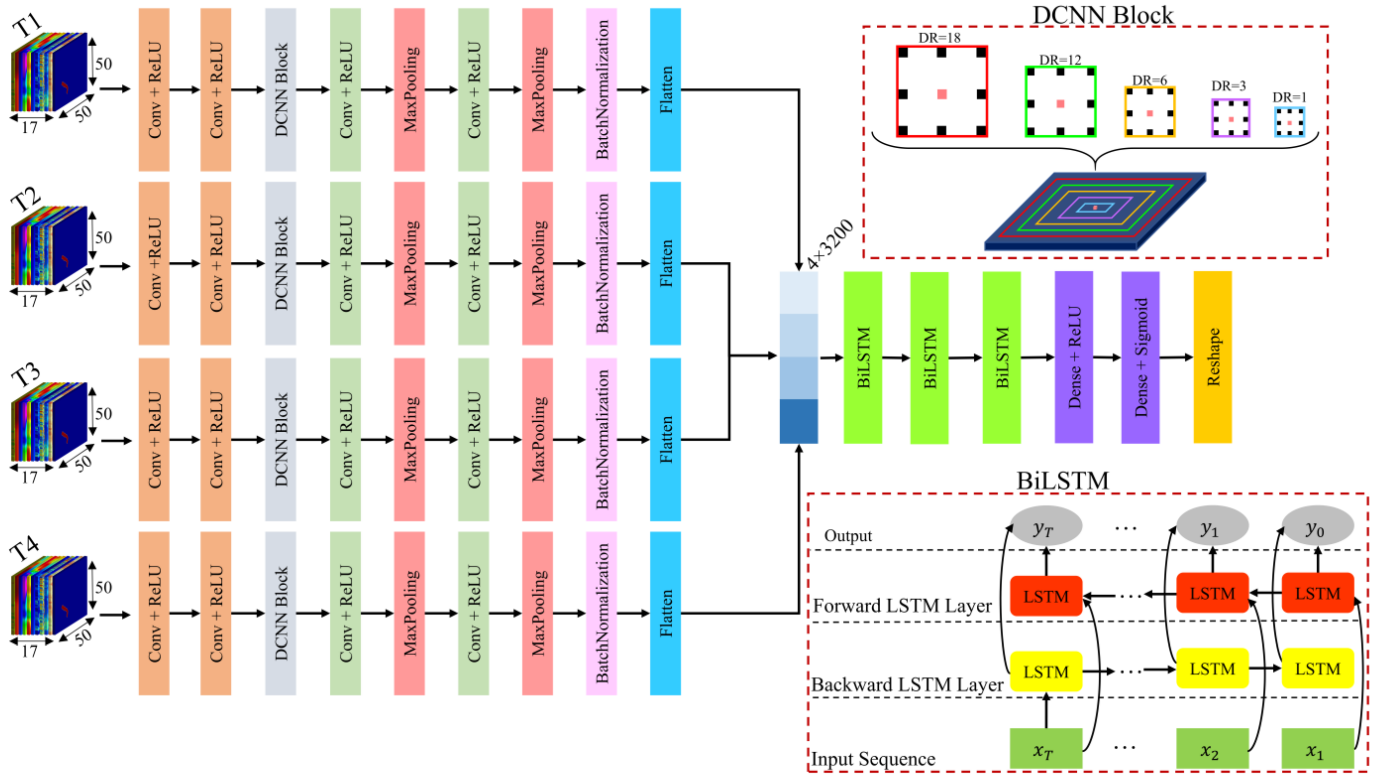
Figure 11: The sample architecture of the separated spatial and temporal modeling method (Marjani et al., 2024b)

Additionally, Chen et al. (2022) incorporated a GNN into the knowledge graph framework proposed by Ge et al. (2022) to enable automated learning and prediction of burn areas. Specifically, the model first constructs a knowledge graph in triples and uses RotaE to compute representation vectors for each entity. These entity vectors are associated with nodes in the graph, and the vectors are subsequently fed into the GNN to facilitate automatic updates. Finally, link prediction algorithms are employed to predict the burn areas associated with the recorded nodes. Experiments conducted in Portugal's Montesinho Natural Park demonstrated that this algorithm significantly outperformed traditional machine learning algorithms such as RF, SVM, and MLP.

Moreover, Li and Rad (2024) introduced spatial attention mechanisms and focal modulation into a U-shaped encoder-decoder network based on Transformers, known as Swin Unet. This end-to-end image segmentation approach utilizes wildfire risk driving factors from the previous day to predict wildfire risk for the following day across the continental United States. Comparative experiments using the extended Next Day Wildfire Spread dataset (Huot et al., 2022) showed that this model outperforms baseline models, including the standard UNet and Swin Unet. In addition, Prapas et al. (2023) introduced a Tele-ViT model that incorporates teleconnections to model long-range spatial interactions globally, aiming to predict subseasonal to seasonal wildfire patterns. This model combines fine-grained local-scale inputs with coarse-grained global-scale data, improving prediction accuracy for global wildfire patterns

up to four months in advance.

7.4. Spatiotemporal Prediction Methods

The previously discussed time series prediction methods and image segmentation/classification methods each have their strengths in capturing temporal and spatial dependencies, respectively. However, they are unable to simultaneously handle both spatial and temporal dependencies and capture the complex cross-spatiotemporal interaction patterns. For instance, Prapas et al. (2021) pointed out that focusing only on spatial scale modeling could overestimate a model's real-world performance. To integrate spatial structure and time series data, many studies have attempted to combine CNN, GNN, and Transformer models with RNN, LSTM, and GRU methods. This transforms the task of time series prediction or spatially localized optimization between consecutive wildfire states (Jiang et al., 2023) into spatiotemporal sequence prediction tasks. There are three primary approaches to achieving this combination: separated spatial and temporal modeling, coupled spatiotemporal modeling, and spatially enhanced coupled spatiotemporal modeling.

Specifically, separated spatial and temporal modeling involves abstracting spatial features into 1D feature vectors using spatial modeling methods, which are then input into temporal prediction models. Coupled spatiotemporal modeling converts the 1D tensors in RNNs into 3D tensors, incorporating spatial dimensions (rows and columns) and using convolutions or graphs (instead of weight matrix multiplication) to determine

a grid cell's future state based on its neighbors' current and past states. Lastly, spatially enhanced coupled spatiotemporal modeling introduces CNNs or graph-based methods to extract spatial features before the temporal modeling stage.

7.4.1. Separated Spatial and Temporal Modeling Methods

The approach of separately extracting spatial and temporal features is quite common. The structure of a typical spatiotemporal wildfire risk prediction model is illustrated in the Fig.11. In this model, multiple CNNs are employed to process multi-dimensional spatial images at each time step, with dimensionality reduction applied before feeding the data into the LSTM. Finally, the output from the LSTM is mapped to output probabilities using a CNN, or directly without it, along with the application of a sigmoid function.

For example, Jin et al. (2020b) proposed enhancing spatial feature extraction by employing CNNs and GCNs to extract spatial information, which is then passed through a feed-forward network (FFN) to unify the data into a 1D vector before being input into a GRU. The output 1D vector is then restored to its original size using deconvolution layers, performing urban fire situation prediction through an end-to-end semantic segmentation approach. Compared to traditional machine learning methods like RF, XGBoost, as well as GRUN and Conv-GRUN, this model showed significant performance improvements.

Similarly, Huot et al. (2021) used the Next Day Wildfire Spread dataset and categorized wildfire risk prediction into two tasks: next-day wildfire probability prediction and final burning area prediction. They experimented with four models: convolutional autoencoder and residual UNet for segmentation, and convolutional autoencoder and residual UNet combined with LSTM for temporal prediction. The results showed that, among the segmentation models, the convolutional autoencoder outperformed UNet. When combining the two models with LSTM for final burning area prediction, there was no significant performance difference between the models.

Zhang et al. (2022) designed and compared four deep neural networks with identical structures but different depths, combining 2D CNN and LSTM models to predict global monthly burned area maps using seven meteorological and two biophysical predictors from the previous 12 months. Each model reduced spatial dimensions through convolution, ReLU, and maxpooling operations and used fully connected layers to flatten the input patches into 1D features before feeding them into LSTM layers. The primary difference among the models was the number of CNN and LSTM layers. Ultimately, the CNN-LSTM network with two convolutional layers and two LSTM layers was selected for its balance of performance and efficiency. The results showed that the combination of convolution and LSTM methods outperformed standalone LSTM and CNN models.

Furthermore, Marjani et al. (2024b) combined CNN with bidirectional LSTM (BiLSTM) for a study in Australia, using wildfire driving factors from the previous four days and wildfire masks to predict next-day wildfire spread. The method first employed four CNN layers to extract spatial features, which were then flattened and input into a three-layer BiLSTM. The model produced binary outputs through dilated con-

volution, dense layers, and sigmoid activation functions. Comparative experiments demonstrated that this approach outperformed LSTM and Conv-LSTM methods, and the study also confirmed that using longer time steps improved prediction capabilities. In another study, Li et al. (2021b) not only introduced CNN before the LSTM but also incorporated an attention mechanism within the LSTM to assign different weights to the hidden states, reducing information loss and improving prediction accuracy. Applied in Portugal's Montesinho Natural Park, the model used various meteorological factors from the Fire Weather Index (FWI), historical burned areas, and time and location data to predict future wildfire risk. Comparisons with SVM, XGBoost, neural networks, RNN, and basic LSTM showed that deep learning models significantly outperformed machine learning models, with LSTM surpassing RNN and the CNN-attention LSTM performing best overall.

Rösch et al. (2024) applied graph convolution combined with GRU to develop Spatiotemporal Graph Neural Networks (ST-GNNs) for predicting wildfire spread in Portugal and the Mediterranean region. These models used an H3 grid system built from weather data, land cover, fuel types, DEM, and fire weather indices. However, the models exhibited high false positive rates.

In another study, Bhowmik et al. (2023) proposed a U-shaped LSTM network combining UNet and LSTM, using seven days of meteorological, environmental, vegetation, and geological data to predict wildfire risk. The U-shaped LSTM network first used a three-layer UNet encoder to extract semantic information, which was then flattened and input into an LSTM. The LSTM output was passed through a UNet decoder to produce end-to-end pixel-level predictions of wildfire heatmaps for the next 24 hours to two weeks. This model achieved over 97% accuracy in predicting large-scale wildfires in California, outperforming CNN models.

Similarly, Yoon and Voulgaris (2022) conducted research on wildfire risk prediction in the western United States, using a convolutional encoder to reduce the dimensionality of input time series data into vectors, which were then fed into a GRU model. A dual deconvolution decoder was designed to restore image size, predicting wildfire risk at different time steps (one, two, three, and four weeks). Compared to logistic regression, generative networks, and GRU, the combination of CNN and GRU showed significant performance improvement.

Lastly, Marjani et al. (2023) developed a spatiotemporal prediction model combining CNNs and RNNs to predict wildfire spread at time step $t + 1$, using environmental variables and burned areas from time steps t and $t - 1$. Data were divided into three blocks: hourly block (6-hour averaged wind speed and direction), daily block (temperature, precipitation, and wildfire burning map), and constant variables (land cover type, population, terrain, etc.). Each block was processed by CNNs and flattened into 1D features, then fed into RNNs with 64 and 31 neurons, respectively. Constant variables were similarly processed and flattened. The RNN outputs were concatenated with the constant variables and passed through convolution, reshape, dropout, and sigmoid layers to produce a burning probability map. Comparative results showed the superiority of this spa-

tiotemporal modeling approach over CNN and the deep convolutional inverse graphics network proposed by Hodges and Lattimer (2019). Additionally, experiments assessing data availability, noise addition, and Monte Carlo dropout were conducted to evaluate model uncertainty.

7.4.2. Coupled Spatiotemporal Modeling Methods

Compared to the separated spatial and temporal modeling methods, time-series prediction algorithms like ConvLSTM are also widely used. For instance, Burge et al. (2021) evaluated the feasibility of using ConvLSTM to simulate wildfire propagation dynamics on three simulated datasets with varying terrain, wind, humidity, and vegetation density distributions. The experiments demonstrated that ConvLSTM's predictive capability surpassed that of CNN. In the study by Prapas et al. (2021), which compared traditional machine learning models (RF), time series prediction algorithms (LSTM), image classification methods (CNN), and spatiotemporal modeling methods (ConvLSTM) for next-day wildfire danger prediction across Greece, several key findings emerged. For the RF model, training data was constructed by averaging each driving factor for the 10 days preceding the prediction date at each spatial location, resulting in a dataset with dimensions $f \times 1$, where f is the number of driving factors. The LSTM model used time series input, with data dimensions of $f \times t$, where t represents the time series length (10 days). For the image classification task, the spatial data was constructed as spatial patches centered on the target point, with dimensions $f \times h \times w$, where h and w are the height and width of the image. Lastly, for the spatiotemporal prediction task using ConvLSTM, the dataset dimensions were $f \times h \times w \times t$. The results showed that LSTM and ConvLSTM performed better than RF and CNN. Evaluating the binary classification results, LSTM outperformed ConvLSTM overall, but when using the area under the ROC curve as the evaluation metric, ConvLSTM slightly surpassed LSTM, with AUC scores of 0.926 and 0.920, respectively.

Similarly, Khalaf et al. (2024) compared ConvLSTM with cellular automata and FlamMap in simulating wildfire spread in Iran's Golestan National Park. The results indicated that ConvLSTM had the highest accuracy in predicting burned areas, but for spread rate evaluation, the CA algorithm performed better than the other models. In another study, Michail et al. (2024) compared temporally-enabled GNN, GRU, and ConvLSTM using the SeasFire Datacube (Alonso et al., 2023), finding that GNN was better at capturing global information, thus improving the understanding of complex patterns. The study also emphasized the importance of long time series information and a large receptive field in global wildfire risk prediction, especially for seasonal forecasts. It showed that longer input sequences provided more reliable predictions, and integrating spatial information to capture the spatiotemporal dynamics of wildfires improved model performance. Therefore, to improve predictions over longer forecast horizons, it is essential to consider a larger spatial receptive field.

Masrur and Yu (2023); Masrur et al. (2024) further proposed two ConvLSTM models based on spatiotemporal attention to predict wildfire spread over the next 10 days using the previous 10 days' NDVI, wind components, and soil moisture. These models were designed to capture local-to-global and short-to-long-term spatiotemporal dependencies. The models were trained and tested on both simulated and real-world datasets. Pairwise self-attention was used to calculate attention scores for input variables, while patchwise self-attention replaced convolution operations in ConvLSTM. Comparisons on simulated datasets showed that the pairwise self-attention model performed better, while the standard ConvLSTM outperformed the patchwise self-attention model. Moreover, they employed integrated gradients (Sundararajan et al., 2017) to enhance the interpretability of the contributions of time steps and driving factors to the model's predictions. The spatial patterns from integrated gradients confirmed the importance of capturing both local and global spatial dependencies. However, in real-world scenarios, replacing ConvLSTM's convolution operations with patchwise self-attention significantly improved the standard ConvLSTM's prediction accuracy and model transferability, surpassing even the pairwise self-attention ConvLSTM in both aspects.

7.4.3. Spatially Enhanced Coupled Spatiotemporal Modeling Methods

In addition, there are studies that combine convolutional layers with ConvLSTM to further emphasize spatial feature extraction. Similar to the separated spatial and temporal sequence wildfire risk prediction models, the spatially enhanced coupled spatiotemporal wildfire risk prediction method, as shown in the Fig.12, first extracts spatial features using convolution operations and reduces dimensionality before feeding the data into a ConvLSTM. For the output of the ConvLSTM, either a CNN is further applied followed by sigmoid mapping, or the sigmoid mapping is directly applied to the output.
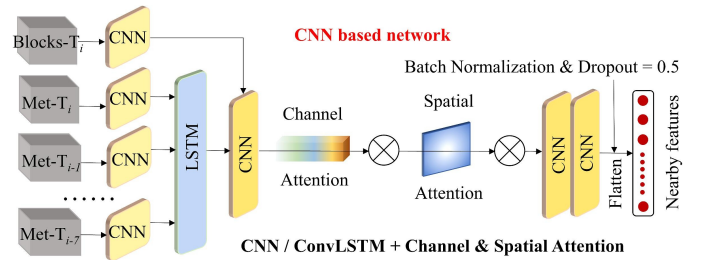

Figure 12: A typical spatial feature-enhanced coupled spatiotemporal wildfire risk prediction model proposed by He et al. (2024).

For example, Deng et al. (2023) used terrain, vegetation, climate, and human activity factors in Yunnan Province, China, to build a 3D CNN and ConvLSTM hybrid model for next-day wildfire prediction. During data preprocessing, Pearson correlation analysis was used to exclude the minimum and average temperatures from the dataset. Variance inflation factors and tolerance were then employed to assess multicollinearity among wildfire driving factors. Information gain ratio analysis revealed that precipitation and slope had the highest impact. In the proposed model, 3D CNN was primarily responsible for extracting spatial features and reducing the input patch's spatial

dimensions, which were then fed into a many-to-many ConvLSTM for prediction. The results showed that the combined 3D CNN and ConvLSTM model outperformed both standalone ConvLSTM and 3D CNN models.

Similarly, Burge et al. (2023) built upon the model proposed by Hodges and Lattimer (2019) by introducing fuel embedding layers and inserting ConvLSTM between the encoder and decoder for end-to-end wildfire spread simulation. The experimental results demonstrated that incorporating LSTM improved prediction accuracy.

Furthermore, Ji et al. (2024b), following a similar branch structure to Eddin et al. (2023) and Jiang et al. (2023), proposed a static location-aware model based on ConvLSTM. This model aimed to integrate global static features (sine and cosine values of longitude and latitude, along with climate variables) with dynamic variables (e.g., meteorological, human, and vegetation cover factors) to predict global wildfire probability on sub-seasonal to seasonal scales. In this model, global static features were first convolved and max-pooled, and the resulting feature maps were multiplied with climate variables for data fusion. SKNet was then employed to extract higher-order features, which were upsampled and merged with the static features generated by the encoder. Finally, upsampling and skip connections were used to restore the image size and supplement the spatial details of global static location variables. The dynamic and static variables were concatenated and input into ConvLSTM. The hidden state output from the last time step of ConvLSTM was combined with the static and global features, and a 1×1 convolution was applied to produce the final wildfire probability prediction. Comparing accuracy, recall, F1 score, precision, and Kappa coefficient with different variants of vision Transformer and ConvLSTM demonstrated the effectiveness of incorporating global location information and climate variables for enhancing predictive capabilities.

Similarly, He et al. (2024) developed a next-day wildfire risk prediction model for eastern China by combining CNN, ConvLSTM, and vision Transformer models, also employing a branch structure. In this model, eight CNN modules were used to model eight meteorological variables, while another CNN module modeled terrain, vegetation, and anthropogenic factors from the last day of each time step. The sequence feature maps generated by the temporal meteorological variables were input into LSTM, and its output was merged with the other variables' CNN outputs. Channel attention, spatial attention, and CNN were used to extract higher-order features. To emphasize the high-resolution structural features of vegetation and scattered small settlements, Landsat data were used to generate 30-meter monthly high-resolution NDVI products, and vision Transformer was applied to extract these structural features. The flattened outputs from the vision Transformer and CNN were concatenated and classified using an artificial neural network (ANN) binary classifier. Ablation studies demonstrated the effectiveness of incorporating attention mechanisms, high-resolution spatial structure features, and vision Transformer. Sensitivity analysis also confirmed that meteorological factors were the most important among wildfire drivers.

Finally, Chen et al. (2024a) designed an end-to-end encoder-

decoder network structure similar to that of Bhowmik et al. (2023) and Yoon and Voulgaris (2022), combining GCN and ConvLSTM. The GCN component was introduced to model the long-distance spatial dependencies required for global wildfire risk prediction, while mitigating the impact of missing data from ocean regions. Explicitly modeling information flow through the graph edges improved the interpretability of the prediction results. Specifically, the Earth's land surface pixels, as simulated by the JULES-INFERNO model, were treated as graph nodes, and the correlation coefficients between nodes were used to establish the graph's edges. Spatial dependencies were modeled using a spatial graph convolution model, followed by LSTM for long-term temporal dependencies. The model was trained and validated using 30 years of simulated data from 1961 to 1990 in the JULES-INFERNO dataset, and its performance was compared against LSTM, ConvLSTM, and convolutional autoencoder with LSTM. The proposed model demonstrated superior performance, with ConvLSTM being the best among the comparative models. Additionally, the study used the Louvain method to identify potential wildfire communities, and integrated gradient analysis revealed that short-term (one-month) wildfire risk is primarily driven by lightning, while long-term (11-month) risk is more influenced by temperature, followed by lightning. Node importance analysis also showed that even geographically distant locations could have strong interactions regarding wildfire risk. Similarly, Zhao et al. (2024) aimed to improve model interpretability by combining causal GNN with LSTM, comparing its performance with LSTM and GRU in predicting future.

7.5. Promising Deep Learning New Methods

Currently, the number and variety of features used in most wildfire risk prediction models have reached a plateau. However, due to the nonlinear and complex spatiotemporal relationships between various factors influencing wildfire ignition and spread, the trend in developing deep learning models for wildfire prediction focuses on enhancing their ability to model long-range spatiotemporal semantic dependencies. This approach aims to capture these subtle relationships more effectively. Specifically, there is a progression from time-series prediction to spatiotemporal sequence prediction and further to spatially enhanced spatiotemporal sequence prediction. Efforts are being made to improve the model's spatiotemporal scale and resolution by incorporating higher-resolution geospatial data over extended time sequences.

With the rapid advancement of computing hardware, particularly GPUs, the scale of input data for deep learning models has continued to expand. However, current wildfire risk prediction models using RNNs, CNNs, Transformers, or GNNs are still limited by their efficiency and capacity to model large spatiotemporal scales, especially when compared to newer models like Mamba (Gu and Dao, 2024). Moreover, many of these models rely on multi-branch networks that use only images or nodes to capture long-range semantic dependencies, neglecting the potential efficiency gains offered by multimodal approaches, such as incorporating textual descriptions. This section will introduce recent advancements in deep learning for im-

age segmentation tasks using multimodal techniques, followed by an overview of the parameter-efficient Mamba model.

7.5.1. Multimodal Models

Multimodal learning is a universal approach to building AI models, enabling the extraction and association of information from various sources, such as different sensors (Baltrušaitis et al., 2018). Unlike unimodal image-based learning, multimodal learning can acquire, interpret, and reason across multiple information sources, resembling human perception (Xu et al., 2023a). A key advantage of multimodal learning over unimodal approaches is its ability to more easily embed domain knowledge or abstract, knowledge-driven perspectives (Baltrušaitis et al., 2018). Currently, multimodal learning has been extensively studied in image segmentation and classification (Roy et al., 2023; Yao et al., 2023; Nasir et al., 2023; Chng et al., 2024; Wang and Ke, 2024; Xu et al., 2023b), data fusion (Khan et al., 2023; Kalamkar et al., 2023), generation, and visual-language pretraining models (Liu et al., 2023; Li et al., 2023a; Oquab et al., 2024). Given that this research focuses on exploring the potential applications of segmentation and classification methods in wildfire risk prediction, we will delve into Referring Image Segmentation (RIS) in subsequent sections.

RIS refers to models that understand natural language descriptions and correspond them to specific objects in images at the pixel level, outputting an object mask (Wu et al., 2024). RIS requires processing both text and visual modalities, with the latter typically being high-dimensional and exhibiting strong spatial characteristics encapsulating attributes such as color, texture, shape, and size. In contrast, natural language is generally low-dimensional and continuous, abstractly describing these visual features (Ji et al., 2024a). The key challenge of RIS lies in designing appropriate multimodal fusion methods to establish a relationship between language and visual modalities, thereby bridging the modality gap between the two (Chng et al., 2024). Generally, fusion methods can be categorized into early fusion and late fusion, commonly known as decoder-fusion and encoder-fusion, respectively (Wu et al., 2024).

Decoder fusion extracts visual and language features separately using different encoders, such as CNNs for visual data and LSTMs for language data, and designs specific fusion modules to combine these features at the decoder stage. For example, (?) developed Bottom-Up Shift and Bidirectional Attentive Refinement modules to progressively fuse the output features of the language and image modules. Similarly, Jain and Gandhi (2022) utilized CNNs to extract multi-stage image features and LSTMs for text feature extraction, integrating these features through a hierarchical cross-modal aggregation module. In another approach, Wang et al. (2022b) designed a knowledge transfer method to adapt image-level knowledge from Contrastive Language-Image Pretraining (CLIP) into RIS for pixel-level segmentation tasks, implementing a Neck module to fuse outputs from both the text and image encoders. Similarly, Yan et al. (2023) introduced a Fusion Neck module to combine image and text encoding information, alongside a multi-query generator module to aid segmentation.

Encoder fusion, in contrast, integrates multimodal features at the encoder stage using auxiliary losses or alignment modules (Chng et al., 2024). This method is considered more effective (Feng et al., 2021; Yang et al., 2022b) and has gained traction in recent studies (Wu et al., 2024). For example, Xu et al. (2023b) introduced a Bridger module, based on self-attention and cross-attention mechanisms, to facilitate cross-modal information exchange between each level of the text encoder and image encoder. Furthermore, the study designed a task decoder with hierarchical and global alignment to further fuse multimodal information and generate the mask prediction. Similarly, Yuan et al. (2024) employed BERT (Devlin et al., 2019) for text feature extraction and Swin Transformer (Liu et al., 2021b) for image feature extraction, combining them with a self-attention-based language-guided cross-scale enhancer and a pixel-word attention module for feature fusion. Moreover, Shah et al. (2024) incorporated a Gaussian Enhancement Module between textual and visual encoders to extract both local and global visual-language relationships, enhancing overall representation. In a similar vein, Chng et al. (2024) designed a Cross-modal Alignment Module between multiple layers of text and image encoders, addressing the granularity mismatch between the two modalities through bidirectional interactions. Additionally, they introduced a mask encoder branch and a Transformer-based masked token decoder to predict the mask.

In summary, multimodal tasks offer greater flexibility and intuitive interaction by incorporating natural language to guide the model, compared to unimodal tasks. Multimodal information provides additional contextual data that unimodal models often lack, allowing the language encoder to construct a relation graph for numerical geospatial relations (Yuan et al., 2024). Therefore, multimodal models, especially RIS, hold significant potential in wildfire risk prediction by capturing subtle spatiotemporal semantic dependencies that are difficult to model using only images or geospatial data.

7.5.2. Mamba

The aforementioned deep learning-based methods for spatial, temporal, and spatiotemporal modeling face challenges in capturing long-term and spatial dependencies. As a result, when these methods are applied to wildfire risk prediction on a regional scale, they often neglect the influence of climate factors outside the study area. Furthermore, global-scale wildfire risk prediction is limited by computational capacity, resulting in relatively low spatial resolution in the predictions. Additionally, whether modeling wildfire risk on a regional or global scale, the time series of driving factors considered is often short (a few days) or constructed using monthly or yearly averages for long-term sequences. This calls for more efficient models capable of handling longer temporal scales and higher spatial resolution.

One potential solution is Mamba: linear time sequence modeling with selective state spaces (Gu and Dao, 2024), a parameter-efficient model designed to handle long sequence modeling (Xu et al., 2024) such as videos or remote sensing imagery over long temporal scales. Mamba's proposal is primarily aimed at addressing the computational complexity found in prevalent transformer-based networks. Specifically, the self-

attention mechanism in transformers involves a computational complexity of $O(n^2)$, where n represents the sequence length. Mamba reduces this complexity from $O(n^2)$ to $O(n)$. Compared to the Transformer network, which uses the self-attention mechanism, the recurrent neural network (RNN)—a previously dominant approach to sequence modeling—suffers from short memory when handling long sequences. Moreover, while RNNs are efficient in the inference stage, they are less efficient during the training phase. Mamba is built on top of the State Space Model (SSM), which, similar to RNNs, is used for sequence modeling. The state-space model can be represented as:

$$\text{State Equation:} \quad x_t = Ax_{t-1} + Bu_t + w_t \tag{23}$$

$$\text{Observation Equation:} \quad y_t = Cx_t + Du_t + v_t \tag{24}$$

Where x_t is the state vector at time t, u_t is the control/input vector, y_t is the observation/output vector, A is the state transition matrix, B is the input matrix, C is the observation matrix, D is the direct transmission matrix (optional, sometimes set to 0), and w_t and v_t are process and observation noise, respectively, often assumed to be Gaussian noise and were often removed from most SSM equations.

By revising the vanilla State Space Model (SSM), as shown in Equations 23 and 24, the Structured State Space Model for Sequences (S4) was proposed by Gu et al. (2021). Specifically, since the data used in language and image processing are discrete, the SSM needed to be adapted into a discretized version. The zero-order hold technique was applied to discretize the SSM. Furthermore, the SSM equations were reformulated into a combination of recurrent and convolutional structures. This allows the S4 models to be trained in a convolutional neural network (CNN) manner while being tested in a recurrent neural network (RNN) manner, thus improving efficiency in both the training and inference stages.

To address the short memory issue typically found in RNNs, S4 employs the HiPPO matrix to replace matrix A in Equation 23. This modification enables the model to store long sequence information in a compact and sparse matrix format. However, one limitation of the S4 models is that the matrices A, B, and C are not data-dependent, which restricts their adaptability — this property is known as Linear Time Invariance (LTI).

To enhance flexibility, a gate-like operation was introduced to matrix A, allowing it to become data-dependent in a parameter-efficient manner. Similarly, matrices B, C, and the time step were adapted to be data-dependent using linear projection functions. Since all parameters are now data-dependent or dynamic, Gu and Dao (2023) proposed a parallel scan algorithm to efficiently operate the model on GPUs, enabling SSM models to scale for parallel computation.

While Mamba demonstrated effectiveness, especially with longer sequence lengths, it still did not fully capitalize on the power of GPUs. To address this, Gu and Dao (2024) introduced Mamba2, which applies a state-space duality approach. This new model leverages GPU capabilities more effectively, further improving the computational efficiency while maintaining high performance in long sequence modeling.

8. Conclusion

In the pursuit of wildfire prediction, researchers have employed a variety of data sources, proposing diverse models and methodologies. However, a comprehensive and systematic review of these data and methods remains lacking, particularly in the case of deep learning techniques, which have seen rapid development and widespread application in wildfire risk prediction in recent years. This paper presents a thorough review of various wildfire driving factor data, feature collinearity, machine learning model interpretability, and wildfire risk prediction algorithms.

First, the development of wildfire prediction models requires multiple input data sources, as well as ground truth data for training and validation. These input data include fuel, weather, and climate conditions, topographical variables, hydrological features, and socio-economic factors. Researchers select different data sources and design appropriate data preprocessing workflows based on the characteristics of the study area and the availability of data. It has been found that most studies prioritize meteorological and climatic parameters, followed by fuel and terrain conditions, with socio-economic and hydrological factors being considered to a lesser extent. Additionally, to facilitate modeling for deep learning-based wildfire risk assessments, we introduced several publicly available wildfire burn prediction datasets, such as FireCube, Next Day Wildfire Spread, Wildfire DB, WildfireSpreadTS, CFSDS, and the SeasFire Datacube. Regarding feature collinearity and the interpretability of deep learning models, this review also highlighted the use of feature collinearity evaluation methods, including Variance Inflation Factor (VIF), tolerance, and Pearson correlation coefficients, as well as interpretability methods for deep learning, such as Permutation Feature Importance, Explainable Feature Engineering, and SHapley Additive exPlanations.

Another crucial aspect of wildfire prediction models is the choice of algorithms. The most commonly used models include traditional machine learning models, wildfire danger rating systems, and deep learning models. While traditional machine learning models have been extensively reviewed in the literature, deep learning models, despite their growing attention, have lacked a systematic overview. In this paper, deep learning models were categorized into three types: time series prediction, image segmentation and classification, and spatiotemporal prediction models. The review of these models revealed a growing trend towards the consideration of longer time series and the development of higher spatiotemporal resolution wildfire risk assessment models.

Looking ahead, we foresee the potential for more efficient architectures, such as Mamba, and multimodal models to further enhance the performance and scalability of deep learning-based wildfire risk prediction systems.

References

Abatzoglou, J.T., Kolden, C.A., 2011. Relative importance of weather and climate on wildfire growth in interior alaska. International Journal of Wildland Fire 20, 479–486.

Abatzoglou, J.T., Kolden, C.A., 2013. Relationships between climate and macroscale area burned in the western united states. International Journal of Wildland Fire 22, 1003–1020.

Abatzoglou, J.T., Kolden, C.A., Balch, J.K., Bradley, B.A., 2016. Controls on interannual variability in lightning-caused fire activity in the western us. Environmental Research Letters 11, 045005.

Abdollahi, A., Pradhan, B., 2023. Explainable artificial intelligence (XAI) for interpreting the contributing factors feed into the wildfire susceptibility prediction model. SCIENCE OF THE TOTAL ENVIRONMENT 879, 163004. URL: https://www.webofscience.com/api/gateway?GWVersion=2&SrcAuth=DynamicDOIArticle&SrcApp=WOS&KeyAID=10.1016%2Fj.scitotenv.2023.163004&DestApp=DOI&SrcAppSID=USW2EC0D7EfQ4jdthTkoDVukmMmGx&SrcJTitle=SCIENCE+OF+THE+TOTAL+ENVIRONMENT&DestDOIRegistrantName=Elsevier, doi:10.1016/j.scitotenv.2023.163004. num Pages: 14 Place: Amsterdam Publisher: Elsevier Web of Science ID: WOS:000973651700001.

Achu, A.L., Thomas, J., Aju, C.D., Gopinath, G., Kumar, S., Reghunath, R., 2021. Machine-learning modelling of fire susceptibility in a forest-agriculture mosaic landscape of southern India. Ecological Informatics 64, 101348. URL: https://www.sciencedirect.com/science/article/pii/S1574954121001394, doi:10.1016/j.ecoinf.2021.101348.

Adhikari, B., Xu, C., Hodza, P., Minckley, T., 2021. Developing a geospatial data-driven solution for rapid natural wildfire risk assessment. Applied Geography 126, 102382. URL: https://www.sciencedirect.com/science/article/pii/S0143622820314818, doi:10.1016/j.apgeog.2020.102382.

Agee, J.K., Skinner, C.N., 2005. Basic principles of forest fuel reduction treatments. Forest ecology and management 211, 83–96.

Ager, A.A., Day, M.A., McHugh, C.W., Short, K., Gilbertson-Day, J., Finney, M.A., Calkin, D.E., 2014a. Wildfire exposure and fuel management on western US national forests. Journal of Environmental Management 145, 54–70. URL: https://linkinghub.elsevier.com/retrieve/pii/S0301479714002916, doi:10.1016/j.jenvman.2014.05.035.

Ager, A.A., Preisler, H.K., Arca, B., Spano, D., Salis, M., 2014b. Wildfire risk estimation in the mediterranean area. Environmetrics 25, 384–396.

Ager, A.A., Vaillant, N.M., Finney, M.A., 2010. A comparison of landscape fuel treatment strategies to mitigate wildland fire risk in the urban interface and preserve old forest structure. Forest Ecology and Management 259, 1556–1570. URL: https://www.sciencedirect.com/science/article/pii/S0378112710000514, doi:10.1016/j.foreco.2010.01.032.

Albini, F.A., 1976. Estimating wildfire behavior and effects. volume 30. Department of Agriculture, Forest Service, Intermountain Forest and Range . . . .

Aldersley, A., Murray, S.J., Cornell, S.E., 2011. Global and regional analysis of climate and human drivers of wildfire. Science of The Total Environment 409, 3472–3481. URL: https://www.sciencedirect.com/science/article/pii/S0048969711005353, doi:10.1016/j.scitotenv.2011.05.032.

Alexander, M., 1989. Fiji adopts canadian system of fire danger rating. International Forest Fire News 2, 3.

Ali, S., Abuhmed, T., El-Sappagh, S., Muhammad, K., Alonso-Moral, J.M., Confalonieri, R., Guidotti, R., Del Ser, J., Díaz-Rodríguez, N., Herrera, F., 2023. Explainable artificial intelligence (xai): What we know and what is left to attain trustworthy artificial intelligence. Information fusion 99, 101805.

Allaire, F., Mallet, V., Filippi, J.B., 2021. Emulation of wildland fire spread simulation using deep learning. Neural networks 141, 184–198.

Alonso, L., Gans, F., Karasante, I., Ahuja, A., Prapas, I., Kondylatos, S., Papoutsis, I., Panagiotou, E., Mihail, D., Cremer, F., Weber, U., Carvalhais, N., 2023. SeasFire Cube: A Global Dataset for Seasonal Fire Modeling in the Earth System. URL: https://doi.org/10.5281/zenodo.8055879, doi:10.5281/zenodo.8055879.

Alonso-Rego, C., Arellano-Pérez, S., Cabo, C., Ordoñez, C., Álvarez-González, J.G., Díaz-Varela, R.A., Ruiz-González, A.D., 2020. Estimating fuel loads and structural characteristics of shrub communities by using terrestrial laser scanning. Remote Sensing 12, 3704.

Andela, N., Morton, D.C., Giglio, L., Paugam, R., Chen, Y., Hantson, S., Van Der Werf, G.R., Randerson, J.T., 2019. The global fire atlas of individual fire size, duration, speed and direction. Earth System Science Data 11, 529–552.

Andersen, H.E., McGaughey, R.J., Reutebuch, S.E., 2005. Estimating forest canopy fuel parameters using lidar data. Remote sensing of Environment 94, 441–449.

Anderson, W.R., Cruz, M.G., Fernandes, P.M., McCaw, L., Vega, J.A., Bradstock, R.A., Fogarty, L., Gould, J., McCarthy, G., Marsden-Smedley, J.B., et al., 2015. A generic, empirical-based model for predicting rate of fire spread in shrublands. International Journal of Wildland Fire 24, 443–460.

Aragoneses, E., Chuvieco, E., 2021. Generation and mapping of fuel types for fire risk assessment. Fire 4, 59.

Aragoneses, E., García, M., Ruiz-Benito, P., Chuvieco, E., 2024. Mapping forest canopy fuel parameters at european scale using spaceborne lidar and satellite data. Remote Sensing of Environment 303, 114005.

Arellano-Pérez, S., Castedo-Dorado, F., López-Sánchez, C.A., González-Ferreiro, E., Yang, Z., Díaz-Varela, R.A., Álvarez-González, J.G., Vega, J.A., Ruiz-González, A.D., 2018. Potential of sentinel-2a data to model surface and canopy fuel characteristics in relation to crown fire hazard. Remote Sensing 10, 1645.

Arroyo, L.A., Pascual, C., Manzanera, J.A., 2008. Fire models and methods to map fuel types: The role of remote sensing. Forest ecology and management 256, 1239–1252.

Artés, T., Oom, D., De Rigo, D., Durrant, T.H., Maianti, P., Libertà, G., San-Miguel-Ayanz, J., 2019. A global wildfire dataset for the analysis of fire regimes and fire behaviour. Scientific data 6, 296.

Asif, N.A., Sarker, Y., Chakrabortty, R.K., Ryan, M.J., Ahamed, M.H., Saha, D.K., Badal, F.R., Das, S.K., Ali, M.F., Moyeen, S.I., Islam, M.R., Tasneem, Z., 2021. Graph neural network: A comprehensive review on non-euclidean space. IEEE Access 9, 60588–60606. doi:10.1109/ACCESS.2021.3071274.

Badia-Perpinyà, A., Pallares-Barbera, M., 2006. Spatial distribution of ignitions in mediterranean periurban and rural areas: the case of catalonia. International journal of Wildland fire 15, 187–196.

Bakke, S.J., Wanders, N., Van Der Wiel, K., Tallaksen, L.M., 2023. A data-driven model for Fennoscandian wildfire danger. Natural Hazards and Earth System Sciences 23, 65–89. URL: https://www.duo.uio.no/handle/10852/108719, doi:10.5194/nhess-23-65-2023. accepted: 2024-02-27T18:29:41Z.

Balch, J.K., Bradley, B.A., Abatzoglou, J.T., Nagy, R.C., Fusco, E.J., Mahood, A.L., 2017. Human-started wildfires expand the fire niche across the united states. Proceedings of the National Academy of Sciences 114, 2946–2951.

Baltrušaitis, T., Ahuja, C., Morency, L.P., 2018. Multimodal machine learning: A survey and taxonomy. IEEE transactions on pattern analysis and machine intelligence 41, 423–443.

Bar Massada, A., Syphard, A.D., Hawbaker, T.J., Stewart, S.I., Radeloff, V.C., 2011. Effects of ignition location models on the burn patterns of simulated wildfires. Environmental Modelling & Software 26, 583–592. URL: https://www.sciencedirect.com/science/article/pii/S1364815210003233, doi:10.1016/j.envsoft.2010.11.016.

Barber, Q.E., Jain, P., Whitman, E., Thompson, D.K., Guindon, L., Parks, S.A., Wang, X., Hethcoat, M.G., Parisien, M.A., 2024. The canadian fire spread dataset. Scientific data 11, 764.

Benali, A., Russo, A., Sá, A.C., Pinto, R.M., Price, O., Koutsias, N., Pereira, J.M., 2016. Determining fire dates and locating ignition points with satellite data. Remote Sensing 8, 326.

Bergado, J.R., Persello, C., Reinke, K., Stein, A., 2021. Predicting wildfire burns from big geodata using deep learning. Safety Science 140, 105276. URL: https://www.sciencedirect.com/science/article/pii/S0925753521001211, doi:10.1016/j.ssci.2021.105276.

Bergonse, R., Oliveira, S., Gonçalves, A., Nunes, S., DaCamara, C., Zêzere, J.L., 2021. Predicting burnt areas during the summer season in Portugal by combining wildfire susceptibility and spring meteorological conditions. Geomatics, Natural Hazards and Risk 12, 1039–1057. URL: https://doi.org/10.1080/19475705.2021.1909664, doi:10.1080/19475705.2021.1909664. publisher: Taylor & Francis _eprint: https://doi.org/10.1080/19475705.2021.1909664.

Bessie, W., Johnson, E., 1995. The relative importance of fuels and weather on fire behavior in subalpine forests. Ecology 76, 747–762.

Bhowmik, R.T., Jung, Y.S., Aguilera, J.A., Prunicki, M., Nadeau, K., 2023. A multi-modal wildfire prediction and early-warning system based on a novel machine learning framework. Journal of Environmental Management 341, 117908. URL: https://www.sciencedirect.com/science/

article/pii/S0301479723006965, doi:10.1016/j.jenvman.2023.117908.

Bianchi, L.O., Defossé, G.E., 2015. Live fuel moisture content and leaf ignition of forest species in Andean Patagonia, Argentina. International Journal of Wildland Fire 24, 340–348. URL: https://www.publish.csiro.au/wf/WF13099, doi:10.1071/WF13099. publisher: CSIRO PUBLISHING.

Bjånes, A., De La Fuente, R., Mena, P., 2021. A deep learning ensemble model for wildfire susceptibility mapping. Ecological Informatics 65, 101397.

Bommer, P.L., Kretschmer, M., Hedström, A., Bareeva, D., Höhne, M.M.C., 2024. Finding the right xai method—a guide for the evaluation and ranking of explainable ai methods in climate science. Artificial Intelligence for the Earth Systems 3, e230074.

Bowd, E.J., Blair, D.P., Lindenmayer, D.B., 2021. Prior disturbance legacy effects on plant recovery post-high-severity wildfire. Ecosphere 12, e03480.

Bowyer, P., Danson, F., 2004. Sensitivity of spectral reflectance to variation in live fuel moisture content at leaf and canopy level. Remote Sensing of Environment 92, 297–308.

Braun, W.J., Jones, B.L., Lee, J.S., Woolford, D.G., Wotton, B.M., 2010. Forest fire risk assessment: an illustrative example from ontario, canada. Journal of Probability and Statistics 2010, 823018.

Bright, B.C., Hudak, A.T., Meddens, A.J., Hawbaker, T.J., Briggs, J.S., Kennedy, R.E., 2017. Prediction of forest canopy and surface fuels from lidar and satellite time series data in a bark beetle-affected forest. Forests 8, 322.

Brillinger, D.R., Preisler, H.K., Benoit, J.W., 2003. Risk assessment: a forest fire example. Lecture Notes-Monograph Series , 177–196.

Burgan, R.E., 1984. Behave: fire behavior prediction and fuel modeling system, fuel subsystem. volume 167. US Department of Agriculture, Forest Service, Intermountain Forest and Range . . . .

Burgan, R.E., 1988. 1988 revisions to the 1978 national fire-danger rating system. volume 273. US Department of Agriculture, Forest Service, Southeastern Forest Experiment . . . .

Burge, J., Bonanni, M., Ihme, M., Hu, L., 2021. Convolutional lstm neural networks for modeling wildland fire dynamics. URL: https://arxiv.org/abs/2012.06679, arXiv:2012.06679.

Burge, J., Bonanni, M.R., Hu, R.L., Ihme, M., 2023. Recurrent convolutional deep neural networks for modeling time-resolved wildfire spread behavior. Fire Technology 59, 3327–3354.

Burrows, N., Gill, M., Sharples, J., 2018. Development and validation of a model for predicting fire behaviour in spinifex grasslands of arid australia. International Journal of Wildland Fire 27, 271–279.

Byrne, B., Liu, J., Bowman, K.W., Pascolini-Campbell, M., Chatterjee, A., Pandey, S., Miyazaki, K., van der Werf, G.R., Wunch, D., Wennberg, P.O., et al., 2024. Carbon emissions from the 2023 canadian wildfires. Nature , 1–5.

Cahuantzi, R., Chen, X., Güttel, S., 2023. A comparison of lstm and gru networks for learning symbolic sequences, in: Science and Information Conference, Springer. pp. 771–785.

Calviño-Cancela, M., Chas-Amil, M.L., García-Martínez, E.D., Touza, J., 2016. Wildfire risk associated with different vegetation types within and outside wildland-urban interfaces. Forest Ecology and Management 372, 1–9.

Calviño-Cancela, M., Chas-Amil, M.L., García-Martínez, E.D., Touza, J., 2017. Interacting effects of topography, vegetation, human activities and wildland-urban interfaces on wildfire ignition risk. Forest Ecology and Management 397, 10–17.

Canisius, F., Chen, J.M., 2007. Retrieving forest background reflectance in a boreal region from Multi-angle Imaging SpectroRadiometer (MISR) data. Remote Sensing of Environment 107, 312–321. URL: https://www.sciencedirect.com/science/article/pii/S0034425706004184, doi:10.1016/j.rse.2006.07.023.

Cao, Y., Zhou, X., Yu, Y., Rao, S., Wu, Y., Li, C., Zhu, Z., 2024. Forest fire prediction based on time series networks and remote sensing images. Forests 15, 1221.

Capps, S.B., Zhuang, W., Liu, R., Rolinski, T., Qu, X., 2021. Modelling chamise fuel moisture content across california: A machine learning approach. International Journal of Wildland Fire 31, 136–148.

Castro, F.X., Tudela, A., Sebastià, M.T., 2003. Modeling moisture content in shrubs to predict fire risk in Catalonia (Spain). Agricultural and Forest Meteorology 116, 49–59. URL: https://www.sciencedirect.com/science/article/pii/S0168192302002484,

doi:10.1016/S0168-1923(02)00248-4.

Catchpole, E., Catchpole, W., Viney, N., McCaw, W., Marsden-Smedley, J., 2001. Estimating fuel response time and predicting fuel moisture content from field data. International Journal of Wildland Fire 10, 215–222.

Catry, F.X., Rego, F.C., Bação, F.L., Moreira, F., 2009. Modeling and mapping wildfire ignition risk in portugal. International Journal of Wildland Fire 18, 921–931.

Cavalcante, R.B., Souza, B.M., Ramos, S.J., Gastauer, M., NASCIMENTO, W.R., Caldeira, C.F., Souza-Filho, P.W., 2021. Assessment of fire hazard weather indices in the eastern amazon: a case study for different land uses. Acta Amazonica 51, 352–362.

Cawson, J.G., Nyman, P., Schunk, C., Sheridan, G.J., Duff, T.J., Gibos, K., Bovill, W.D., Conedera, M., Pezzatti, G.B., Menzel, A., 2020. Estimation of surface dead fine fuel moisture using automated fuel moisture sticks across a range of forests worldwide. International Journal of Wildland Fire 29, 548–559.

Chavalithumrong, A., Yoon, H.J., Voulgaris, P., 2021. Learning Wildfire Model from Incomplete State Observations. URL: http://arxiv.org/abs/2111.14038. arXiv:2111.14038 [cs].

Chen, D., Cheng, S., Hu, J., Kasoar, M., Arcucci, R., 2024a. Explainable global wildfire prediction models using graph neural networks. arXiv preprint arXiv:2402.07152 .

Chen, J., Yang, Y., Peng, L., Chen, L., Ge, X., 2022. Knowledge graph representation learning-based forest fire prediction. Remote Sensing 14, 4391.

Chen, R., He, B., Li, Y., Fan, C., Yin, J., Zhang, H., Zhang, Y., 2024b. Estimation of potential wildfire behavior characteristics to assess wildfire danger in southwest China using deep learning schemes. Journal of Environmental Management 351, 120005. URL: https://linkinghub.elsevier.com/retrieve/pii/S0301479723027937, doi:10.1016/j.jenvman.2023.120005.

Chen, R., He, B., Li, Y., Fan, C., Yin, J., Zhang, H., Zhang, Y., 2024c. Estimation of potential wildfire behavior characteristics to assess wildfire danger in southwest china using deep learning schemes. Journal of environmental management 351, 120005.

Chen, R., He, B., Li, Y., Zhang, Y., Liao, Z., Fan, C., Yin, J., Zhang, H., 2024d. Incorporating fire spread simulation and machine learning algorithms to estimate crown fire potential for pine forests in sichuan, china. International Journal of Applied Earth Observation and Geoinformation 132, 104080.

Chen, W., Panahi, M., Khosravi, K., Pourghasemi, H.R., Rezaie, F., Parvinnezhad, D., 2019. Spatial prediction of groundwater potentiality using ANFIS ensembled with teaching-learning-based and biogeography-based optimization. Journal of Hydrology 572, 435–448. URL: https://www.sciencedirect.com/science/article/pii/S0022169419302604, doi:10.1016/j.jhydrol.2019.03.013.

Chen, Y., Morton, D.C., Andela, N., Giglio, L., Randerson, J.T., 2016. How much global burned area can be forecast on seasonal time scales using sea surface temperatures? Environmental Research Letters 11, 045001. URL: https://dx.doi.org/10.1088/1748-9326/11/4/045001, doi:10.1088/1748-9326/11/4/045001. publisher: IOP Publishing.

Chen, Y., Zhu, X., Yebra, M., Harris, S., Tapper, N., 2017. Development of a predictive model for estimating forest surface fuel load in Australian eucalypt forests with LiDAR data. Environmental Modelling & Software 97, 61–71. URL: https://www.sciencedirect.com/science/article/pii/S1364815216304418, doi:10.1016/j.envsoft.2017.07.007.

Cheney, N.P., Gould, J.S., McCaw, W.L., Anderson, W.R., 2012. Predicting fire behaviour in dry eucalypt forest in southern australia. Forest Ecology and Management 280, 120–131.

Cheng, S., Chassagnon, H., Kasoar, M., Guo, Y., Arcucci, R., 2024. Deep learning surrogate models of jules-inferno for wildfire prediction on a global scale. IEEE Transactions on Emerging Topics in Computational Intelligence .

Cheng, S., Prentice, I.C., Huang, Y., Jin, Y., Guo, Y.K., Arcucci, R., 2022. Data-driven surrogate model with latent data assimilation: Application to wildfire forecasting. Journal of Computational Physics 464, 111302.

Cheng, T., Wang, J., 2008. Integrated spatio-temporal data mining for forest fire prediction. Transactions in GIS 12, 591–611.

Chicas, S.D., Østergaard Nielsen, J., Valdez, M.C., Chen, C.F., 2022. Modelling wildfire susceptibility in belize's ecosystems and protected areas using machine learning and knowledge-based methods. Geocarto International 37, 15823–15846.

Chino, D.Y., Avalhais, L.P., Rodrigues, J.F., Traina, A.J., 2015. Bowfire: detection of fire in still images by integrating pixel color and texture analysis, in: 2015 28th SIBGRAPI conference on graphics, patterns and images, IEEE. pp. 95–102.

Chng, Y.X., Zheng, H., Han, Y., Qiu, X., Huang, G., 2024. Mask grounding for referring image segmentation, in: Proceedings of the IEEE/CVF Conference on Computer Vision and Pattern Recognition (CVPR), pp. 26573–26583.

Chung, J., Gulcehre, C., Cho, K., Bengio, Y., 2014. Empirical evaluation of gated recurrent neural networks on sequence modeling. arXiv preprint arXiv:1412.3555 .

Chuvieco, E., Aguado, I., Jurdao, S., Pettinari, M.L., Yebra, M., Salas, J., Hantson, S., de la Riva, J., Ibarra, P., Rodrigues, M., et al., 2012. Integrating geospatial information into fire risk assessment. International journal of wildland fire 23, 606–619.

Chuvieco, E., Aguado, I., Salas, J., García, M., Yebra, M., Oliva, P., 2020. Satellite remote sensing contributions to wildland fire science and management. Current Forestry Reports 6, 81–96.

Chuvieco, E., Cocero, D., Riano, D., Martin, P., Martınez-Vega, J., De La Riva, J., Pérez, F., 2004. Combining ndvi and surface temperature for the estimation of live fuel moisture content in forest fire danger rating. Remote Sensing of Environment 92, 322–331.

Chuvieco, E., Congalton, R.G., 1989. Application of remote sensing and geographic information systems to forest fire hazard mapping. Remote sensing of Environment 29, 147–159.

Chuvieco, E., Deshayes, M., Stach, N., Cocero, D., Riaño, D., 1999. Short-term fire risk: foliage moisture content estimation from satellite data, in: Chuvieco, E. (Ed.), Remote Sensing of Large Wildfires: in the European Mediterranean Basin. Springer, Berlin, Heidelberg, pp. 17–38. URL: https://doi.org/10.1007/978-3-642-60164-4_3, doi:10.1007/978-3-642-60164-4_3.

Chuvieco, E., Riaño, D., Aguado, I., Cocero, D., 2002. Estimation of fuel moisture content from multitemporal analysis of landsat thematic mapper reflectance data: applications in fire danger assessment. International journal of remote sensing 23, 2145–2162.

Chuvieco, E., Riaño, D., Van Wagtendok, J., Morsdof, F., 2003. Fuel loads and fuel type mapping, in: Wildland fire danger estimation and mapping: The role of remote sensing data. World Scientific, pp. 119–142.

Clark, K.L., Skowronski, N., Hom, J., Duveneck, M., Pan, Y., Van Tuyl, S., Cole, J., Patterson, M., Maurer, S., 2009. Decision support tools to improve the effectiveness of hazardous fuel reduction treatments in the new jersey pine barrens. International journal of wildland fire 18, 268–277.

Coen, J.L., Cameron, M., Michalakes, J., Patton, E.G., Riggan, P.J., Yedinak, K.M., 2013. WRF-Fire: Coupled Weather–Wildland Fire Modeling with the Weather Research and Forecasting Model. Journal of Applied Meteorology and Climatology 52, 16–38. URL: https://journals.ametsoc.org/view/journals/apme/52/1/jamc-d-12-023.1.xml, doi:10.1175/JAMC-D-12-023.1. publisher: American Meteorological Society Section: Journal of Applied Meteorology and Climatology.

Cohen, J.D., 1985. The national fire-danger rating system: basic equations. volume 82. US Department of Agriculture, Forest Service, Pacific Southwest Forest and . . . .

Coskuner, K.A., 2022. Assessing the performance of modis and viirs active fire products in the monitoring of wildfires: a case study in turkey. iForest-Biogeosciences and Forestry 15, 85.

Cruz, M., Gould, J., Alexander, M., Sullivan, A., McCaw, W., Matthews, S., Land, C., Flagship, W., of Alberta, U., of Parks, W.A.D., Wildlife, M., Fire, A., Limited, E.S.A.C., et al., 2015. A Guide to Rate of Fire Spread Models for Australian Vegetation. Australasian Fire & Emergency Service Authorities. URL: https://books.google.ca/books?id=OlR6rgEACAAJ.

Cruz, M.G., Alexander, M.E., Wakimoto, R.H., 2003. Assessing canopy fuel stratum characteristics in crown fire prone fuel types of western north america. International Journal of Wildland Fire 12, 39–50.

Cruz, M.G., Alexander, M.E., Wakimoto, R.H., 2004. Modeling the likelihood of crown fire occurrence in conifer forest stands. Forest Science 50, 640–658.

Cruz, M.G., Alexander, M.E., Wakimoto, R.H., 2005. Development and testing of models for predicting crown fire rate of spread in conifer forest stands. Canadian Journal of Forest Research 35, 1626–1639.

Cruz, M.G., McCaw, W.L., Anderson, W.R., Gould, J.S., 2013. Fire behaviour modelling in semi-arid mallee-heath shrublands of southern australia. Environmental Modelling & Software 40, 21–34.

Dal Pozzolo, A., Caelen, O., Johnson, R.A., Bontempi, G., 2015. Calibrating probability with undersampling for unbalanced classification, in: 2015 IEEE symposium series on computational intelligence, IEEE. pp. 159–166.

Deeming, J.E., 1972. National fire-danger rating system. volume 84. Rocky Mountain Forest and Range Experiment Station, Forest Service, US . . . .

Deeming, J.E., Burgan, R.E., Cohen, J.D., 1977. The national fire-danger rating system, 1978. volume 39. Department of Agriculture, Forest Service, Intermountain Forest and Range . . . .

Deng, J., Wang, W., Gu, G., Chen, Z., Liu, J., Xie, G., Weng, S., Ding, L., Li, C., 2023. Wildfire susceptibility prediction using a multisource and spatiotemporal cooperative approach. Earth Science Informatics 16, 3511–3529.

Depicker, A., De Baets, B., Baetens, J.M., 2020. Wildfire ignition probability in belgium. Natural hazards and earth system sciences 20, 363–376.

Devlin, J., Chang, M.W., Lee, K., Toutanova, K., 2019. BERT: Pre-training of deep bidirectional transformers for language understanding, in: Burstein, J., Doran, C., Solorio, T. (Eds.), Proceedings of the 2019 Conference of the North American Chapter of the Association for Computational Linguistics: Human Language Technologies, Volume 1 (Long and Short Papers), Association for Computational Linguistics, Minneapolis, Minnesota. pp. 4171–4186. URL: https://aclanthology.org/N19-1423, doi:10.18653/v1/N19-1423.

Dimitrakopoulos, A., Bemmerzouk, A., Mitsopoulos, I., 2011. Evaluation of the canadian fire weather index system in an eastern mediterranean environment. Meteorological Applications 18, 83–93.

Dong, Z., Zhao, F., Wang, G., Tian, Y., Li, H., 2024. A deep learning framework: Predicting fire radiative power from the combination of polar-orbiting and geostationary satellite data during wildfire spread. IEEE Journal of Selected Topics in Applied Earth Observations and Remote Sensing .

Donovan, V.M., Wonkka, C.L., Wedin, D.A., Twidwell, D., 2020. Land-use type as a driver of large wildfire occurrence in the us great plains. Remote Sensing 12, 1869.

Dorigo, W., Wagner, W., Albergel, C., Albrecht, F., Balsamo, G., Brocca, L., Chung, D., Ertl, M., Forkel, M., Gruber, A., et al., 2017. Esa cci soil moisture for improved earth system understanding: State-of-the art and future directions. Remote Sensing of Environment 203, 185–215.

Duff, T.J., Bell, T.L., York, A., 2012. Predicting continuous variation in forest fuel load using biophysical models: a case study in south-eastern Australia. International Journal of Wildland Fire 22, 318–332. URL: https://www.publish.csiro.au/wf/WF11087, doi:10.1071/WF11087. publisher: CSIRO PUBLISHING.

Duff, T.J., Keane, R.E., Penman, T.D., Tolhurst, K.G., 2017. Revisiting wildland fire fuel quantification methods: the challenge of understanding a dynamic, biotic entity. Forests 8, 351.

Dutta, R., Aryal, J., Das, A., Kirkpatrick, J.B., 2013. Deep cognitive imaging systems enable estimation of continental-scale fire incidence from climate data. Scientific reports 3, 3188.

Dzulhijjah, D.A., Majid, M.N., Alwanda, A.Y., Kusuma, D.C., Zakaria, F., Kusrini, K., Kusnawi, K., 2023. Comparative analysis of hybrid long short-term memory models for fire danger index forecasting with weather data, in: 2023 6th International Conference on Information and Communications Technology (ICOIACT), pp. 165–170. doi:10.1109/ICOIACT59844.2023.10455879.

D'Este, M., Elia, M., Giannico, V., Spano, G., Lafortezza, R., Sanesi, G., 2021. Machine learning techniques for fine dead fuel load estimation using multisource remote sensing data. Remote Sensing 13, 1658.

Eames, T., Russell-Smith, J., Yates, C., Edwards, A., Vernooij, R., Ribeiro, N., Steinbruch, F., van der Werf, G.R., 2021. Instantaneous pre-fire biomass and fuel load measurements from multi-spectral uas mapping in southern african savannas. Fire 4, 2.

Eddin, M.H.S., Roscher, R., Gall, J., 2023. Location-aware adaptive normalization: a deep learning approach for wildfire danger forecasting. IEEE Transactions on Geoscience and Remote Sensing 61, 1–18.

El-Madafri, I., Peña, M., Olmedo-Torre, N., 2023. The wildfire dataset: Enhancing deep learning-based forest fire detection with a diverse evolving open-source dataset focused on data representativeness and a novel multitask learning approach. Forests 14, 1697.

Elia, M., Giannico, V., Spano, G., Lafortezza, R., Sanesi, G., 2020. Likelihood and frequency of recurrent fire ignitions in highly urbanised mediterranean landscapes. International journal of wildland fire 29, 120–131.

Elkan, C., 2001. The foundations of cost-sensitive learning, in: International

joint conference on artificial intelligence, Lawrence Erlbaum Associates Ltd. pp. 973–978.

Erhan, D., Bengio, Y., Courville, A., Vincent, P., 2009. Visualizing higher-layer features of a deep network. Ph.D. thesis. University of Montreal.

Erni, S., Wang, X., Swystun, T., Taylor, S.W., Parisien, M.A., Robinne, F.N., Eddy, B., Oliver, J., Armitage, B., Flannigan, M.D., 2024. Mapping wildfire hazard, vulnerability, and risk to canadian communities. International Journal of Disaster Risk Reduction 101, 104221.

Fan, C., He, B., 2021. A physics-guided deep learning model for 10-h dead fuel moisture content estimation. Forests 12, 933.

Fan, C., He, B., Yin, J., Chen, R., Zhang, H., 2024. Process-based and geostationary meteorological satellite-enhanced dead fuel moisture content estimation. GIScience & Remote Sensing 61, 2324556.

FAO, 2006. Fire management-Global assessment 2006. Technical Report. Food and Agriculture Organization of the United Nations.

Feng, G., Hu, Z., Zhang, L., Lu, H., 2021. Encoder fusion network with co-attention embedding for referring image segmentation, in: Proceedings of the IEEE/CVF Conference on Computer Vision and Pattern Recognition (CVPR), pp. 15506–15515.

Fensholt, R., Sandholt, I., 2003. Derivation of a shortwave infrared water stress index from MODIS near- and shortwave infrared data in a semiarid environment. Remote Sensing of Environment 87, 111–121. URL: https://www.sciencedirect.com/science/article/pii/S0034425703001895, doi:10.1016/j.rse.2003.07.002.

Ferguson, S.A., Ruthford, J.E., McKay, S.J., Wright, D., Wright, C., Ottmar, R., 2002. Measuring moisture dynamics to predict fire severity in longleaf pine forests. International Journal of Wildland Fire 11, 267–279.

Fernandes, P.M., Botelho, H., Rego, F., Loureiro, C., 2008. Using fuel and weather variables to predict the sustainability of surface fire spread in maritime pine stands. Canadian Journal of Forest Research 38, 190–201.

Fernandes, P.M., Botelho, H.S., 2003. A review of prescribed burning effectiveness in fire hazard reduction. International Journal of wildland fire 12, 117–128.

Finney, M.A., 1998. FARSITE, Fire Area Simulator–model development and evaluation. 4, US Department of Agriculture, Forest Service, Rocky Mountain Research Station.

Finney, M.A., 2002. Fire growth using minimum travel time methods. Canadian Journal of Forest Research 32, 1420–1424.

Fogarty, L., Pearce, H., Catchpole, W., Alexander, M., 1998. Adoption vs. adaptation: lessons from applying the canadian forest fire danger rating system in new zealand, in: Proceedings, 3rd International Conference on Forest Fire Research and 14th Fire and Forest Meteorology Conference, Luso, Coimbra, Portugal, pp. 1011–1028.

Fogarty, L., Sullivan, A., Heemstra, S., Chladil, M., 2010. Review of grassland fire danger indicies for scaled bushfire advice warning. Technical Report. Science sub group.

Frandsen, W.H., Andrews, P.L., Forest, I., Range Experiment Station (Ogden, U., 1979. Fire behavior in nonuniform fuels. volume no.232. Ogden, Utah, Intermountain Forest and Range Experiment Station, Forest Service, U.S. Dept. of Agriculture, 1979. URL: https://www.biodiversitylibrary.org/item/136922. https://www.biodiversitylibrary.org/bibliography/68702.

Fuller, M., 1991. Forest fires: an introduction to wildland fire behavior, management, firefighting, and prevention. John Wiley & Sons, Inc.

Fusco, E.J., Finn, J.T., Abatzoglou, J.T., Balch, J.K., Dadashi, S., Bradley, B.A., 2019. Detection rates and biases of fire observations from modis and agency reports in the conterminous united states. Remote Sensing of Environment 220, 30–40.

Gao, S., Huang, Y., Zhang, S., Han, J., Wang, G., Zhang, M., Lin, Q., 2020. Short-term runoff prediction with gru and lstm networks without requiring time step optimization during sample generation. Journal of Hydrology 589, 125188.

Gao, Y., Wang, R., Zhou, E., 2021. Stock prediction based on optimized lstm and gru models. Scientific Programming 2021, 4055281.

García, M., Popescu, S., Riaño, D., Zhao, K., Neuenschwander, A., Agca, M., Chuvieco, E., 2012. Characterization of canopy fuels using icesat/glas data. Remote Sensing of Environment 123, 81–89.

García-Llamas, P., Suárez-Seoane, S., Taboada, A., Fernández-García, V., Fernández-Guisuraga, J.M., Fernández-Manso, A., Quintano, C., Marcos, E., Calvo, L., 2019. Assessment of the influence of biophysical properties related to fuel conditions on fire severity using remote sensing techniques: a case study on a large fire in NW Spain. International Journal of Wildland Fire 28, 512–520. URL: https://www.publish.csiro.au/wf/WF18156, doi:10.1071/WF18156. publisher: CSIRO PUBLISHING.

Ge, X., Yang, Y., Peng, L., Chen, L., Li, W., Zhang, W., Chen, J., 2022. Spatio-temporal knowledge graph based forest fire prediction with multi source heterogeneous data. Remote Sensing 14, 3496.

Gentilucci, M., Barbieri, M., Younes, H., Rihab, H., Pambianchi, G., 2024. Analysis of Wildfire Susceptibility by Weight of Evidence, Using Geomorphological and Environmental Factors in the Marche Region, Central Italy. Geosciences 14, 112. URL: https://www.mdpi.com/2076-3263/14/5/112, doi:10.3390/geosciences14050112. number: 5 Publisher: Multidisciplinary Digital Publishing Institute.

Gerard, S., Zhao, Y., Sullivan, J., 2023. Wildfirespreadts: A dataset of multi-modal time series for wildfire spread prediction. Advances in Neural Information Processing Systems 36, 74515–74529.

Gers, F.A., Schmidhuber, J., Cummins, F., 2000. Learning to forget: Continual prediction with lstm. Neural computation 12, 2451–2471.

Ghorbanzadeh, O., Blaschke, T., 2018. Wildfire Susceptibility Evaluation By Integrating an Analytical Network Process Approach Into GIS-Based Analyses, in: Wildfire Susceptibility Evaluation By Integrating an Analytical Network Process Approach Into GIS-Based Analyses. URL: https://uni-salzburg.elsevierpure.com/en/publications/wildfire-susceptibility-evaluation-by-integrating-an-analytical-n.

Ghorbanzadeh, O., Blaschke, T., Gholamnia, K., Aryal, J., 2019. Forest Fire Susceptibility and Risk Mapping Using Social/Infrastructural Vulnerability and Environmental Variables. Fire 2, 50. URL: https://www.mdpi.com/2571-6255/2/3/50, doi:10.3390/fire2030050. number: 3 Publisher: Multidisciplinary Digital Publishing Institute.

Giannakopoulos, C., LeSager, P., Moriondo, M., Bindi, M., Karali, A., Hatzaki, M., Kostopoulou, E., 2012. Comparison of fire danger indices in the mediterranean for present day conditions. Iforest-Biogeosciences and Forestry 5, 197.

Giglio, L., Descloitres, J., Justice, C.O., Kaufman, Y.J., 2003. An enhanced contextual fire detection algorithm for modis. Remote Sensing of Environment 87, 273–282. URL: https://www.sciencedirect.com/science/article/pii/S0034425703001846, doi:https://doi.org/10.1016/S0034-4257(03)00184-6.

Giglio, L., Schroeder, W., Justice, C.O., 2016. The collection 6 modis active fire detection algorithm and fire products. Remote Sensing of Environment 178, 31–41. URL: https://www.sciencedirect.com/science/article/pii/S0034425716300827, doi:https://doi.org/10.1016/j.rse.2016.02.054.

Gilreath, J., 2006. Validation of Variables for the Creation of a Descriptive Fire Potential Model for the Southeastern Fire District of Mississippi. Theses and Dissertations URL: https://scholarsjunction.msstate.edu/td/4942.

Gincheva, A., Pausas, J.G., Edwards, A., Provenzale, A., Cerdà, A., Hanes, C., Royé, D., Chuvieco, E., Mouillot, F., Vissio, G., et al., 2024. A monthly gridded burned area database of national wildland fire data. Scientific data 11, 352.

Good, P.I., Hardin, J.W., 2012. Common errors in statistics (and how to avoid them). John Wiley & Sons.

Gopu, A., Ramakrishnan, A., Balasubramanian, G., Srinidhi, K., 2023. A comparative study on forest fire prediction using arima, sarima, lstm, and gru methods, in: 2023 IEEE International Conference on Contemporary Computing and Communications (InC4), IEEE. pp. 1–5.

Gould, J.S., McCaw, W.L., Cheney, N.P., 2011. Quantifying fine fuel dynamics and structure in dry eucalypt forest (eucalyptus marginata) in western australia for fire management. Forest ecology and management 262, 531–546.

Greenwell, B.M., et al., 2017. pdp: An r package for constructing partial dependence plots. R J. 9, 421.

Gregor, M., David, S., 2017. Fire Risk Assessment: A measure to quantify fire risk for New Zealand locations. Technical Report. Ministry for the Environment, National Institute of water & Atmospheric Research Ltd.

de Groot, W.J., Hanes, C.C., Wang, Y., 2022. Crown fuel consumption in canadian boreal forest fires. International Journal of Wildland Fire 31, 255–276.

Groot, W.J.d., Field, R.D., Brady, M.A., Roswintiarti, O., Mohamad, M., 2007. Development of the indonesian and malaysian fire danger rating systems. Mitigation and Adaptation Strategies for Global Change 12, 165–180.

Group, C.F.C.F.D., Science, C.F.C., Directorate, S.D., 1992. Development and structure of the Canadian forest fire behavior prediction system. volume 3. Forestry Canada, Science and Sustainable Development Directorate.

Gu, A., Dao, T., 2023. Mamba: Linear-Time Sequence Modeling with Selective State Spaces. URL: http://arxiv.org/abs/2312.00752, doi:10.48550/arXiv.2312.00752. arXiv:2312.00752 [cs].

Gu, A., Dao, T., 2024. Mamba: Linear-time sequence modeling with selective state spaces. URL: https://arxiv.org/abs/2312.00752, arXiv:2312.00752.

Gu, A., Goel, K., Ré, C., 2021. Efficiently modeling long sequences with structured state spaces. arXiv preprint arXiv:2111.00396 .

Guerra-Hernández, J., Pereira, J.M., Stovall, A., Pascual, A., 2024. Impact of fire severity on forest structure and biomass stocks using nasa gedi data. insights from the 2020 and 2021 wildfire season in spain and portugal. Science of Remote Sensing 9, 100134.

Guo, F., Wang, G., Su, Z., Liang, H., Wang, W., Lin, F., Liu, A., 2016. What drives forest fire in Fujian, China? Evidence from logistic regression and Random Forests. International Journal of Wildland Fire 25, 505–519. URL: https://www.publish.csiro.au/wf/WF15121, doi:10.1071/WF15121. publisher: CSIRO PUBLISHING.

Hair Jr, J.F., Anderson, R.E., Tatham, R.L., 1986. Multivariate data analysis with readings. Macmillan Publishing Co., Inc.

Hall, J.V., Argueta, F., Zubkova, M., Chen, Y., Randerson, J.T., Giglio, L., 2024. Glocab: global cropland burned area from mid-2002 to 2020. Earth System Science Data 16, 867–885.

Hall, S.A., Burke, I.C., 2006. Considerations for characterizing fuels as inputs for fire behavior models. Forest Ecology and Management 227, 102–114.

Hantson, S., Padilla, M., Corti, D., Chuvieco, E., 2013. Strengths and weaknesses of MODIS hotspots to characterize global fire occurrence. Remote Sensing of Environment 131, 152–159. URL: https://www.sciencedirect.com/science/article/pii/S0034425712004610, doi:10.1016/j.rse.2012.12.004.

Hardy, C.C., 2005. Wildland fire hazard and risk: Problems, definitions, and context. Forest ecology and management 211, 73–82.

Hardy, C.C., Hardy, C.E., 2007. Fire danger rating in the united states of america: an evolution since 1916. International journal of wildland fire 16, 217–231.

Hargrove, W.W., Kumar, J., Norman, S.P., Hoffman, F.M., 2022. Statistically determined global fire regimes (gfrs) empirically characterized using historical modis hotspots. URL: https://doi.org/10.5281/zenodo.6522071, doi:10.5281/zenodo.6522071.

Harris, L.B., Taylor, A.H., Kassa, H., Leta, S., Powell, B., 2023. Humans and climate modulate fire activity across ethiopia. Fire Ecology 19, 15.

Harrison, S.P., Prentice, I.C., Bloomfield, K.J., Dong, N., Forkel, M., Forrest, M., Ningthoujam, R.K., Pellegrini, A., Shen, Y., Baudena, M., et al., 2021. Understanding and modelling wildfire regimes: an ecological perspective. Environmental Research Letters 16, 125008.

He, Z., Fan, G., Li, Z., Li, S., Gao, L., Li, X., Zeng, Z.C., 2024. Deep learning modeling of human activity affected wildfire risk by incorporating structural features: A case study in eastern china. Ecological Indicators 160, 111946.

Helman, D., Lensky, I.M., Tessler, N., Osem, Y., 2015. A Phenology-Based Method for Monitoring Woody and Herbaceous Vegetation in Mediterranean Forests from NDVI Time Series. Remote Sensing 7, 12314–12335. URL: https://www.mdpi.com/2072-4292/7/9/12314, doi:10.3390/rs70912314. number: 9 Publisher: Multidisciplinary Digital Publishing Institute.

Hochreiter, S., 1997. Long short-term memory. Neural Computation MIT-Press .

Hodges, J.L., Lattimer, B.Y., 2019. Wildland fire spread modeling using convolutional neural networks. Fire technology 55, 2115–2142.

Holder, A.L., Ahmed, A., Vukovich, J.M., Rao, V., 2023. Hazardous air pollutant emissions estimates from wildfires in the wildland urban interface. PNAS nexus 2, pgad186.

Holdrege, M.C., Schlaepfer, D.R., Palmquist, K.A., Crist, M., Doherty, K.E., Lauenroth, W.K., Remington, T.E., Riley, K., Short, K.C., Tull, J.C., Wiechman, L.A., Bradford, J.B., 2024. Wildfire probability estimated from recent climate and fine fuels across the big sagebrush region. Fire Ecology 20, 22. URL: https://doi.org/10.1186/s42408-024-00252-4, doi:10.1186/s42408-024-00252-4.

Hollis, J.J., Matthews, S., Fox-Hughes, P., Grootemaat, S., Heemstra, S., Kenny, B.J., Sauvage, S., 2024. Introduction to the australian fire danger rating system. International Journal of Wildland Fire 33.

Hong, H., Jaafari, A., Zenner, E.K., 2019. Predicting spatial patterns of wildfire susceptibility in the Huichang County, China: An integrated model to analysis of landscape indicators. Ecological Indicators 101, 878–891. URL: https://www.sciencedirect.com/science/article/pii/S1470160X19300792, doi:10.1016/j.ecolind.2019.01.056.

Hu, P., Tanchak, R., Wang, Q., 2023. Developing Risk Assessment Framework for Wildfire in the United States – A Deep Learning Approach to Safety and Sustainability. Journal of Safety and Sustainability URL: https://www.sciencedirect.com/science/article/pii/S2949926723000033, doi:10.1016/j.jsasus.2023.09.002.

Hu, W.S., Li, H.C., Pan, L., Li, W., Tao, R., Du, Q., 2020. Spatial–spectral feature extraction via deep convlstm neural networks for hyperspectral image classification. IEEE Transactions on Geoscience and Remote Sensing 58, 4237–4250. doi:10.1109/TGRS.2019.2961947.

Hua, L., Shao, G., 2017. The progress of operational forest fire monitoring with infrared remote sensing. Journal of Forestry Research 28, 215–229. URL: https://doi.org/10.1007/s11676-016-0361-8, doi:10.1007/s11676-016-0361-8.

Hunt Jr, E.R., Rock, B.N., Nobel, P.S., 1987. Measurement of leaf relative water content by infrared reflectance. Remote sensing of environment 22, 429–435.

Huot, F., Hu, R.L., Goyal, N., Sankar, T., Ihme, M., Chen, Y.F., 2022. Next day wildfire spread: A machine learning dataset to predict wildfire spreading from remote-sensing data. IEEE Transactions on Geoscience and Remote Sensing 60, 1–13.

Huot, F., Hu, R.L., Ihme, M., Wang, Q., Burge, J., Lu, T., Hickey, J., Chen, Y.F., Anderson, J., 2021. Deep Learning Models for Predicting Wildfires from Historical Remote-Sensing Data. URL: http://arxiv.org/abs/2010.07445. arXiv:2010.07445 [cs].

Iban, M.C., Aksu, O., 2024. Shap-driven explainable artificial intelligence framework for wildfire susceptibility mapping using modis active fire pixels: An in-depth interpretation of contributing factors in izmir, türkiye. Remote Sensing 16, 2842.

Iban, M.C., Sekertekin, A., 2022. Machine learning based wildfire susceptibility mapping using remotely sensed fire data and gis: A case study of adana and mersin provinces, turkey. Ecological Informatics 69, 101647.

Jaafari, A., Gholami, D.M., Zenner, E.K., 2017. A Bayesian modeling of wildfire probability in the Zagros Mountains, Iran. Ecological Informatics 39, 32–44. URL: https://linkinghub.elsevier.com/retrieve/pii/S1574954117300912, doi:10.1016/j.ecoinf.2017.03.003.

Jaafari, A., Mafi-Gholami, D., Thai Pham, B., Tien Bui, D., 2019. Wildfire Probability Mapping: Bivariate vs. Multivariate Statistics. Remote Sensing 11, 618. URL: https://www.mdpi.com/2072-4292/11/6/618, doi:10.3390/rs11060618. number: 6 Publisher: Multidisciplinary Digital Publishing Institute.

Jain, K., Gandhi, V., 2022. Comprehensive multi-modal interactions for referring image segmentation, in: Muresan, S., Nakov, P., Villavicencio, A. (Eds.), Findings of the Association for Computational Linguistics: ACL 2022, Association for Computational Linguistics, Dublin, Ireland. pp. 3427–3435. URL: https://aclanthology.org/2022.findings-acl.270, doi:10.18653/v1/2022.findings-acl.270.

Jain, P., Barber, Q.E., Taylor, S.W., Whitman, E., Castellanos Acuna, D., Boulanger, Y., Chavardès, R.D., Chen, J., Englefield, P., Flannigan, M., et al., 2024. Drivers and impacts of the record-breaking 2023 wildfire season in canada. Nature Communications 15, 6764.

Jain, P., Coogan, S.C., Subramanian, S.G., Crowley, M., Taylor, S., Flannigan, M.D., 2020. A review of machine learning applications in wildfire science and management. Environmental Reviews 28, 478–505. URL: https://cdnsciencepub.com/doi/10.1139/er-2020-0019, doi:10.1139/er-2020-0019. publisher: NRC Research Press.

Jalilian, S., Jouibary, S.S., 2023. Forest wildfire risk mapping, performance comparison of machine learning algorithms. Research Square .

Jenks, G.F., Caspall, F.C., 1971. Error on choroplethic maps: definition, measurement, reduction. Annals of the Association of American Geographers 61, 217–244.

Ji, L., Du, Y., Dang, Y., Gao, W., Zhang, H., 2024a. A survey of methods for addressing the challenges of referring image segmentation. Neurocomputing 583, 127599.

Ji, Y., Wang, D., Li, Q., Liu, T., Bai, Y., 2024b. Global wildfire danger predictions based on deep learning taking into account static and dynamic vari-

ables. Forests 15, 216.

Jia, S., Kim, S.H., Nghiem, S.V., Kafatos, M., 2019. Estimating live fuel moisture using smap l-band radiometer soil moisture for southern california, usa. Remote Sensing 11, 1575.

Jiang, S., Sweet, L.b., Blougouras, G., Brenning, A., Li, W., Reichstein, M., Denzler, J., Shangguan, W., Yu, G., Huang, F., et al., 2024a. How interpretable machine learning can benefit process understanding in the geosciences. Earth's Future 12, e2024EF004540.

Jiang, W., Qiao, Y., Su, G., Li, X., Meng, Q., Wu, H., Quan, W., Wang, J., Wang, F., 2023. Wfnet: A hierarchical convolutional neural network for wildfire spread prediction. Environmental Modelling & Software 170, 105841.

Jiang, W., Qiao, Y., Zheng, X., Zhou, J., Jiang, J., Meng, Q., Su, G., Zhong, S., Wang, F., 2024b. Wildfire risk assessment using deep learning in Guangdong Province, China. International Journal of Applied Earth Observation and Geoinformation 128, 103750. URL: https://www.sciencedirect.com/science/article/pii/S1569843224001043, doi:10.1016/j.jag.2024.103750.

Jiang, W., Wang, F., Su, G., Li, X., Wang, G., Zheng, X., Wang, T., Meng, Q., 2022. Modeling wildfire spread with an irregular graph network. Fire 5, 185.

Jin, G., Wang, Q., Zhu, C., Feng, Y., Huang, J., Hu, X., 2020a. Urban fire situation forecasting: Deep sequence learning with spatio-temporal dynamics. Applied Soft Computing 97, 106730.

Jin, G., Zhu, C., Chen, X., Sha, H., Hu, X., Huang, J., 2020b. Ufsp-net: a neural network with spatio-temporal information fusion for urban fire situation prediction, in: IOP Conference Series: Materials Science and Engineering, IOP Publishing. p. 012050.

Jolly, W.M., Cochrane, M.A., Freeborn, P.H., Holden, Z.A., Brown, T.J., Williamson, G.J., Bowman, D.M., 2015. Climate-induced variations in global wildfire danger from 1979 to 2013. Nature communications 6, 7537.

Jolly, W.M., Freeborn, P.H., Bradshaw, L.S., Wallace, J., Brittain, S., 2024. Modernizing the us national fire danger rating system (version 4): Simplified fuel models and improved live and dead fuel moisture calculations. Environmental Modelling & Software , 106181.

Jones, M.W., Kelley, D.I., Burton, C.A., Di Giuseppe, F., Barbosa, M.L.F., Brambleby, E., Hartley, A.J., Lombardi, A., Mataveli, G., McNorton, J.R., et al., 2024. State of wildfires 2023–2024. Earth System Science Data 16, 3601–3685.

Josephson, J.R., Josephson, S.G., 1996. Abductive inference: Computation, philosophy, technology. Cambridge University Press.

Kadir, E.A., Kung, H.T., AlMansour, A.A., Irie, H., Rosa, S.L., Fauzi, S.S.M., 2023. Wildfire hotspots forecasting and mapping for environmental monitoring based on the long short-term memory networks deep learning algorithm. Environments 10, 124.

Kalamkar, S., et al., 2023. Multimodal image fusion: A systematic review. Decision Analytics Journal , 100327.

Kalantar, B., Ueda, N., Idrees, M.O., Janizadeh, S., Ahmadi, K., Shabani, F., 2020. Forest Fire Susceptibility Prediction Based on Machine Learning Models with Resampling Algorithms on Remote Sensing Data. Remote Sensing 12, 3682. URL: https://www.mdpi.com/2072-4292/12/22/3682, doi:10.3390/rs12223682. number: 22 Publisher: Multidisciplinary Digital Publishing Institute.

Kanwal, R., Rafaqat, W., Iqbal, M., Weiguo, S., 2023. Data-Driven Approaches for Wildfire Mapping and Prediction Assessment Using a Convolutional Neural Network (CNN). Remote Sensing 15, NA–NA. URL: https://go.gale.com/ps/i.do?p=AONE&sw=w&issn=20724292&v=2.1&it=r&id=GALE%7CA772535779&sid=googleScholar&linkaccess=abs, doi:10.3390/rs15215099. publisher: MDPI AG.

Keane, R.E., Burgan, R., Wagtendonk, J.v., 2001. Mapping wildland fuels for fire management across multiple scales: Integrating remote sensing, GIS, and biophysical modeling. International Journal of Wildland Fire 10, 301–319. URL: https://www.publish.csiro.au/wf/wf01028, doi:10.1071/wf01028. publisher: CSIRO PUBLISHING.

Khalaf, M.W.A., Jouibary, S.S., Jahdi, R., 2024. Performance analysis of convlstm, flammap, and ca algorithms to predict wildfire spread in golestan national park, ne iran. Environmental Modeling & Assessment , 1–14.

Khan, S.U., Khan, M.A., Azhar, M., Khan, F., Lee, Y., Javed, M., 2023. Multimodal medical image fusion towards future research: A review. Journal of King Saud University-Computer and Information Sciences 35, 101733.

Kiefer, M.T., Zhong, S., 2015. The role of forest cover and valley geometry in cold-air pool evolution. Journal of Geophysical Research: Atmospheres 120, 8693–8711. URL: https://onlinelibrary.wiley.com/doi/abs/10.1002/2014JD022998, doi:10.1002/2014JD022998. _eprint: https://agupubs.onlinelibrary.wiley.com/doi/pdf/10.1002/2014JD022998.

Kilgore, B.M., Sando, R.W., 1975. Crown-fire potential in a sequoia forest after prescribed burning. Forest Science 21, 83–87.

Kim, D.W., Chung, W., Lee, B., 2016. Exploring tree crown spacing and slope interaction effects on fire behavior with a physics-based fire model. Forest Science and Technology 12, 167–175.

Knipling, E.B., 1970. Physical and physiological basis for the reflectance of visible and near-infrared radiation from vegetation. Remote sensing of environment 1, 155–159.

Kondylatos, S., Prapas, I., Camps-Valls, G., Papoutsis, I., 2023. Mesogeos: A multi-purpose dataset for data-driven wildfire modeling in the mediterranean, in: Thirty-seventh Conference on Neural Information Processing Systems Datasets and Benchmarks Track. URL: https://openreview.net/forum?id=VH1vxapUTs.

Kondylatos, S., Prapas, I., Ronco, M., Papoutsis, I., Camps-Valls, G., Piles, M., Fernández-Torres, M.A., Carvalhais, N., 2022. Wildfire Danger Prediction and Understanding With Deep Learning. Geophysical Research Letters 49, e2022GL099368. doi:10.1029/2022GL099368. _eprint: https://onlinelibrary.wiley.com/doi/pdf/10.1029/2022GL099368.

Kramer, H.A., Collins, B.M., Kelly, M., Stephens, S.L., 2014. Quantifying ladder fuels: A new approach using lidar. Forests 5, 1432–1453.

Krizhevsky, A., Sutskever, I., Hinton, G.E., 2012. Imagenet classification with deep convolutional neural networks. Advances in neural information processing systems 25.

Krueger, E.S., Levi, M.R., Achieng, K.O., Bolten, J.D., Carlson, J.D., Coops, N.C., Holden, Z.A., Magi, B.I., Rigden, A.J., Ochsner, T.E., 2022. Using soil moisture information to better understand and predict wildfire danger: a review of recent developments and outstanding questions. International Journal of Wildland Fire 32, 111–132. URL: https://www.publish.csiro.au/wf/WF22056, doi:10.1071/WF22056. publisher: CSIRO PUBLISHING.

Labenski, P., Ewald, M., Schmidtlein, S., Heinsch, F.A., Fassnacht, F.E., 2023. Quantifying surface fuels for fire modelling in temperate forests using airborne lidar and Sentinel-2: potential and limitations. Remote Sensing of Environment 295, 113711. URL: https://www.sciencedirect.com/science/article/pii/S0034425723002626, doi:10.1016/j.rse.2023.113711.

Lall, S., Mathibela, B., 2016. The application of artificial neural networks for wildfire risk prediction, in: 2016 International Conference on Robotics and Automation for Humanitarian Applications (RAHA), IEEE. pp. 1–6.

Lawson, B.D., Armitage, O., 2008. Weather guide for the Canadian forest fire danger rating system. Technical Report. Canadian Forest Service, Northern Forestry Centre.

Lecina-Diaz, J., Alvarez, A., Retana, J., 2014. Extreme Fire Severity Patterns in Topographic, Convective and Wind-Driven Historical Wildfires of Mediterranean Pine Forests. PLOS ONE 9, e85127. URL: https://journals.plos.org/plosone/article?id=10.1371/journal.pone.0085127, doi:10.1371/journal.pone.0085127. publisher: Public Library of Science.

Lee, S.J., Lee, Y.J., Ryu, J.Y., Kwon, C.G., Seo, K.W., Kim, S.Y., 2022. Prediction of wildfire fuel load for pinus densiflora stands in south korea based on the forest-growth model. Forests 13, 1372.

Leite, R.V., Amaral, C., Neigh, C.S., Cosenza, D.N., Klauberg, C., Hudak, A.T., Aragão, L., Morton, D.C., Coffield, S., McCabe, T., et al., 2024. Leveraging the next generation of spaceborne earth observations for fuel monitoring and wildland fire management. Remote Sensing in Ecology and Conservation .

Leite, R.V., Silva, C.A., Broadbent, E.N., Do Amaral, C.H., Liesenberg, V., De Almeida, D.R.A., Mohan, M., Godinho, S., Cardil, A., Hamamura, C., et al., 2022. Large scale multi-layer fuel load characterization in tropical savanna using gedi spaceborne lidar data. Remote Sensing of Environment 268, 112764.

Leuenberger, M., Parente, J., Tonini, M., Pereira, M.G., Kanevski, M., 2018. Wildfire susceptibility mapping: Deterministic vs. stochastic approaches. Environmental Modelling & Software 101, 194–203.

Li, B.S., Rad, R., 2024. Wildfire spread prediction in north america using satellite imagery and vision transformer, in: 2024 IEEE Conference on Artificial Intelligence (CAI), IEEE. pp. 1536–1541.

Li, F., Zhang, H., Xu, H., Liu, S., Zhang, L., Ni, L.M., Shum, H.Y., 2023a.

Mask dino: Towards a unified transformer-based framework for object detection and segmentation, in: Proceedings of the IEEE/CVF Conference on Computer Vision and Pattern Recognition (CVPR), pp. 3041–3050.

Li, F., Zhu, Q., Riley, W.J., Zhao, L., Xu, L., Yuan, K., Chen, M., Wu, H., Gui, Z., Gong, J., et al., 2023b. Attentionfire_v1. 0: interpretable machine learning fire model for burned-area predictions over tropics. Geoscientific Model Development 16, 869–884.

Li, W., Xu, Q., Yi, J., Liu, J., 2022a. Predictive model of spatial scale of forest fire driving factors: a case study of Yunnan Province, China. Scientific Reports 12, 19029. doi:10.1038/s41598-022-23697-6. publisher: Nature Publishing Group.

Li, X., Wang, X., Sun, S., Wang, Y., Li, S., Li, D., 2023c. Predicting the wildland fire spread using a mixed-input cnn model with both channel and spatial attention mechanisms. Fire Technology 59, 2683–2717.

Li, Y., Chen, R., He, B., Veraverbeke, S., 2022b. Forest foliage fuel load estimation from multi-sensor spatiotemporal features. International Journal of Applied Earth Observation and Geoinformation 115, 103101. URL: https://www.sciencedirect.com/science/article/pii/S1569843222002898, doi:10.1016/j.jag.2022.103101.

Li, Y., Quan, X., Liao, Z., He, B., 2021a. Forest fuel loads estimation from landsat etm+ and alos palsar data. Remote Sensing 13, 1189.

Li, Z., Huang, Y., Li, X., Xu, L., 2021b. Wildland Fire Burned Areas Prediction Using Long Short-Term Memory Neural Network with Attention Mechanism. Fire Technology 57, 1–23. URL: https://doi.org/10.1007/s10694-020-01028-3, doi:10.1007/s10694-020-01028-3.

Li, Z., Shi, H., Vogelmann, J.E., Hawbaker, T.J., Peterson, B., 2020. Assessment of fire fuel load dynamics in shrubland ecosystems in the western united states using modis products. Remote Sensing 12, 1911.

Liang, H., Zhang, M., Wang, H., 2019. A Neural Network Model for Wildfire Scale Prediction Using Meteorological Factors. IEEE Access 7, 176746–176755. URL: https://ieeexplore.ieee.org/document/8924693, doi:10.1109/ACCESS.2019.2957837. conference Name: IEEE Access.

Liang, M., Duncanson, L., Silva, J.A., Sedano, F., 2023. Quantifying aboveground biomass dynamics from charcoal degradation in mozambique using gedi lidar and landsat. Remote sensing of environment 284, 113367.

Liao, D., Valliant, R., 2012a. Variance inflation factors in the analysis of complex survey data. Survey Methodology 38, 53–62.

Liao, D., Valliant, R., 2012b. Variance inflation factors in the analysis of complex survey data. Survey Methodology 38, 53–62.

Liu, S., Zeng, Z., Ren, T., Li, F., Zhang, H., Yang, J., Li, C., Yang, J., Su, H., Zhu, J., et al., 2023. Grounding dino: Marrying dino with grounded pre-training for open-set object detection. arXiv preprint arXiv:2303.05499.

Liu, X., Lin, Z., Feng, Z., 2021a. Short-term offshore wind speed forecast by seasonal arima-a comparison against gru and lstm. Energy 227, 120492.

Liu, Y., Stanturf, J., Goodrick, S., 2010. Wildfire potential evaluation during a drought event with a regional climate model and NDVI. Ecological Informatics 5, 418–428. URL: https://www.sciencedirect.com/science/article/pii/S1574954110000531, doi:10.1016/j.ecoinf.2010.04.001.

Liu, Z., Lin, Y., Cao, Y., Hu, H., Wei, Y., Zhang, Z., Lin, S., Guo, B., 2021b. Swin transformer: Hierarchical vision transformer using shifted windows, in: Proceedings of the IEEE/CVF International Conference on Computer Vision (ICCV), pp. 10012–10022.

Lizundia-Loiola, J., Otón, G., Ramo, R., Chuvieco, E., 2020. A spatio-temporal active-fire clustering approach for global burned area mapping at 250 m from modis data. Remote Sensing of Environment 236, 111493.

Lopez, A.M., Avila, C.C.E., VanderRoest, J.P., Roth, H.K., Fendorf, S., Borch, T., 2024. Molecular insights and impacts of wildfire-induced soil chemical changes. Nature Reviews Earth & Environment , 1–16.

López, A.S., San-Miguel-Ayanz, J., Burgan, R.E., 2002. Integration of satellite sensor data, fuel type maps and meteorological observations for evaluation of forest fire risk at the pan-european scale. International Journal of Remote Sensing 23, 2713–2719.

Lu, Y., Wei, C., 2021. Evaluation of microwave soil moisture data for monitoring live fuel moisture content (lfmc) over the coterminous united states. Science of The Total Environment 771, 145410.

Lundberg, S.M., Lee, S.I., 2017. A Unified Approach to Interpreting Model Predictions, in: Advances in Neural Information Processing Systems, Curran Associates, Inc. URL: https://proceedings.neurips.cc/paper/2017/hash/8a20a8621978632d76c43dfd28b67767-Abstract.html.

Luo, L., Zhai, Q., Su, Y., Ma, Q., Kelly, M., Guo, Q., 2018. Simple method for direct crown base height estimation of individual conifer trees using airborne lidar data. Optics express 26, A562–A578.

Malik, A., Rao, M.R., Puppala, N., Koouri, P., Thota, V.A.K., Liu, Q., Chiao, S., Gao, J., 2021. Data-Driven Wildfire Risk Prediction in Northern California. Atmosphere 12, 109. URL: https://www.mdpi.com/2073-4433/12/1/109, doi:10.3390/atmos12010109. number: 1 Publisher: Multidisciplinary Digital Publishing Institute.

Mansuy, N., Miller, C., Parisien, M.A., Parks, S.A., Batllori, E., Moritz, M.A., 2019. Contrasting human influences and macro-environmental factors on fire activity inside and outside protected areas of North America. Environmental Research Letters 14, 064007. URL: https://dx.doi.org/10.1088/1748-9326/ab1bc5, doi:10.1088/1748-9326/ab1bc5. publisher: IOP Publishing.

Marjani, M., Ahmadi, S.A., Mahdianpari, M., 2023. Firepred: A hybrid multi-temporal convolutional neural network model for wildfire spread prediction. Ecological Informatics 78, 102282.

Marjani, M., Mahdianpari, M., Ahmadi, S.A., Hemmati, E., Mohammadimanesh, F., Mesgari, M.S., 2024a. Application of explainable artificial intelligence in predicting wildfire spread: an aspp-enabled cnn approach. IEEE Geoscience and Remote Sensing Letters .

Marjani, M., Mahdianpari, M., Mohammadimanesh, F., 2024b. Cnn-bilstm: A novel deep learning model for near-real-time daily wildfire spread prediction. Remote Sensing 16, 1467.

Martell, D.L., Bevilacqua, E., Stocks, B.J., 1989. Modelling seasonal variation in daily people-caused forest fire occurrence. Canadian Journal of Forest Research 19, 1555–1563. URL: https://cdnsciencepub.com/doi/10.1139/x89-237, doi:10.1139/x89-237. publisher: NRC Research Press.

Martínez, J., Vega-Garcia, C., Chuvieco, E., 2009. Human-caused wildfire risk rating for prevention planning in Spain. Journal of Environmental Management 90, 1241–1252. URL: https://www.sciencedirect.com/science/article/pii/S0301479708001758, doi:10.1016/j.jenvman.2008.07.005.

Masrur, A., Yu, M., 2023. Chapter 6 - spatiotemporal attention convlstm networks for predicting and physically interpreting wildfire spread, in: Sun, Z., Cristea, N., Rivas, P. (Eds.), Artificial Intelligence in Earth Science. Elsevier, pp. 119–156. URL: https://www.sciencedirect.com/science/article/pii/B9780323917377000098, doi:https://doi.org/10.1016/B978-0-323-91737-7.00009-8.

Masrur, A., Yu, M., Taylor, A., 2024. Capturing and interpreting wildfire spread dynamics: attention-based spatiotemporal models using convlstm networks. Ecological Informatics 82, 102760.

Matthews, S., 2013. Dead fuel moisture research: 1991–2012. International journal of wildland fire 23, 78–92.

May, N., Ellicott, E., Gollner, M., 2019. An examination of fuel moisture, energy release and emissions during laboratory burning of live wildland fuels. International Journal of Wildland Fire 28, 187–197.

Mbow, C., Goïta, K., Bénié, G.B., 2004. Spectral indices and fire behavior simulation for fire risk assessment in savanna ecosystems. Remote Sensing of Environment 91, 1–13. doi:10.1016/j.rse.2003.10.019.

McArthur, A.G., 1958. The preparation and use of fire danger tables. Technical Report. Forestry and Timber Bureau: Canberra, Australia.

McArthur, A.G., 1960. Fire danger rating tables for annual grassland. Technical Report. (Forestry and Timber Bureau: Canberra, Australia.

McArthur, A.G., 1966. Weather and grassland fire behaviour. Technical Report. Department of National Development, Forestry and Timber Bureau: Canberra, Australia.

McArthur, A.G., 1967. Fire behaviour in eucalypt forests. Technical Report. Forest Research Institute, Forestry and Timber Bureau: Canberra, Australia.

McArthur, A.G., 1973. Grassland fire danger meter Mk IV. Technical Report. Forest Research Institute, Forestry and Timber Bureau: Canberra, ACT.

McCandless, T.C., Kosovic, B., Petzke, W., 2020. Enhancing wildfire spread modelling by building a gridded fuel moisture content product with machine learning. Machine Learning: Science and Technology 1, 035010.

McLauchlan, K.K., Higuera, P.E., Miesel, J., Rogers, B.M., Schweitzer, J., Shuman, J.K., Tepley, A.J., Varner, J.M., Veblen, T.T., Adalsteinsson, S.A., et al., 2020. Fire as a fundamental ecological process: Research advances and frontiers. Journal of Ecology 108, 2047–2069.

McNorton, J.R., Di Giuseppe, F., 2024. A global fuel characteristic model and dataset for wildfire prediction. Biogeosciences 21, 279–300. doi:10.5194/bg-21-279-2024. publisher: Copernicus GmbH.

Meikle, S., Heine, J., 1987. A fire danger index system for the transvaal lowveld and adjoining escarpment areas. South African Forestry Journal 143, 55–56.

Mell, W., Jenkins, M.A., Gould, J., Cheney, P., 2007. A physics-based approach to modelling grassland fires. International Journal of Wildland Fire 16, 1–22. URL: https://www.publish.csiro.au/wf/WF06002, doi:10.1071/WF06002. publisher: CSIRO PUBLISHING.

Menning, K.M., Stephens, S.L., 2007. Fire climbing in the forest: a semiqualitative, semiquantitative approach to assessing ladder fuel hazards. Western Journal of Applied Forestry 22, 88–93.

Miao, X., Li, J., Mu, Y., He, C., Ma, Y., Chen, J., Wei, W., Gao, D., 2023. Time Series Forest Fire Prediction Based on Improved Transformer. Forests 14, 1596. URL: https://www.mdpi.com/1999-4907/14/8/1596, doi:10.3390/f14081596. number: 8 Publisher: Multidisciplinary Digital Publishing Institute.

Michail, D., Panagiotou, L.I., Davalas, C., Prapas, I., Kondylatos, S., Bountos, N.I., Papoutsis, I., 2024. Seasonal Fire Prediction using Spatio-Temporal Deep Neural Networks. URL: http://arxiv.org/abs/2404.06437. arXiv:2404.06437 [cs].

Miller, C., Ager, A.A., 2012. A review of recent advances in risk analysis for wildfire management. International journal of wildland fire 22, 1–14.

Miller, C., Parisien, M.A., Ager, A., Finney, M., 2008. Evaluating spatially-explicit burn probabilities for strategic fire management planning. WIT Transactions on Ecology and the Environment 119, 245–252.

Mills, G.A., McCaw, W.L., 2010. Atmospheric stability environments and fire weather in Australia: extending the Haines Index. volume 20. Centre for Australian Weather and Climate Research Melbourne, Australia.

Moayedi, H., Khasmakhi, M.A.S.A., 2023. Wildfire susceptibility mapping using two empowered machine learning algorithms. Stochastic Environmental Research and Risk Assessment 37, 49–72.

Molnar, C., König, G., Herbinger, J., Freiesleben, T., Dandl, S., Scholbeck, C.A., Casalicchio, G., Grosse-Wentrup, M., Bischl, B., 2020. General pitfalls of model-agnostic interpretation methods for machine learning models, in: International Workshop on Extending Explainable AI Beyond Deep Models and Classifiers, Springer. pp. 39–68.

Monner, D., Reggia, J.A., 2012. A generalized lstm-like training algorithm for second-order recurrent neural networks. Neural Networks 25, 70–83.

Moritz, M.A., Batllori, E., Bradstock, R.A., Gill, A.M., Handmer, J., Hessburg, P.F., Leonard, J., McCaffrey, S., Odion, D.C., Schoennagel, T., et al., 2014. Learning to coexist with wildfire. Nature 515, 58–66.

Mou, L., Hua, Y., Jin, P., Zhu, X.X., 2020. Era: A data set and deep learning benchmark for event recognition in aerial videos [software and data sets]. IEEE Geoscience and Remote Sensing Magazine 8, 125–133.

Myoung, B., Kim, S.H., Nghiem, S.V., Jia, S., Whitney, K., Kafatos, M.C., 2018. Estimating live fuel moisture from modis satellite data for wildfire danger assessment in southern california usa. Remote Sensing 10, 87.

Myroniuk, V., Zibtsev, S., Bogomolov, V., Goldammer, J.G., Soshenskyi, O., Levchenko, V., Matsala, M., 2023. Combining landsat time series and gedi data for improved characterization of fuel types and canopy metrics in wildfire simulation. Journal of Environmental Management 345, 118736.

Naderpour, M., Rizeei, H.M., Ramezani, F., 2020. Wildfire Prediction: Handling Uncertainties Using Integrated Bayesian Networks and Fuzzy Logic, in: 2020 IEEE International Conference on Fuzzy Systems (FUZZ-IEEE), pp. 1–7. URL: https://ieeexplore.ieee.org/document/9177700, doi:10.1109/FUZZ48607.2020.9177700. iSSN: 1558-4739.

Nami, M.H., Jaafari, A., Fallah, M., Nabiuni, S., 2018. Spatial prediction of wildfire probability in the Hyrcanian ecoregion using evidential belief function model and GIS. International Journal of Environmental Science and Technology 15, 373–384. URL: https://doi.org/10.1007/s13762-017-1371-6, doi:10.1007/s13762-017-1371-6.

Nasir, N., Kansal, A., Barneih, F., Al-Shaltone, O., Bonny, T., Al-Shabi, M., Al Shammaa, A., 2023. Multi-modal image classification of covid-19 cases using computed tomography and x-rays scans. Intelligent Systems with Applications 17, 200160.

Natekar, S., Patil, S., Nair, A., Roychowdhury, S., 2021. Forest fire prediction using lstm, in: 2021 2nd International Conference for Emerging Technology (INCET), pp. 1–5. doi:10.1109/INCET51464.2021.9456113.

Nelson Jr, R.M., 2000. Prediction of diurnal change in 10-h fuel stick moisture content. Canadian Journal of Forest Research 30, 1071–1087. URL: https://cdnsciencepub.com/doi/abs/10.1139/x00-032, doi:10.1139/x00-032. publisher: NRC Research Press.

Nieto, H., Aguado, I., Chuvieco, E., Sandholt, I., 2010. Dead fuel moisture estimation with msg–seviri data. retrieval of meteorological data for the calculation of the equilibrium moisture content. Agricultural and Forest Meteorology 150, 861–870.

Noble, I., Gill, A., Bary, G., 1980. Mcarthur's fire-danger meters expressed as equations. Australian journal of ecology 5, 201–203.

Nolan, R.H., de Dios, V.R., Boer, M.M., Caccamo, G., Goulden, M.L., Bradstock, R.A., 2016. Predicting dead fine fuel moisture at regional scales using vapour pressure deficit from modis and gridded weather data. Remote Sensing of Environment 174, 100–108.

Nolan, R.H., Price, O.F., Samson, S.A., Jenkins, M.E., Rahmani, S., Boer, M.M., 2022. Framework for assessing live fine fuel loads and biomass consumption during fire. Forest Ecology and Management 504, 119830.

Nur, A.S., Kim, Y.J., Lee, C.W., 2022. Creation of wildfire susceptibility maps in plumas national forest using insar coherence, deep learning, and metaheuristic optimization approaches. Remote Sensing 14, 4416.

Nur, A.S., Kim, Y.J., Lee, J.H., Lee, C.W., 2023. Spatial Prediction of Wildfire Susceptibility Using Hybrid Machine Learning Models Based on Support Vector Regression in Sydney, Australia. Remote Sensing 15, 760. URL: https://www.mdpi.com/2072-4292/15/3/760, doi:10.3390/rs15030760. number: 3 Publisher: Multidisciplinary Digital Publishing Institute.

Oak, O., Nazre, R., Naigaonkar, S., Sawant, S., Joshi, A., 2024. A novel transfer learning based cnn model for wildfire susceptibility prediction, in: 2024 5th International Conference for Emerging Technology (INCET), IEEE. pp. 1–6.

Oliveira, S., Gonçalves, A., Zêzere, J.L., 2021a. Reassessing wildfire susceptibility and hazard for mainland portugal. Science of the total environment 762, 143121.

Oliveira, S., Rocha, J., Sá, A., 2021b. Wildfire risk modeling. Current Opinion in Environmental Science & Health 23, 100274. URL: https://www.sciencedirect.com/science/article/pii/S2468584421000465, doi:10.1016/j.coesh.2021.100274.

Oquab, M., Darcet, T., Moutakanni, T., Vo, H., Szafraniec, M., Khalidov, V., Fernandez, P., Haziza, D., Massa, F., El-Nouby, A., Assran, M., Ballas, N., Galuba, W., Howes, R., Huang, P.Y., Li, S.W., Misra, I., Rabbat, M., Sharma, V., Synnaeve, G., Xu, H., Jegou, H., Mairal, J., Labatut, P., Joulin, A., Bojanowski, P., 2024. Dinov2: Learning robust visual features without supervision. URL: https://arxiv.org/abs/2304.07193, arXiv:2304.07193.

Ottmar, R.D., Sandberg, D.V., Riccardi, C.L., Prichard, S.J., 2007. An overview of the fuel characteristic classification system—quantifying, classifying, and creating fuelbeds for resource planning. Canadian Journal of Forest Research 37, 2383–2393.

Parks, S.A., Abatzoglou, J.T., 2020. Warmer and Drier Fire Seasons Contribute to Increases in Area Burned at High Severity in Western US Forests From 1985 to 2017. Geophysical Research Letters 47, e2020GL089858. URL: https://onlinelibrary.wiley.com/doi/abs/10.1029/2020GL089858, doi:10.1029/2020GL089858. _eprint: https://onlinelibrary.wiley.com/doi/pdf/10.1029/2020GL089858.

Pelletier, N., Millard, K., Darling, S., 2023. Wildfire likelihood in Canadian treed peatlands based on remote-sensing time-series of surface conditions. Remote Sensing of Environment 296, 113747. URL: https://www.sciencedirect.com/science/article/pii/S0034425723002985, doi:10.1016/j.rse.2023.113747.

Pellizzaro, G., Duce, P., Ventura, A., Zara, P., 2007. Seasonal variations of live moisture content and ignitability in shrubs of the mediterranean basin. International Journal of Wildland Fire 16, 633–641.

Pettinari, M.L., Chuvieco, E., 2016. Generation of a global fuel data set using the fuel characteristic classification system. Biogeosciences 13, 2061–2076.

Pettinari, M.L., Chuvieco, E., 2020. Fire danger observed from space. Surveys in Geophysics 41, 1437–1459.

Pettinari, M.L., Ottmar, R.D., Prichard, S.J., Andreu, A.G., Chuvieco, E., 2013. Development and mapping of fuel characteristics and associated fire potentials for south america. International Journal of Wildland Fire 23, 643–654.

Phelps, N., Woolford, D.G., 2021. Comparing calibrated statistical and machine learning methods for wildland fire occurrence prediction: a case study of human-caused fires in Lac La Biche, Alberta, Canada. International Journal of Wildland Fire 30, 850–870. URL: https://www.publish.csiro.au/wf/WF20139, doi:10.1071/WF20139. publisher: CSIRO PUBLISHING.

Pisek, J., Rautiainen, M., Nikopensius, M., Raabe, K., 2015. Estimation of seasonal dynamics of understory NDVI in northern forests using

41

MODIS BRDF data: Semi-empirical versus physically-based approach. Remote Sensing of Environment 163, 42–47. URL: https://www.sciencedirect.com/science/article/pii/S0034425715000991, doi:10.1016/j.rse.2015.03.003.

Ploton, P., Mortier, F., Réjou-Méchain, M., Barbier, N., Picard, N., Rossi, V., Dormann, C., Cornu, G., Viennois, G., Bayol, N., et al., 2020. Spatial validation reveals poor predictive performance of large-scale ecological mapping models. Nature communications 11, 4540.

Pollina, J.B., Colle, B.A., Charney, J.J., 2013. Climatology and Meteorological Evolution of Major Wildfire Events over the Northeast United States. Weather and Forecasting 28, 175–193. URL: https://journals.ametsoc.org/view/journals/wefo/28/1/waf-d-12-00009_1.xml, doi:10.1175/WAF-D-12-00009.1. publisher: American Meteorological Society Section: Weather and Forecasting.

Prapas, I., Bountos, N.I., Kondylatos, S., Michail, D., Camps-Valls, G., Papoutsis, I., 2023. TeleViT: Teleconnection-Driven Transformers Improve Subseasonal to Seasonal Wildfire Forecasting, pp. 3754–3759. URL: https://openaccess.thecvf.com/content/ICCV2023W/AIHADR/html/Prapas_TeleViT_Teleconnection-Driven_Transformers_Improve_Subseasonal_to_Seasonal_Wildfire_Forecasting_ICCVW_2023_paper.html.

Prapas, I., Kondylatos, S., Papoutsis, I., 2022. FireCube: A Daily Datacube for the Modeling and Analysis of Wildfires in Greece. URL: https://doi.org/10.5281/zenodo.6475592, doi:10.5281/zenodo.6475592.

Prapas, I., Kondylatos, S., Papoutsis, I., Camps-Valls, G., Ronco, M., Ángel Fernández-Torres, M., Guillem, M.P., Carvalhais, N., 2021. Deep learning methods for daily wildfire danger forecasting. URL: https://arxiv.org/abs/2111.02736, arXiv:2111.02736.

Preisler, H.K., Brillinger, D.R., Burgan, R.E., Benoit, J., 2004. Probability based models for estimation of wildfire risk. International Journal of wildland fire 13, 133–142.

Prior, T., Eriksen, C., 2013. Wildfire preparedness, community cohesion and social–ecological systems. Global Environmental Change 23, 1575–1586. URL: https://www.sciencedirect.com/science/article/pii/S0959378013001684, doi:10.1016/j.gloenvcha.2013.09.016.

Pye, J.M., Prestemon, J.P., Butry, D.T., Abt, K.L., 2003. Prescribed burning and wildfire risk in the 1998 fire season in florida, in: In: Omi, Philip N.; Joyce, Linda A., technical editors. Fire, fuel treatments, and ecological restoration: Conference proceedings; 2002 16-18 April; Fort Collins, CO. Proceedings RMRS-P-29. Fort Collins, CO: US Department of Agriculture, Forest Service, Rocky Mountain Research Station. p. 15-26, pp. 15–26.

Qadir, A., Talukdar, N.R., Uddin, M.M., Ahmad, F., Goparaju, L., 2021. Predicting forest fire using multispectral satellite measurements in Nepal. Remote Sensing Applications: Society and Environment 23, 100539. URL: https://www.sciencedirect.com/science/article/pii/S2352938521000756, doi:10.1016/j.rsase.2021.100539.

Quan, X., Wang, W., Xie, Q., He, B., Resco De Dios, V., Yebra, M., Jiao, M., Chen, R., 2023. Improving wildfire occurrence modelling by integrating time-series features of weather and fuel moisture content. Environmental Modelling & Software 170, 105840. doi:10.1016/j.envsoft.2023.105840.

Rakhmatulina, E., Stephens, S., Thompson, S., 2021. Soil moisture influences on sierra nevada dead fuel moisture content and fire risks. Forest Ecology and Management 496, 119379.

Rao, K., Williams, A.P., Flefil, J.F., Konings, A.G., 2020a. Sar-enhanced mapping of live fuel moisture content. Remote Sensing of Environment 245, 111797.

Rao, K., Williams, A.P., Flefil, J.F., Konings, A.G., 2020b. SAR-enhanced mapping of live fuel moisture content. Remote Sensing of Environment 245, 111797. URL: https://www.sciencedirect.com/science/article/pii/S003442572030167X, doi:10.1016/j.rse.2020.111797.

Ray, D., Nepstad, D., Brando, P., 2010. Predicting moisture dynamics of fine understory fuels in a moist tropical rainforest system: results of a pilot study undertaken to identify proxy variables useful for rating fire danger. New Phytologist 187, 720–732.

Razavi Termeh, S.V., Kornejady, A., Pourghasemi, H.R., Keesstra, S., 2018. Flood susceptibility mapping using novel ensembles of adaptive neuro fuzzy inference system and metaheuristic algorithms. Science of The Total Environment 615, 438–451. URL: https://www.

sciencedirect.com/science/article/pii/S0048969717326141, doi:10.1016/j.scitotenv.2017.09.262.

Rezaie, F., Panahi, M., Bateni, S.M., Lee, S., Jun, C., Trauernicht, C., Neale, C.M.U., 2023. Development of novel optimized deep learning algorithms for wildfire modeling: A case study of Maui, Hawai'i. Engineering Applications of Artificial Intelligence 125, 106699. URL: https://www.sciencedirect.com/science/article/pii/S0952197623008837, doi:10.1016/j.engappai.2023.106699.

Riaño, D., Chuvieco, E., Salas, J., Palacios-Orueta, A., Bastarrika, A., 2002. Generation of fuel type maps from landsat tm images and ancillary data in mediterranean ecosystems. Canadian Journal of Forest Research 32, 1301–1315.

Ritter, S.M., Hoffman, C.M., Battaglia, M.A., Linn, R., Mell, W.E., 2023. Vertical and horizontal crown fuel continuity influences group-scale ignition and fuel consumption. Fire 6, 321.

Rogger, M., Agnoletti, M., Alaoui, A., Bathurst, J., Bodner, G., Borga, M., Chaplot, V., Gallart, F., Glatzel, G., Hall, J., et al., 2017. Land use change impacts on floods at the catchment scale: Challenges and opportunities for future research. Water resources research 53, 5209–5219.

Romero-Calcerrada, R., Novillo, C., Millington, J.D., Gomez-Jimenez, I., 2008. Gis analysis of spatial patterns of human-caused wildfire ignition risk in the sw of madrid (central spain). Landscape ecology 23, 341–354.

Rösch, M., Nolde, M., Ullmann, T., Riedlinger, T., 2024. Data-driven wildfire spread modeling of european wildfires using a spatiotemporal graph neural network. Fire 7, 207.

Rothermel, R.C., Wilson, R., Morris, G.A., Sackett, S.S., 1986. Modeling Moisture Content of Fine Dead Wildland Fuels:. United States Department of Agriculture, Forest Service, Intermountain . . . .

Roy, S.K., Deria, A., Hong, D., Rasti, B., Plaza, A., Chanussot, J., 2023. Multimodal fusion transformer for remote sensing image classification. IEEE Transactions on Geoscience and Remote Sensing 61, 1–20. doi:10.1109/TGRS.2023.3286826.

Rubí, J.N.S., Gondim, P.R.L., 2023. A performance comparison of machine learning models for wildfire occurrence risk prediction in the Brazilian Federal District region. Environment Systems and Decisions URL: https://doi.org/10.1007/s10669-023-09921-2, doi:10.1007/s10669-023-09921-2.

Ruffault, J., Martin-StPaul, N., Pimont, F., Dupuy, J.L., 2018. How well do meteorological drought indices predict live fuel moisture content (lfmc)? an assessment for wildfire research and operations in mediterranean ecosystems. Agricultural and Forest Meteorology 262, 391–401.

Saatchi, S., Halligan, K., Despain, D.G., Crabtree, R.L., 2007. Estimation of Forest Fuel Load From Radar Remote Sensing. IEEE Transactions on Geoscience and Remote Sensing 45, 1726–1740. URL: https://ieeexplore.ieee.org/abstract/document/4215087, doi:10.1109/TGRS.2006.887002. conference Name: IEEE Transactions on Geoscience and Remote Sensing.

Sadasivuni, R., Cooke, W.H., Bhushan, S., 2013. Wildfire risk prediction in Southeastern Mississippi using population interaction. Ecological Modelling 251, 297–306. URL: https://www.sciencedirect.com/science/article/pii/S0304380013000070, doi:10.1016/j.ecolmodel.2012.12.024.

Salis, M., Arca, B., Del Giudice, L., Palaiologou, P., Alcasena-Urdiroz, F., Ager, A., Fiori, M., Pellizzaro, G., Scarpa, C., Schirru, M., Ventura, A., Casula, M., Duce, P., 2021. Application of simulation modeling for wildfire exposure and transmission assessment in Sardinia, Italy. International Journal of Disaster Risk Reduction 58, 102189. URL: https://linkinghub.elsevier.com/retrieve/pii/S2212420921001552, doi:10.1016/j.ijdrr.2021.102189.

San-Miguel-Ayanz, J., Durrant, T., Boca, R., Libertà, G., Branco, A., DE, R., Ferrari, D., Maianti, P., ARTES, V.T., PFEIFFER, H., et al., 2018. Forest Fires in Europe, Middle East and North Africa 2018. Publications Office of the European Union, Luxembourg.

Sandberg, D.V., Ottmar, R.D., Cushon, G.H., 2001. Characterizing fuels in the 21st century. International Journal of Wildland Fire 10, 381–387.

Santopaolo, A., Saif, S.S., Pietrabissa, A., Giuseppi, A., 2021. Forest fire risk prediction from satellite data with convolutional neural networks, in: 2021 29th Mediterranean Conference on Control and Automation (MED), IEEE. pp. 360–367.

Sayad, Y.O., Mousannif, H., Al Moatassime, H., 2019. Predictive modeling of

wildfires: A new dataset and machine learning approach. Fire safety journal 104, 130–146.

Scheller, R.M., Domingo, J.B., Sturtevant, B.R., Williams, J.S., Rudy, A., Gustafson, E.J., Mladenoff, D.J., 2007. Design, development, and application of landis-ii, a spatial landscape simulation model with flexible temporal and spatial resolution. ecological modelling 201, 409–419.

Schroeder, W., Oliva, P., Giglio, L., Csiszar, I.A., 2014. The new viirs 375 m active fire detection data product: Algorithm description and initial assessment. Remote Sensing of Environment 143, 85–96.

Scott, J.H., 2001. Assessing crown fire potential by linking models of surface and crown fire behavior. 29, US Department of Agriculture, Forest Service, Rocky Mountain Research Station.

Shadrin, D., Illarionova, S., Gubanov, F., Evteeva, K., Mironenko, M., Levchunets, I., Belousov, R., Burnaev, E., 2024a. Wildfire spreading prediction using multimodal data and deep neural network approach. Scientific Reports 14, 2606. URL: https://www.ncbi.nlm.nih.gov/pmc/articles/PMC10831103/, doi:10.1038/s41598-024-52821-x.

Shadrin, D., Illarionova, S., Gubanov, F., Evteeva, K., Mironenko, M., Levchunets, I., Belousov, R., Burnaev, E., 2024b. Wildfire spreading prediction using multimodal data and deep neural network approach. Scientific Reports 14, 2606.

Shah, N.A., VS, V., Patel, V.M., 2024. Lqmformer: Language-aware query mask transformer for referring image segmentation, in: Proceedings of the IEEE/CVF Conference on Computer Vision and Pattern Recognition (CVPR), pp. 12903–12913.

Shamsoshoara, A., Afghah, F., Razi, A., Zheng, L., Fulé, P., Blasch, E., 2020. The flame dataset: Aerial imagery pile burn detection using drones (uavs). URL: https://dx.doi.org/10.21227/qad6-r683, doi:10.21227/qad6-r683.

Shapley, L.S., 1953. Stochastic games. Proceedings of the national academy of sciences 39, 1095–1100.

Short, K.C., 2014. A spatial database of wildfires in the united states, 1992-2011. Earth System Science Data 6, 1–27.

Singla, S., Diao, T., Mukhopadhyay, A., Eldawy, A., Shachter, R., Kochenderfer, M., 2020. Wildfiredb: A spatio-temporal dataset combining wildfire occurrence with relevant covariates, in: 34th Conference on Neural Information Processing Systems (NeurIPS 2020).

Skowronski, N.S., Clark, K.L., Duveneck, M., Hom, J., 2011. Three-dimensional canopy fuel loading predicted using upward and downward sensing LiDAR systems. Remote Sensing of Environment 115, 703–714. URL: https://www.sciencedirect.com/science/article/pii/S0034425710003172, doi:10.1016/j.rse.2010.10.012.

Song, Y., Wang, Y., 2020. Global Wildfire Outlook Forecast with Neural Networks. Remote Sensing 12, 2246. URL: https://www.mdpi.com/2072-4292/12/14/2246, doi:10.3390/rs12142246. number: 14 Publisher: Multidisciplinary Digital Publishing Institute.

Srivastava, S.K., Saran, S., de By, R.A., Dadhwal, V.K., 2014. A geo-information system approach for forest fire likelihood based on causative and anti-causative factors. International Journal of Geographical Information Science 28, 427–454. URL: https://doi.org/10.1080/13658816.2013.797984, doi:10.1080/13658816.2013.797984. publisher: Taylor & Francis _eprint: https://doi.org/10.1080/13658816.2013.797984.

Stocks, B.J., Lawson, B.D., Alexander, M.E., Wagner, C.E.V., McAlpine, R.S., Lynham, T.J., Dubé, D.E., 1989a. The Canadian Forest Fire Danger Rating System: An Overview. The Forestry Chronicle 65, 450–457. URL: https://pubs.cif-ifc.org/doi/abs/10.5558/tfc65450-6, doi:10.5558/tfc65450-6. publisher: Canadian Institute of Forestry.

Stocks, B.J., Lynham, T., Lawson, B., Alexander, M., Wagner, C.V., McAlpine, R., Dube, D., 1989b. Canadian forest fire danger rating system: an overview. The Forestry Chronicle 65, 258–265.

Stojanovic, D., nee Voogdt, J.W., Webb, M., Cook, H., Heinsohn, R., 2016. Loss of habitat for a secondary cavity nesting bird after wildfire. Forest Ecology and Management 360, 235–241.

Su, Z., Zheng, L., Luo, S., Tigabu, M., Guo, F., 2021. Modeling wildfire drivers in Chinese tropical forest ecosystems using global logistic regression and geographically weighted logistic regression. Natural Hazards 108, 1317–1345. URL: https://doi.org/10.1007/s11069-021-04733-6, doi:10.1007/s11069-021-04733-6.

Sundararajan, M., Taly, A., Yan, Q., 2017. Axiomatic attribution for deep networks, in: International conference on machine learning, PMLR. pp. 3319–

3328.

Swetnam, T.W., Betancourt, J.L., 1990. Fire-southern oscillation relations in the southwestern united states. Science 249, 1017–1020.

Taneja, R., Hilton, J., Wallace, L., Reinke, K., Jones, S., 2021. Effect of fuel spatial resolution on predictive wildfire models. International Journal of Wildland Fire 30, 776–789. URL: https://www.publish.csiro.au/wf/WF20192, doi:10.1071/WF20192. publisher: CSIRO PUBLISHING.

Tavakkoli Piralilou, S., Einali, G., Ghorbanzadeh, O., Nachappa, T.G., Gholamnia, K., Blaschke, T., Ghamisi, P., 2022. A Google Earth Engine Approach for Wildfire Susceptibility Prediction Fusion with Remote Sensing Data of Different Spatial Resolutions. Remote Sensing 14, 672. URL: https://www.mdpi.com/2072-4292/14/3/672, doi:10.3390/rs14030672. number: 3 Publisher: Multidisciplinary Digital Publishing Institute.

Taylor, S.W., Alexander, M.E., 2006. Science, technology, and human factors in fire danger rating: the canadian experience. International Journal of Wildland Fire 15, 121–135.

Tesch, T., Kollet, S., Garcke, J., 2023. Causal deep learning models for studying the earth system. Geoscientific Model Development 16, 2149–2166.

Thompson, M.P., Vaillant, N.M., Haas, J.R., Gebert, K.M., Stockmann, K.D., 2013. Quantifying the potential impacts of fuel treatments on wildfire suppression costs. Journal of Forestry 111, 49–58.

Tolhurst, K., Shields, B., Chong, D., 2008. Phoenix: development and application of a bushfire risk management tool. Australian Journal of Emergency Management, The 23, 47–54.

Toulouse, T., Rossi, L., Campana, A., Celik, T., Akhloufi, M.A., 2017. Computer vision for wildfire research: An evolving image dataset for processing and analysis. Fire Safety Journal 92, 188–194.

Tran, T.T.K., Bateni, S.M., Rezaie, F., Panahi, M., Jun, C., Trauernicht, C., Neale, C.M.U., 2023. Enhancing predictive ability of optimized group method of data handling (GMDH) method for wildfire susceptibility mapping. Agricultural and Forest Meteorology 339, 109587. URL: https://www.sciencedirect.com/science/article/pii/S0168192323002782, doi:10.1016/j.agrformet.2023.109587.

Tran, T.T.K., Janizadeh, S., Bateni, S.M., Jun, C., Kim, D., Trauernicht, C., Rezaie, F., Giambelluca, T.W., Panahi, M., 2024. Improving the prediction of wildfire susceptibility on hawai'i island, hawai'i, using explainable hybrid machine learning models. Journal of environmental management 351, 119724.

Trucchia, A., Meschi, G., Fiorucci, P., Gollini, A., Negro, D., 2022. Defining Wildfire Susceptibility Maps in Italy for Understanding Seasonal Wildfire Regimes at the National Level. Fire 5, 30. URL: https://www.mdpi.com/2571-6255/5/1/30, doi:10.3390/fire5010030. number: 1 Publisher: Multidisciplinary Digital Publishing Institute.

Tucker, C.J., 1979. Red and photographic infrared linear combinations for monitoring vegetation. Remote Sensing of Environment 8, 127–150. URL: https://www.sciencedirect.com/science/article/pii/0034425779900130, doi:10.1016/0034-4257(79)90013-0.

Tymstra, C., Bryce, R., Wotton, B., Taylor, S., Armitage, O., et al., 2010. Development and structure of prometheus: the canadian wildland fire growth simulation model. Natural Resources Canada, Canadian Forest Service, Northern Forestry Centre, Information Report NOR-X-417.(Edmonton, AB) .

Ujjwal, K., Hilton, J., Garg, S., Aryal, J., 2022. A probability-based risk metric for operational wildfire risk management. Environmental Modelling & Software 148, 105286.

Umunnakwe, A., Parvania, M., Nguyen, H., Horel, J.D., Davis, K.R., 2022. Data-driven spatio-temporal analysis of wildfire risk to power systems operation. IET Generation, Transmission & Distribution 16, 2531–2546.

Van Wagner, C.E., et al., 1974. Structure of the Canadian forest fire weather index. volume 1333. Environment Canada, Forestry Service Ottawa, ON, Canada.

Vaswani, A., Shazeer, N., Parmar, N., Uszkoreit, J., Jones, L., Gomez, A.N., Kaiser, L., Polosukhin, I., 2017. Attention is all you need, in: Advances in Neural Information Processing Systems.

Vega, J.A., Arellano-Pérez, S., Álvarez-González, J.G., Fernández, C., Jiménez, E., Fernández-Alonso, J.M., Vega-Nieva, D.J., Briones-Herrera, C., Alonso-Rego, C., Fontúrbel, T., et al., 2022. Modelling aboveground biomass and fuel load components at stand level in shrub communities in nw spain. Forest Ecology and Management 505, 119926.

Viegas, D.X., Bovio, G., Ferreira, A., Nosenzo, A., Sol, B., 1999. Comparative study of various methods of fire danger evaluation in southern europe.

International Journal of wildland fire 9, 235–246.

Vilar, L., Camia, A., San-Miguel-Ayanz, J., Martín, M.P., 2016. Modeling temporal changes in human-caused wildfires in mediterranean europe based on land use-land cover interfaces. Forest Ecology and Management 378, 68–78.

Viney, N.R., 1991a. A review of fine fuel moisture modelling. International Journal of Wildland Fire 1, 215–234.

Viney, N.R., 1991b. A Review of Fine Fuel Moisture Modelling. International Journal of Wildland Fire 1, 215–234. URL: https://www.publish.csiro.au/wf/wf9910215, doi:10.1071/wf9910215. publisher: CSIRO PUBLISHING.

Vissio, G., Turco, M., Provenzale, A., 2023. Testing drought indicators for summer burned area prediction in Italy. Natural Hazards 116, 1125–1137. URL: https://doi.org/10.1007/s11069-022-05714-z, doi:10.1007/s11069-022-05714-z.

Viswanathan, S., Anand Kumar, M., Soman, K., 2019. A sequence-based machine comprehension modeling using lstm and gru, in: Emerging Research in Electronics, Computer Science and Technology: Proceedings of International Conference, ICERECT 2018, Springer. pp. 47–55.

Vitolo, C., Di Giuseppe, F., Barnard, C., Coughlan, R., San-Miguel-Ayanz, J., Libertá, G., Krzeminski, B., 2020. ERA5-based global meteorological wildfire danger maps. Scientific Data 7, 216. URL: https://www.nature.com/articles/s41597-020-0554-z, doi:10.1038/s41597-020-0554-z. publisher: Nature Publishing Group.

Wagner, C.V., 1993. Prediction of crown fire behavior in two stands of jack pine. Canadian Journal of Forest Research 23, 442–449.

Walker, X.J., Rogers, B.M., Veraverbeke, S., Johnstone, J.F., Baltzer, J.L., Barrett, K., Bourgeau-Chavez, L., Day, N., de Groot, W., Dieleman, C., et al., 2020. Fuel availability not fire weather controls boreal wildfire severity and carbon emissions. Nature Climate Change 10, 1130–1136.

Wang, J., Ke, L., 2024. Llm-seg: Bridging image segmentation and large language model reasoning, in: Proceedings of the IEEE/CVF Conference on Computer Vision and Pattern Recognition (CVPR) Workshops, pp. 1765–1774.

Wang, Q., Ihme, M., Gazen, C., Chen, Y.F., Anderson, J., 2024. Firebench: A high-fidelity ensemble simulation framework for exploring wildfire behavior and data-driven modeling. arXiv preprint arXiv:2406.08589 .

Wang, S.S.C., Qian, Y., Leung, L.R., Zhang, Y., 2021. Identifying Key Drivers of Wildfires in the Contiguous US Using Machine Learning and Game Theory Interpretation. Earth's Future 9, e2020EF001910. URL: https://onlinelibrary.wiley.com/doi/abs/10.1029/2020EF001910, doi:10.1029/2020EF001910. _eprint: https://onlinelibrary.wiley.com/doi/pdf/10.1029/2020EF001910.

Wang, Y., Xi, X., Wang, C., Yang, X., Wang, P., Nie, S., Du, M., 2022a. A novel method based on kernel density for estimating crown base height using uav-borne lidar data. IEEE Geoscience and Remote Sensing Letters 19, 1–5. doi:10.1109/LGRS.2022.3171316.

Wang, Z., Lu, Y., Li, Q., Tao, X., Guo, Y., Gong, M., Liu, T., 2022b. Cris: Clip-driven referring image segmentation, in: 2022 IEEE/CVF Conference on Computer Vision and Pattern Recognition (CVPR), pp. 11676–11685. doi:10.1109/CVPR52688.2022.01139.

Wing, B.M., Ritchie, M.W., Boston, K., Cohen, W.B., Gitelman, A., Olsen, M.J., 2012. Prediction of understory vegetation cover with airborne lidar in an interior ponderosa pine forest. Remote Sensing of Environment 124, 730–741.

Wu, J., Li, X., Li, X., Ding, H., Tong, Y., Tao, D., 2024. Toward robust referring image segmentation. IEEE Transactions on Image Processing 33, 1782–1794. doi:10.1109/TIP.2024.3371348.

Xie, L., Zhang, R., Zhan, J., Li, S., Shama, A., Zhan, R., Wang, T., Lv, J., Bao, X., Wu, R., 2022. Wildfire risk assessment in liangshan prefecture, china based on an integration machine learning algorithm. Remote Sensing 14, 4592.

Xu, P., Zhu, X., Clifton, D.A., 2023a. Multimodal learning with transformers: A survey. IEEE Transactions on Pattern Analysis and Machine Intelligence 45, 12113–12132. doi:10.1109/TPAMI.2023.3275156.

Xu, R., Yang, S., Wang, Y., Cai, Y., Du, B., Chen, H., 2024. Visual mamba: A survey and new outlooks. URL: https://arxiv.org/abs/2404.18861, arXiv:2404.18861.

Xu, W., Wooster, M.J., 2023. Sentinel-3 slstr active fire (af) detection and frp daytime product-algorithm description and global intercomparison to modis, viirs and landsat af data. Science of Remote Sensing 7, 100087.

Xu, Z., Chen, Z., Zhang, Y., Song, Y., Wan, X., Li, G., 2023b. Bridging vision and language encoders: Parameter-efficient tuning for referring image segmentation, in: Proceedings of the IEEE/CVF International Conference on Computer Vision (ICCV), pp. 17503–17512.

Yahia, O., Ghabi, M., Karoui, M.S., 2023. The Prediction of Regional Wildfire Risk Using High-Resolution Remotely Sensed Soil Moisture Content Estimation, Case Study: Sidi Douma Forest, Saida, Algeria, in: IGARSS 2023 - 2023 IEEE International Geoscience and Remote Sensing Symposium, pp. 3387–3390. URL: https://ieeexplore.ieee.org/abstract/document/10281986, doi:10.1109/IGARSS52108.2023.10281986. iSSN: 2153-7003.

Yan, Y., He, X., Wan, W., Liu, J., 2023. Mmnet: Multi-mask network for referring image segmentation. URL: https://arxiv.org/abs/2305.14969, arXiv:2305.14969.

Yang, C.E., Fu, J.S., Liu, Y., Dong, X., Liu, Y., 2022a. Projections of future wildfires impacts on air pollutants and air toxics in a changing climate over the western United States. Environmental Pollution 304, 119213. URL: https://www.sciencedirect.com/science/article/pii/S0269749122004274, doi:10.1016/j.envpol.2022.119213.

Yang, J., He, H.S., Gustafson, E.J., 2004. A hierarchical fire frequency model to simulate temporal patterns of fire regimes in landis. Ecological Modelling 180, 119–133.

Yang, Z., Wang, J., Tang, Y., Chen, K., Zhao, H., Torr, P.H., 2022b. Lavt: Language-aware vision transformer for referring image segmentation, in: Proceedings of the IEEE/CVF Conference on Computer Vision and Pattern Recognition (CVPR), pp. 18155–18165.

Yao, J., Zhang, B., Li, C., Hong, D., Chanussot, J., 2023. Extended vision transformer (exvit) for land use and land cover classification: A multimodal deep learning framework. IEEE Transactions on Geoscience and Remote Sensing 61, 1–15. doi:10.1109/TGRS.2023.3284671.

Yebra, M., Dennison, P.E., Chuvieco, E., Riaño, D., Zylstra, P., Hunt Jr, E.R., Danson, F.M., Qi, Y., Jurdao, S., 2013a. A global review of remote sensing of live fuel moisture content for fire danger assessment: Moving towards operational products. Remote Sensing of Environment 136, 455–468.

Yebra, M., Dennison, P.E., Chuvieco, E., Riaño, D., Zylstra, P., Hunt, E.R., Danson, F.M., Qi, Y., Jurdao, S., 2013b. A global review of remote sensing of live fuel moisture content for fire danger assessment: Moving towards operational products. Remote Sensing of Environment 136, 455–468. URL: https://www.sciencedirect.com/science/article/pii/S0034425713001831, doi:10.1016/j.rse.2013.05.029.

Ying, L., Cheng, H., Shen, Z., Guan, P., Luo, C., Peng, X., 2021. Relative humidity and agricultural activities dominate wildfire ignitions in yunnan, southwest china: Patterns, thresholds, and implications. Agricultural and Forest Meteorology 307, 108540.

Ying, L., Shen, Z., Yang, M., Piao, S., 2019. Wildfire detection probability of modis fire products under the constraint of environmental factors: A study based on confirmed ground wildfire records. Remote Sensing 11, 3031.

Yoon, H.J., Voulgaris, P., 2022. Multi-time predictions of wildfire grid map using remote sensing local data, in: 2022 IEEE International Conference on Knowledge Graph (ICKG), pp. 365–372. doi:10.1109/ICKG55886.2022.00053.

You, X., Zheng, Z., Yang, K., Yu, L., Liu, J., Chen, J., Lu, X., Guo, S., 2023. A pso-cnn-based deep learning model for predicting forest fire risk on a national scale. Forests 15, 86.

Yuan, Z., Mou, L., Hua, Y., Zhu, X.X., 2024. Rrsis: Referring remote sensing image segmentation. IEEE Transactions on Geoscience and Remote Sensing 62, 1–12. doi:10.1109/TGRS.2024.3369720.

Zacharakis, I., Tsihrintzis, V.A., 2023a. Environmental forest fire danger rating systems and indices around the globe: a review. Land 12, 194.

Zacharakis, I., Tsihrintzis, V.A., 2023b. Integrated wildfire danger models and factors: A review. Science of The Total Environment 899, 165704. URL: https://linkinghub.elsevier.com/retrieve/pii/S0048969723043279, doi:10.1016/j.scitotenv.2023.165704.

Zarzycki, K., Ławryńczuk, M., 2022. Advanced predictive control for gru and lstm networks. Information Sciences 616, 229–254.

Zerveas, G., Jayaraman, S., Patel, D., Bhamidipaty, A., Eickhoff, C., 2021. A Transformer-based Framework for Multivariate Time Series Representation Learning, in: Proceedings of the 27th ACM SIGKDD Conference on Knowledge Discovery & Data Mining, Association for Computing Machinery, New York, NY, USA. pp. 2114–2124. URL: https://dl.acm.org/doi/10.1145/3447548.3467401, doi:10.1145/3447548.3467401.

Zhang, C., Pan, X., Li, H., Gardiner, A., Sargent, I., Hare, J., Atkinson, P.M., 2018. A hybrid MLP-CNN classifier for very fine resolution remotely sensed image classification. ISPRS Journal of Photogrammetry and Remote Sensing 140, 133–144. URL: https://www.sciencedirect.com/science/article/pii/S0924271617300254, doi:10.1016/j.isprsjprs.2017.07.014.

Zhang, G., Wang, M., Liu, K., 2019. Forest Fire Susceptibility Modeling Using a Convolutional Neural Network for Yunnan Province of China. International Journal of Disaster Risk Science 10, 386–403. URL: https://doi.org/10.1007/s13753-019-00233-1, doi:10.1007/s13753-019-00233-1.

Zhang, G., Wang, M., Liu, K., 2021. Deep neural networks for global wildfire susceptibility modelling. Ecological Indicators 127, 107735. URL: https://www.sciencedirect.com/science/article/pii/S1470160X21004003, doi:10.1016/j.ecolind.2021.107735.

Zhang, G., Wang, M., Liu, K., 2022. Dynamic prediction of global monthly burned area with hybrid deep neural networks. Ecological Applications 32, e2610.

Zhang, G., Wang, M., Yang, B., Liu, K., 2024. Current and future patterns of global wildfire based on deep neural networks. Earth's Future 12, e2023EF004088.

Zhao, F., Liu, Y., 2021. Important meteorological predictors for long-range wildfires in China. Forest Ecology and Management 499, 119638. URL: https://www.sciencedirect.com/science/article/pii/S0378112721007283, doi:10.1016/j.foreco.2021.119638.

Zhao, S., Prapas, I., Karasante, I., Xiong, Z., Papoutsis, I., Camps-Valls, G., Zhu, X.X., 2024. Causal graph neural networks for wildfire danger prediction. URL: https://arxiv.org/abs/2403.08414, arXiv:2403.08414.

ZORMPAS, K., VASILAKOS, C., ATHANASIS, N., SOULAKELLIS, N., KALABOKIDIS, K., 2017. Dead fuel moisture content estimation using remote sensing. European Journal of Geography 8.

Zubkova, M., Lötter, M., Bronkhorst, F., Giglio, L., 2024. Assessment of the effectiveness of coarse resolution fire products in monitoring long-term changes in fire regime within protected areas in south africa. International Journal of Applied Earth Observation and Geoinformation 132, 104064.